13

DIFFUSION FLAMES

Diffusion flames are formed when the combustible and oxidizer are not premixed before entering the reaction zone, e.g., the combustion of producer gas with air in steel furnaces and a non-aerated gas burner provide such flames. The burning of fuel droplets as in a gas turbine or a diesel engine is also essentially diffusion flame phenomenon. Unlike as in the case of premixed flames, there are no fundamental characteristics such as burning velocity for diffusion flames. In a diffusion flame, as the gases mix and flow upwards, the combustible gas diffuses outwards and the air inwards. The distinctive characteristic of a diffusion flame is that the burning rate is determined by the rate at which the fuel and the oxidizer are brought together in proper proportions for the reaction. The rate of combustion in a premixed flame is dependent on the rate of energy release and, therefore, on the rate of the oxidation reaction.

Although diffussion flames are used more frequently in industry, they have received less attention in fundamental studies than premixed flames. In a diffusion flame, the reaction is first with oxygen and occurs mainly in the maximum temperature region of the flame, whereas in the premixed flame, the oxidation commences well before the maximum temperature is reached. The rate of consumption of oxygen per unit volume of the flame is thousands of times less in a diffusion flame than in a premixed flame.

13.1 GASEOUS DIFFUSION FLAMES

Burke and Schumann[1] studied the gaseous diffusion flame in a tube in which the fuel stream was surrounded by an annular stream of air, the two streams having the same initial velocity. The shape of the flame depends on whether the annular stream has more oxygen (over-ventilated flame) or less oxygen (under-ventilated flame) than necessary for the

complete combustion of the fuel or fuel-air mixture in the inner stream. The shapes of the flame front under these conditions are shown in Fig. 13.1.

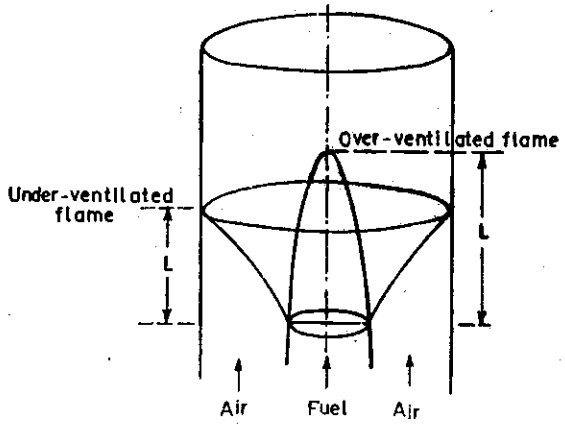

Fig. 13.1 Over-ventilated and under-ventilated diffusion flame. (With permission of the American Chemical Society from *Industrial Engineering Chemistry*, 1928, 20: (10) 999.)

In the over-ventilated flame, the flame boundary converges to the axis of the cylinder, while for the under-ventilated flame it expands towards the outer cylinder walls. Various shapes between these two limits can be obtained by changing the fuel to air ratio. For diffusion flames, the flame boundary is defined as the surface at which combustion is complete. It corresponds to the boundary where the air and fuel are in stoichiometric ratio. John[2] first studied the effect of changing air and fuel supply and obtained various shapes of flames on a burner similar to that of Burke and Schumann. He divided the range of air and fuel flows in ten zones giving various flame shapes. Figure 13.2 shows the various zones and flame shapes obtained:

Zones 1 and 2	Laminar diffusion flames
Zone 3	Meniscus flames
Zone 4	Lambent flames
Zone 5	Rich tilted flames
Zones 6 and 7	Incipient lifting and lifted flames
Zone 8	Vortex flames
Zones 9 and 10	Weak tilted flames

Before considering laminar diffusion flames in zones 1 and 2, we shall take other flames of unconventional shapes. For example, meniscus shaped flames in zone 3 are obtained at very low fuel flow rates. This shape is attributed to the effect of axial diffusion of fuel which is otherwise neglected. The line between zones 1 and 3 indicates the point where the yellow glow of the laminar diffusion flame disappears. Below zone 3

the flame is extinguished because of very low fuel flow. At very low fuel and air flow rates, the convective forces become appreciable and lambent

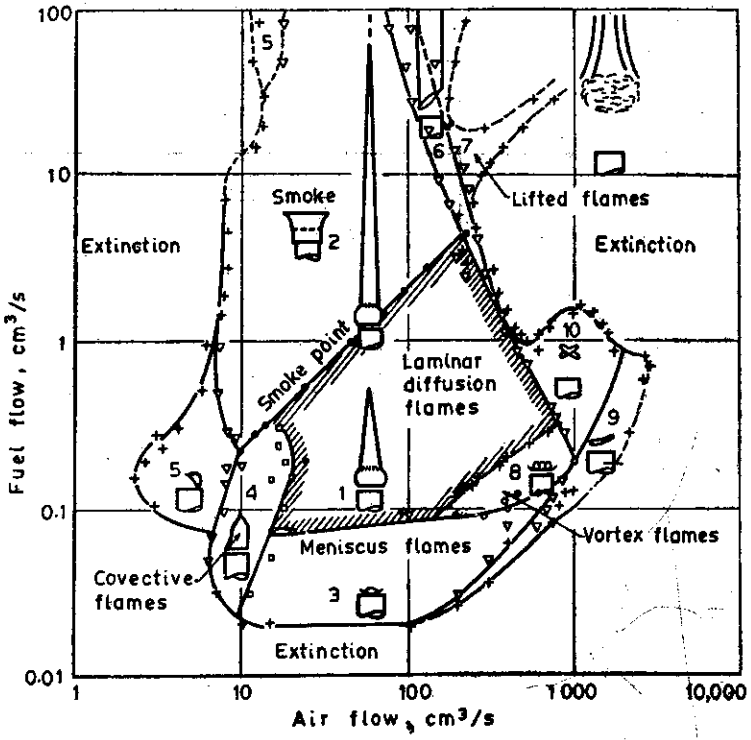

Fig. 13.2 Types of diffusion flames obtained with various flow rates of fuel and air. (With permission of the Combustion Institute, from *Fourth Symposium (International) on Combustion*, 1953, p. 766.)

flames are obtained, the position of flame shifts from one side to another. In the region 4, the flame extinguishes when one corner lifts during convective oscillation. In zone 5, where fuel concentration is high, rich tilted flames are obtained. Above the fuel flow rates of 10 cc/s and at increased air flow in zone 6, one corner of the flame is lifted. A further increase leads to flame lifting and finally to extinction. At very high fuel and air flows, lifted flames have the appearance of tilted highly turbulent flames. In zone 8, i.e., for low fuel flow rates and high air flow rates, torroidal vortex forms near the inner tube mouth. By increasing the air flow, a central streak of glowing carbon appears, and carbon is deposited at the burner tip. A further increase of air flow depresses the flame tip until a central hole appears. A further increase gradually changes the flame to a tilted, elliptical blue flame. Weak tilted flames are formed in zones 9 and 10. These flames sometimes oscillate or rotate at the port.

Laminar diffusion flames, as obtained in zones 1 and 2, were studied by many workers. Such flames are also easily obtainable in quiescent air. The line separating zones 1 and 2 gives the point where the smoke starts appearing. Generally under-ventilated flames are obtained in zone 2, while in zone 1, only over-ventilated flames are obtained. The height of the laminar flame is one of the parameters generally measured and is related to the diameter of the tube, fuel flow rate, etc.

By increasing the air flow, the laminar character of the diffusion flame changes. During the transition period, the tip of the flame becomes turbulent while the base remains laminar. A further increase in the flow velocity results in a reduction of the length of the laminar region. The point where the laminar stream changes to a turbulent one is called the break point. When the break point reaches quite near the fuel nozzle, the height of the flame and the height of the break point above the nozzle remain unchanged. A further increase in the flow velocity only increases the intensity of noise. Figure 13.3 shows the change in

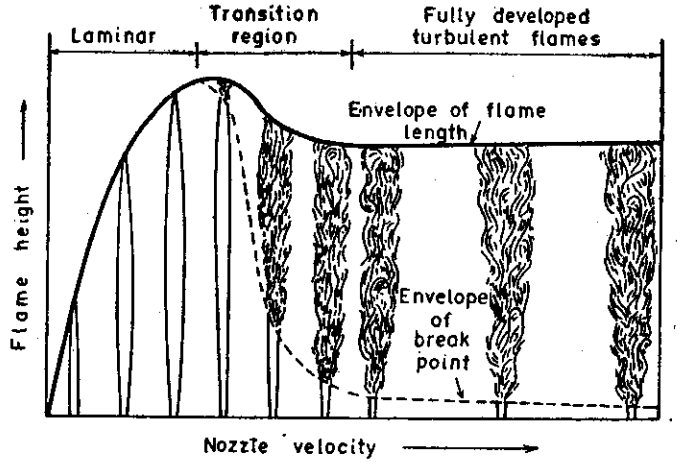

Fig. 13.3 Progressive change in flame type with increase in nozzle velocity. (With permission of Combustion Institute from *Third Symposium (International) on Combustion*, 1949, p. 225.)

height and position of the break point with increasing flow velocity. It can be observed from the figure, that during the laminar region, the height of the flame increases almost linearly with an increase in the flow velocity. The height of the flame is reduced slightly in the turbulent region and is independent of the flow velocity. The break point height also remains constant after a particular flow velocity is attained. In the turbulent region, a lifted flame can also be obtained similar to the one obtained with premixed mixtures.

The distribution of various components at different heights in a laminar diffusion flame was first measured by Hattel and Hawthorne[9]. The results

for the hydrogen-air flame are shown in Fig 13.4. Hydrogen flame was selected because of its simple chemistry. It was observed that the concentrations of both the fuel and air approach zero at the flame front. The concentration of the products is maximum at the flame front. The fuel concentration is zero at the flame front and maximum at the burner axis, while the oxygen concentration increases from zero at the flame front to maximum at the ambient stream. It is assumed that at the flame front, the fuel and oxygen reach in stoichiometric proportions and are instantaneously consumed.

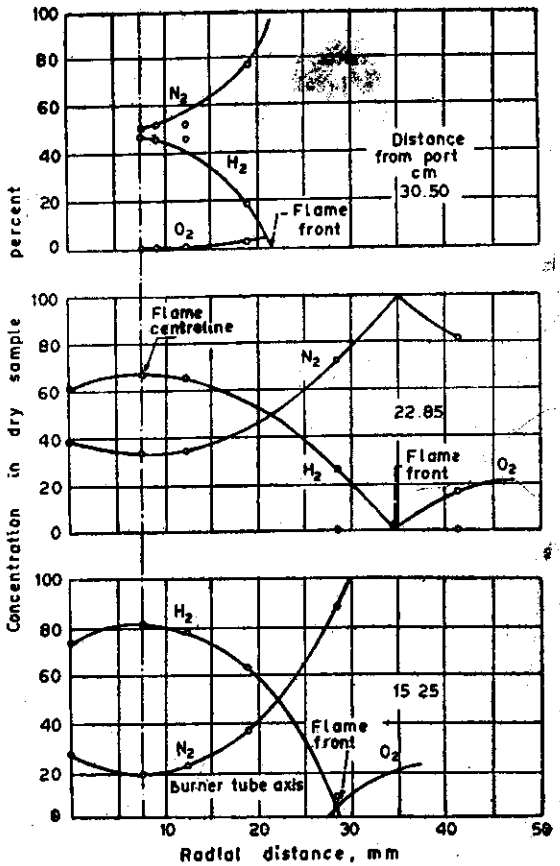

Fig. 13.4 Composition of a hydrogen diffusion flame, (With permission of Combustion Institute from *Third Symposium (International) on Combustion*, 1949, p. 258).

In this treatment, the flame front is assumed to be a thin reaction zone. Figure 13.4 gives the concentrations of hydrogen, nitrogen, and oxygen at different heights above the burner port. The position of the flame front keeps shifting because of the different width of the flame. The measurable

concentration of oxygen on the fuel side is attributed to the air entering the sampling tube because of the flame movement. From these results, a general picture of the structure of a laminar diffusion flame is drawn as shown in Fig. 13.5. This figure shows the change in fuel, oxygen, and product

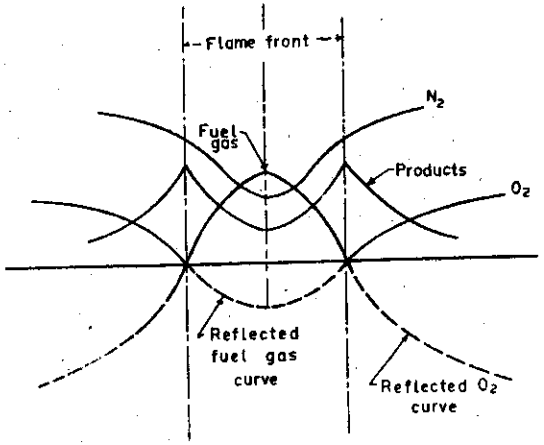

Fig. 13.5 Simplified diagram of concentration profiles in typical laminar diffusion flame. (With permission of Combustion Institute from the *Third Symposium (International) on Combustion*, 1949, p. 258.)

concentrations. The dashed curves shown in Fig. 13.5 represent the reflected fuel and the oxygen concentrations with negative values. The figure does not give any idea of the diffusion or formation of intermediate active species. Spectroscopic studies enable us to obtain the concentration of various intermediate products. It has been observed that the reaction in diffusion flames takes place largely by the pyrolysis of the fuel due to the diffusion of active species.

13.2 THEORY OF DIFFUSION FLAMES

For the diffusion flames in zones 1 and 2 of Fig. 13.2, the flame height is the indicator of the rate of burning of fuel. Therefore, the theoretical treatment of diffusion flames is mostly directed towards the calculation of the height of the flame.

Hawthorne, Weddell, and Hottel[4], from the consideration of the effect of change of scale, derived a simple correlation between the flame length, dimensions of the tube, and flow of gas. Consider the two cylindrical diffusion flame burners as shown in Fig 13.6, the inner tube diameters being d_1 and d_2 and the outer tube diameters d_1' and d_2', respectively. At the outlet of the inner tube, the mixing of the fuel and oxidant begins. At the outlet, the concentration profile of the fuel will be square in shape. At distances L_1 and L_2 the concentration profiles will be curved as shown.

L_1 and L_2 are so chosen that the centreline concentration is the same in both the tubes. The rate of mixing of the fuel and oxidant in the two streams will be proportional to the area normal to the direction of

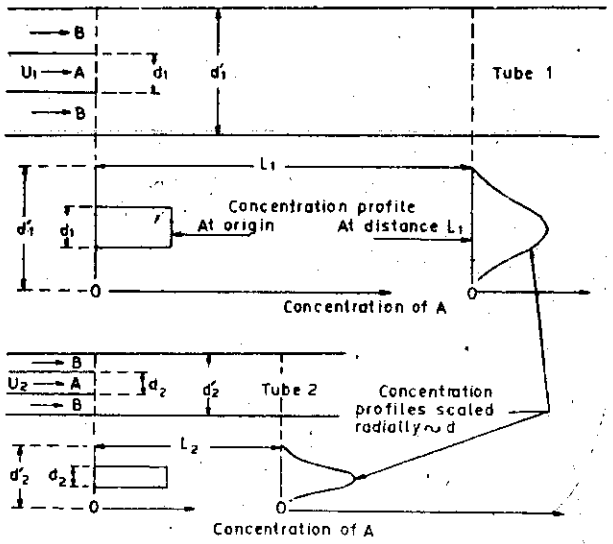

Fig. 13.6 Change of scale in jet mixing. (With permission of the Combustion Institute, from *Third Symposium on Combustion*, p. 267, 1949.)

mixing, and the concentration gradient normal to the area. The proportionality constant will be the diffusion coefficient D for the two gases. Now, the areas of mixing surfaces up to distances L_1 and L_2 will be d_1L_1 and d_2L_2 respectively. Since the concentration curves at the corresponding distances downstream are scaled in one dimension in proportion to the diameter, the ratio of the concentration gradient is $(1/d_1)/(1/d_2)$.

It follows that the ratio of the mixing rates in the two ducts, out to the corresponding points L_1 and L_2 is

$$\frac{d_1 L_1}{d_2 L_2} \cdot \frac{1/d_1}{1/d_2} \cdot \frac{D_1}{D_2}$$

or

$$\frac{L_1 D_1}{L_2 D_2}$$

The ratio of the amounts of fuel flowing per unit time through the tubes, if the flow velocities of fuel in the two burners is U_1 and U_2, will be:

$$U_1 d_1^2 / U_2 d_2^2$$

As the ratio of the fuel flow should be equal to the ratio of the amounts of the fuel mixed with air, therefore,

$$\frac{L_1}{L_2} \frac{D_1}{D_2} = \frac{U_1 d_1^2}{U_2 d_2^2} \tag{13.1}$$

or

$$L \propto \frac{U d^2}{D} \tag{13.2}$$

i.e., the height of the flame is proportional to the fuel flow rate. This expression is valid for the laminar flow. For turbulent flow, the diffusion coefficient D should be replaced by the eddy diffusivity ε which is found to be the product of the scale and intensity of turbulence. As the scale of turbulence is proportional to the diameter, and the intensity of turbulence is proportional to the average velocity U, therefore, from Eq. (13.2) for turbulent flow:

$$L \propto \frac{U d^2}{U d}$$

or

$$L \propto d \tag{13.3}$$

i.e., for turbulent flow, the diffusion flame height is independent of the fuel flow rate and depends only upon the diameter of the burner tube. These two results are found to confirm the experimental investigations of Burke and Schumann[1], Wohl, Gazley, and Kapp[5] and others.

For the study of diffusion flames, slot burners are found to be more suitable than cylindrical burners because they give a flat mixing zone. For the previous treatment, the ratio of the mixing areas of two slot burners will be L_1/L_2. If d denotes the width of the inner slot, the ratio of concentration gradients will be $1/d_1/1/d_2$. Therefore, for the slot burners also, Eq. (13.2) will be the same, the only difference being that d represents the width of the slot instead of the diameter of burner.

Jost[6] estimated the diffusion flame length using the equation of the average square of displacement

$$\overline{x^2} = \xi^2 = 2\,Dt \tag{13.4}$$

where ξ^2 denotes the average of the square of displacement of molecules from some location due to diffusion during time t. Now at a point on the axis of the tube where combustion is complete, the average depth of penetration of air into fuel must be equal to the radius of the tube and this point will give the height of flame. If ξ is identified with the average depth of penetration, taking U to be constant, the time t required for the completion of the diffusion process, i. e., the time required by a gas element to flow from the burner tip to the flame tip is given by

$$t = \frac{L}{U} \tag{13.5}$$

from Eq. (13.4) and taking $\xi = \frac{d}{2}$

$$L = \frac{d^2U}{8D} \tag{13.6}$$

This equation gives the proportionality constant of Eq. (13.2). This can be expressed in terms of the volume flow rate V as:

$$L = \frac{V}{2\pi D} \tag{13.7}$$

Burke and Schumann gave a rigorous mathematical treatment with the following assumptions on a cylindrical diffusion burner model of Fig 13.1.

1. The flow velocities of fuel and air are equal and constant at the burner port so that the ratio of the fuel to air flow is $d^2/(d'^2-d^2)$.
2. The velocity of the fuel and air at the flame region is assumed to be the same as at the port. This assumption is not true as due to expansion, the velocities increase appreciably.
3. The coefficient of inter-diffusion of the fuel and air is assumed to be constant. Burke and Schumann suggested that the increase in the diffusion coefficient at a higher temperature compensates the error due to assumption (1) of constant flow velocity.
4. The inter-diffusion of the two gases is in the radial direction only.
5. Mixing is only due to diffusion. Recirculation eddies and radial flow components are assumed to be absent.
6. The flame zone is assumed to be a thin zone where the fuel and air meet in stoichiometric ratio.
7. To simplify the mathematical treatment, oxygen is treated as a negative fuel. In the reaction,

   $$\text{Fuel} + i\ O_2 \rightarrow \text{Products}$$

   each mole of fuel is equivalent to i moles of oxygen. The oxygen concentration, C_{oxy} may be replaced by its stoichiometric equivalent in terms of fuel. Since at the flame boundary, the fuel and oxygen to be the are in stoichiometric ratio and since the diffusivities are assumed same for all gases, it follows that at the flame boundary

   $$d\,C_f/\,dy = -(1/i)\,(d\,C_{oxy}/dy) \tag{13.8}$$

   where C_f and C_{oxy} are the fuel and oxygen concentrations respectively.
8. It is assumed that the tube containing the fuel has negligible thickness.

With the above assumptions, the problem reduces to the diffusion of a single gas, namely, the fuel.

In cylindrical coordinates, the diffusion equation may be written as

$$\frac{\partial C}{\partial t} = D\left[\frac{\partial^2 C}{\partial r^2} + \frac{1}{r}\frac{\partial C}{\partial r}\right] \tag{13.9}$$

with assumptions (1) and(2), i.e., constant velocity U, t can be replaced by vertical distance x from the burner port as:

$$t = \frac{x}{U}$$

Therefore Eq. (13.9) becomes

$$\frac{\partial C}{\partial x} = \frac{D}{U}\left[\frac{\partial^2 C}{\partial r^2} + \frac{1}{r}\frac{\partial C}{\partial r}\right] \tag{13.10}$$

the boundary conditions are

$$\frac{\partial C}{\partial r} = 0 \quad \text{at} \begin{cases} r=0 \\ r=d'/2 \end{cases}$$

where d' is the diameter of the outer tube.

At $x=0$,

$C=C_1$ from $r=0$ to $r=d/2$

and $$C = -\frac{C_2}{i} \text{ from } r = \frac{d}{2} \text{ to } r = \frac{d'}{2}$$

where C_1 and C_2 are the initial fuel and oxygen concentrations respectively.

The solution of Eq. (13.10) with the above boundary conditions is

$$C = C_0\frac{d^2}{d'^2} - \frac{C_2}{i} + \frac{4C_0}{d'^2}\sum\frac{1}{\varphi}\frac{J_1(\varphi\, d/2)\,J_0(\varphi r)}{\{J_0(\varphi d'/2)\}^2}\exp(-D\,\varphi^2\,x/U) \tag{13.11}$$

where $C_0 = C_1 + \frac{C_2}{i}$ and φ is a constant that assumes all positive roots of the equation $J_1(\varphi\, d'/2) = 0$, and J_0 and J_1 are the Bessel functions of the first kind.

The equation for the flame boundary is obtained by putting $C=0$ and $r=r_f$ wher r_f is the radial distance of the flame boundary from the axis, hence:

$$\sum\frac{1}{\varphi}\frac{J_1(\varphi\, d/2)\,J_0(\varphi r_f)}{\{J_0(\varphi\, d'/2)\}^2}\exp(-D\varphi^2\,x/U) = \frac{d'C_2}{4\,diC_0}\frac{d}{4} \tag{13.12}$$

The shape of the flame will be given by the values of r_f and x that satisfy Eq. (13.12). The height of the flame for the over-ventilated flame is given by the value of x corresponding to $r_f=0$, and x corresponding to $r_f=d'/2$ will give the height of the under-ventilated flame.

To obtain the shape of flame for a known value of d', the number of values of constant φ is obtained from the table of Bessel functions corresponding to the equation $J_1\{\varphi d'/2\}=0$. For each value of φ and known value of d, U and D, a pair of values for x and r_f is selected and the left hand side of Eq.(13.12) is evaluated. If the equation is not satisfied for some value of x, another value of r_f is selected till the

equation is satisfied. This pair of values of r_f and x will give a point on the flame front. The number of such points can be calculated to give the flame shape. Figure 13.7 gives the shape of an over-ventilated

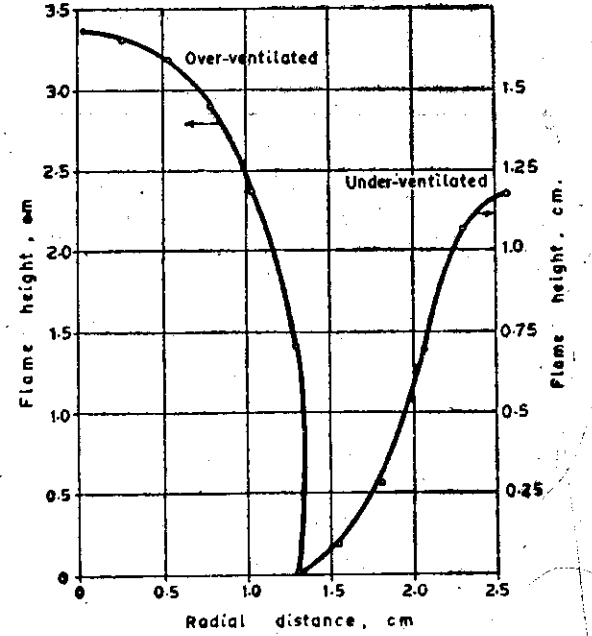

Fig. 13.7 Calculated flame shape for under-ventilated and over-ventilated flame. (With permission of the American Chemical Society, from *Industrial Engineering Chemistry*, vol. 20, p. 1000, 1928.)

and under-ventilated flame for a burner of $d=2.54$ cm, $d'=5.08$ cm, $D=0.492$ cm^2/s and $U=1.55$ cm/s corresponding to a flow of 0.0283 m^3/hr in the inner tube.

Similarly, for a slot burner the equation of diffusion may be written as

$$\frac{\partial C}{\partial x}=\frac{D}{U}\frac{\partial^2 C}{\partial y^2} \tag{13.13}$$

where y corresponds to r in Eq. (13.10). For the corresponding boundary conditions, the solution of Eq. (13.13) is :

$$C=\frac{C_0 d}{d'}-\frac{C_2}{i}+\frac{2C_0}{\pi}\sum_1^\infty \frac{1}{n}\sin\frac{n\pi d}{d'}\cos\frac{2n\pi y}{d'}\exp\left(-4Dn^2\pi^2 x/Ud'^2\right) \tag{13.14}$$

Substituting $C=0$ and $y=y_f$, the equation for the flame boundary is:

$$\sum_1^\infty \frac{1}{n}\sin\frac{n\pi d}{d'}\cos\frac{2n\pi y_f}{d'}\exp\left(-4Dn^2\pi^2 x/Ud'^2\right)=\frac{\pi}{2}\left(\frac{C_2}{iC_0}-\frac{d}{d'}\right) \tag{13.15}$$

Here d and d' represent the width of the inner and outer slots respectively. The shapes of the over-ventilated and under-ventilated flames are similar to that obtained on cylindrical burners. These shapes are found to be similar to those obtained experimentally. However, it should be observed that the flame height calculated by the simple Eq.(13.7) is equally good. Similarly for a comparison of the two flames Eq. (13.2) gives good results.

Further theoretical work on diffusion flames has been carried out by Hottel and Hawthorne[8], and Wohl *et al*[5]. These groups used empirical or semi-empirical relations to predict the flame height in the region where the proportionality Eq. (13.2) or Eq. (13.11) could not be applicable due to assumptions (1) and (2) stated earlier. Similarly, for the diffusion flames burning in an open atmosphere, assumption (1) is not valid. Hottel and Hawthorne assumed fuel as negative oxygen, i.e., the fuel is replaced by $-i\,C_f$. If a sample of gas is taken from some point in the stream and the composition of the mixture is calculated in the unburned state from the sample, one may determine what portion comes from the fuel nozzle. The mole fraction of the gas in this "regenerated" sample is called C. As the surrounding atmosphere contains no fuel,

$$C=m_{\text{fuel}}\,(1+a_0) \tag{13.16}$$

where m_{fuel} is the mole fraction of the fuel in the "regenerated" sample and a_0 is the ratio of the moles of air to moles of fuel in the nozzle. The equation of diffusion is similar to Eq. (13.1).

A dimensionless concentration C_f is defined as

$$C_f=\frac{1+a_0}{1+a_t} \tag{13.17}$$

where a_t is the ratio of mole of air to mole of fuel at flame boundary i.e., $(m_{\text{air}}/m_{\text{fuel}})_{\text{state}}=a_t$, because at flame boundary, the fuel and air are in stoichiometric ratio.

The value of C at any point along the axis is C_m. At the flame tip $C_m=C_f$ at fuel jet C or $C_m=1$, and at an infinite distance from the fuel nozzle it will be zero.

Another dimensionless time parameter θ is defined as

$$\theta=\frac{4\,D\,t}{d^2} \tag{13.18}$$

where t is the time for the gas to flow from the nozzle to the point where $C=C_m$. The solution of Eq. (13.12) is

$$C_m=1-e^{-\theta/4} \tag{13.19}$$

The value of θ at the flame tip is θ_f corresponding to C_f. From Eqs. (13.17) and (13.19)

$$\theta_f=4\ln(1+a_0)/(1+a_t) \tag{13.20}$$

θ_f or the actual time of flow, t_f to the flame tip is correlated with the flame length L by the equation

$$\theta_f = 4\, dt_f/d^2 = \left(\frac{4\,D}{d^2}\right)\int_0^{t_f} dt$$

or
$$\theta_f = \frac{4\,D}{d^2}\int_0^{x}\frac{dx}{U} \tag{13.21}$$

where U is the gas velocity at distance x from the nozzle.

If U is considered constant, Eq. (13.21) can be readily integrated and the flame length now becomes

$$L = \frac{Ud^2\theta_f}{4d} = \frac{V.\theta_f}{\pi D} \tag{13.22}$$

This equation is similar to the proportionality Eq. (13.2) for small flames. For long flames, this equation is not applicable as the assumption of constant U is not valid for long flames.

Wohl, Gazley, and Kapp[5] further simplified Eq. (13.22) by expanding (Eq. 13.19) for the condition at the flame tip, i.e., $C_m = C_f$, $\theta = \theta_f$ and neglecting higher order terms

$$C_f = \frac{1}{4\,\theta_f} \tag{13.23}$$

Therefore Eq. (13.22) may be approximately written as

$$L = \frac{V}{4\pi\, C_f D} \tag{13.24}$$

The above theoretical treatment of diffusion flame considers the reaction zone to be thin. However, in actual practice, the reaction takes place in a thick zone. If the reaction zone is thin, then apart from the diffusional effect, the reaction rate will also govern the rate of fuel consumption.

13.3 THEORY OF TURBULENT DIFFUSION FLAMES

The behaviour of turbulent diffusion flame is explained by two different approaches. In the first approach, the theoretical treatment is the same as for the laminar case, only the molecular diffusion coefficient is replaced by the turbulent eddy diffusivity. In the second approach, the equation for the mixing of turbulent jet is used.

Wohl, Gazley, and Kapp[5] used the turbulent eddy diffusivity instead of the laminar diffusion coefficient. As already discussed in the proportionality Eq. (13.3) for turbulent flame, the eddy diffusivity is defined as the product of mixing length l_1 and intensity of turbulence u'. For fully

developed flow, the maximum value of l_1 occurs at the axis of the burner tube. According to Dryden, the maximum value of l_1 at the axis of the tube is equal to 0.085 d, and the value of $u' = 0.03\ U$. Therefore, the eddy diffusivity ε_m at the axis will be given by

$$\varepsilon_m = l_1 u' = 0.00255\ Ud \tag{13.25}$$

For the flow with a flame on the tube, the value of eddy may change slightly. Wohl *et al.* used the following expression:

$$\varepsilon = 0.00255\, f\, U_0\, d \tag{13.26}$$

where f is a constant with a value near unity, U_0 is the average gas velocity at the nozzle.

Replacing D with ε in Eq. (13.24), we may write

$$L = \frac{V\theta_f}{\pi\varepsilon} = \frac{V\theta_f}{\pi\,(0.00255)\, f\, U_0\, d} \tag{13.27}$$

As
$$V = \frac{\pi U_0\, d^2}{4}$$

Therefore,

$$\frac{L}{d} = \frac{\theta_f}{4\,(0.00255)\, f} \tag{13.28}$$

From Eq. (13.24) we may write

$$\frac{L}{d} = \frac{1}{16\,(0.00255)\, f\, C_t} \tag{13.29}$$

where C_t is the mole fraction of the nozzle fluid at the flame tip. This corresponds to C_f of the laminar flame as defined by Eq. (13.17). At the turbulent jet, the mixture is not homogeneous and the mole fraction value of C is the time average value. Therefore, to differentiate for the turbulent flame, C_f is replaced by C_t.

For city gas, Wohl *et al.* found that

$$\frac{L}{d} = \frac{1}{0.00837\, f} \tag{13.30}$$

Equations (13.29) and (13.30) also emphasize that the height of the turbulent jet is a function of the burner diameter only and is independent of the flow velocity.

Hawthorne, Weddell, and Hottel[4] based their theory on the momentum theorem. It was assumed that the jet has a sharp boundary and that the velocity of the gas is uniform across the cross-section. Now the momentum transported per unit time through any cross-section A of the jet is $\rho U^2 A$ where ρ is the density of the fluid and U is the gas velocity in the plane A. Under steady state condition, the momentum transport through any plane is equal to the momentum of the nozzle fluid, viz., $\rho_0 U_0^2 A_0$ where subscript 0 refers to the plane of the nozzle. We have

$$\rho_0 U_0^2 A_0 = \rho U^2 A \tag{13.31}$$

The mass flowing from the nozzle per unit time is $\rho_0 U_0 A_0$ and for the constant temperature and number of moles, the amount of nozzle fluid through any cross-section in unit time is $\rho_0 CUA$ so that

$$U_0 A_0 = CUA \tag{13.32}$$

Since $A_0 = \pi d^2/4$ and $A = \pi r_b^2$ where r_b is the jet radius eliminating U/U_0 from Eqs. (13.31) and (13.32) we get

$$\frac{1}{C} = \frac{(2r_b)}{d}\sqrt{\rho_0/\rho} \tag{13.33}$$

considering the effect of density, temperature, chemical reaction and buoyancy (for vertical jets), Hawthorne *et al.*[4] gave the following relation for negligible buoyancy and for stoichoimetric ratio

$$\frac{2r_f}{d} = \frac{1}{G_i}\sqrt{\frac{T_F}{\alpha_i T_N} - (C_i + (1-C_i)\frac{M_S}{M_N}} \tag{13.3}$$

where r_f refers to the jet radius, T_f is the adiabatic combustion temperature, T_N is the temperature at the nozzle, α_i is the ratio of the number of moles of reactants to the number of moles of combustion products for a stoichiometric mixture, and M_S and M_N are the average molecular weight of surrounding air and nozzle fluid respectively. C_i has been already defined. This treatment also corroborates the result for turbulent flames; the height is a function of the nozzle diameter and is independent of flow velocity.

13.4 CONFINED DIFFUSION JET FLAMES

Diffusion jet flames are used in blast furnaces and open hearth furnaces where the jet fuel is supplied at right angles to the flow of air or oxygen. Some of the practical jet flame systems are usually concentric tubes with a small tube for the supply of combustible gas and a larger duct for air supply. The flame in such a system is called the confined or enclosed jet system. When a jet mixes with the surrounding air, steep concentration or composition gradients make their exit very close to the nozzle. As the flow is usually turbulent, the gradients become less and within a very short distance downstream the mixture becomes homogeneous.

The mixing pattern of the fuel and air or oxidant is determined purely by diffusion, i.e., a mechanical and physical process of viscous and turbulent shear. The chemical reactions have only a secondary influence as the whole process is diffusion and mixture formation controlled unlike premixed flames which are kinetically controlled.

The profiles of velocity or velocity field may be theoretically and analytically obtained by making use of the mass, momentum, energy and species conservation equations neglecting body forces (electrical, magnetic, etc.). The temperature field is slightly displaced by the effect of combustion and consequent rise in temperature and the influence of viscosity and density. By assuming gross stoichiometric reaction the fields of temperature, velocity and composition can be determined by imposing the condition of combustion also. To summarise, the turbulent diffusion jet flames are thicker and much shorter than laminar flames and the space heating rates are considerably increased. Rummel[6] and Sawai[7] *et al.* agree that if air and fuel jets impinge on one another at right angles, the mixing is most efficient and the flame very short in an open hearth furnace.

Gunther[8] obtained a semi-empirical formula for free turbulent diffusion flames

$$\frac{L}{d} = 6(R+1)\left(\frac{\rho_e}{\rho_f}\right)^{1/3}$$

where R = stoichiometric air-fuel ratio
ρ_e = fuel gas density = 0.677 kg/m^3 for CH_4 at 15°C
ρ_f = flame density = 0.205 kg/m^3 for CH_4 at 1400°C
L = length of flame
d = diameter of burner orifice

Some of the values of L/d for stoichiometric fuels are given below:

Fuel gas	*L/d*
CO	76
Coke oven gas	110
City gas	136
H_2	147
C_2H_2	188
C_3H_8	296
CH_4	200

However, when turbulent flames are enclosed they are elongated due to recirculation and vitiation by burnt gases.

Figure 13.8 shows the recirculation zone in the upper half for the case of the surrounding air being less than that which can be entrained by the jet due to friction. The mass of the recirculation can be evaluated by the integral of the negative velocities. The stagnation points at N and P can be obtained by finding out the recirculated mass. The lower half of the

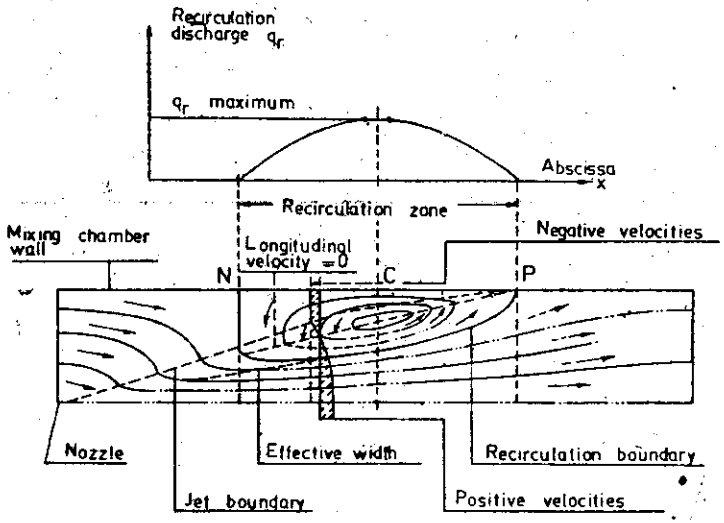

Fig. 13.8 Recirculation zone for ducted axisymmetric jet. (After Barchilon and Curtet.)

diagram shows the deflection of the stream lines when the jet issues at a low velocity.

Thring and Newby[9] used a very simple theoretical treatment assuming that the rate of entrainment of the jet is unaffected by the enclosure and the development of jet is determined by the momentum flux.

The approximate value of x_2 (the distance downstream from the nozzle at which the jet hits the wall and the duct diameter D_d) is given by $x_2 \approx 2.25\ D_d$. When the fuel issues at a very high velocity as shown in the upper half of the curve, the distance of x_1 is given by

$$x_1 \cong 2.5\ d_f \left(1 + \frac{m_a}{m_f} \right)$$

where m_a is the mass of the air entrained.

Thring and Newby by considering small scale mixing models suggested that the density differences can be compensated if the diameter of the nozzle part is modified by the effective diameter

$$d_e = d_f \left(\frac{\rho_f}{\rho_a} \right)^n$$

where $n = 0.5$ for a cylindrical jet
$= 1.0$ for a plane jet

If $\rho_f > \rho_a$, the mixing pattern is lengthened since the velocity and concentration depend on $\frac{x}{d_e}$ rather than $\frac{x}{d_f}$ where x is the axial distance from the nozzle.

Thring and Newby treated primary and secondary flows as a single jet and introducing a parameter θ

$$\theta = \frac{d_e}{D_d} \left(\frac{\rho_f}{\rho_a} \right)^{1/2}$$

where D_d=duct diameter, obtained a relation

$$x_1 = \frac{D_d}{2} \left(2.925 + \frac{\theta}{0.32} \right)$$

Craya and Curtet[10] developed a theory based on Reynolds equation and continuity equation and obtained a similar straight line relationship based on a different parameter showing the same trend. They proposed a modified Thring-Newby parameter θ'.

$$\theta' = \left(\frac{m_a + m_f}{m_f} \right) \left(\frac{d_f}{D_d} \right) \left(\frac{\rho_f}{\rho_a} \right)^{1/2} \text{ and } \frac{m_f}{m_f + m_a} = \frac{0.47}{\theta'} - 0.5$$

The position of points N and C is given by

$$X_N = 6.25\theta' \left(\frac{D_d}{2} \right)$$

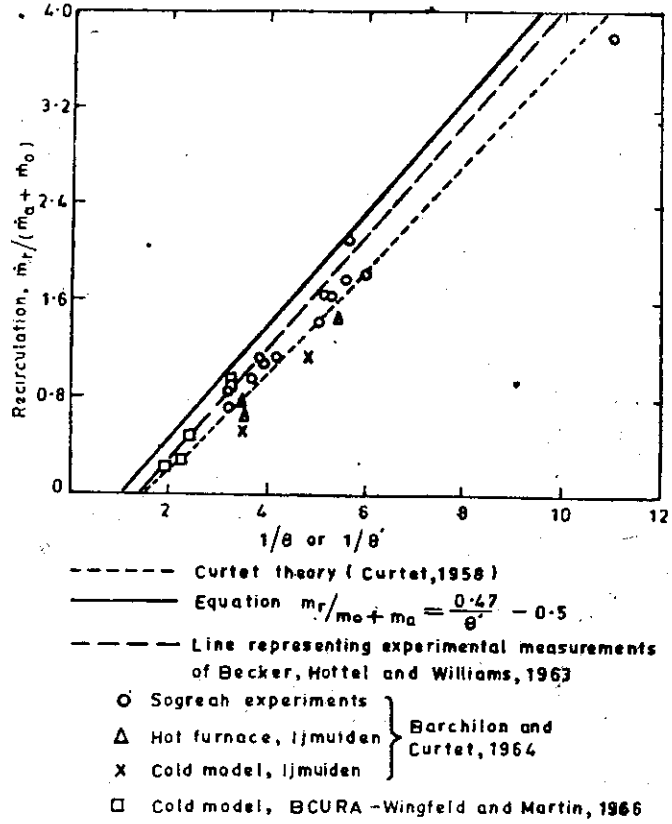

Fig. 13.9 Confined: Maximum quantity of recirculation.

$$X_C = 3.12(\theta' + 0.94)\left(\frac{D_g}{2}\right)$$

The relationship between recirculation and the parameter $\frac{1}{\theta}$ or $\frac{1}{\theta'}$ is shown in the graph to be a straight line (Fig. 13.9).

Eickhoff and Lenz[11] have shown that the free turbulent flame when confined in an enclosure increases as a result of recirculation and depletion of the oxygen concentration in the gas entrained by the jet. Confinement not only increases the length of the flame but also widens the flame. The relationship between the ratio of enclosed to free jet combustion lengths and the reciprocal of recirculation parameter θ (Thring-Newby number) as shown in Fig. 13.10 is linear.

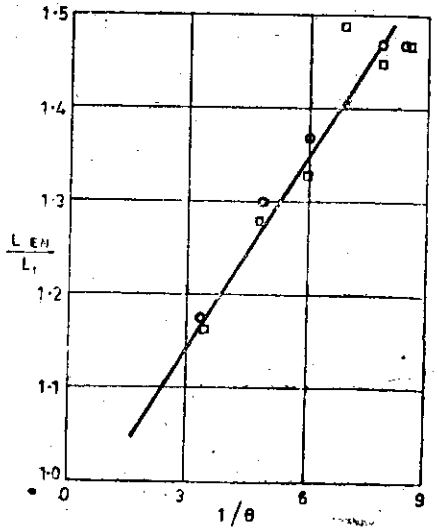

Fig. 13.10 **Relationship between the ratio of enclosed to free jet combustion lengths and the reciprocal of Thring-Newby recirculation parameter. (After Eickhoff and Lenze.)**

REFERENCES

1. S.P. Burke, and T.E.W. Schumann, *Ind. and Eng. Chem.*, 1928, 20 (10): 998-1004.
2. John Barr, *Fourth Symposium (International) on Combustion*, Williams and Wilkins, Baltimore, 1953, 765-771.
3. H.C. Hottel, and W.R. Hawthorne, *Third Symposium on Combustion and Flame and Explosion Phenomena*, Williams and Wilkins, Baltimore, 1949, 254-266.
4. W.R. Hawthorne, D.S. Weddell, and H.C. Hottel, *Third Symposium on Combustion and Flame and Explosion Phenomena*, Williams and Wilkins, Baltimore, 1949, 266-288.
5. K. Wohl, C. Gazley, and N. Kapp, *Third Symposium on Combustion and Flame and Explosion Phenomena*, Williams and Wilkins, Baltimore, 1949, 288-300.

6. Rummel, K., *Arch. Eserihuttenw.*, 1938, pp. 11, 67, 113, 163, 215.
7. Sawai, I., Kunugi, M., and Jinno, H., "Turbulent diffusion flames", *Fourth Symposium International on Combustion*, 1953, p. 805.
8. Gunther, R., *Gaswarme*, 1966, 15, p. 376.
9. Thring, M.W. and Newby, M.P., "Combustion length of enclosed turbulent jet flames", *Fourth Symposium International on Combustion*, Williams and Wilkins, Baltimore, 1953, pp. 789-96.
10. Craya, A. and Curtet, R., *Compt. Rend*, 1955, 241 (1): 621-2.
11. Eickhoff, H. and Lenze, B., "Basic form of jet flames", *Chem. Ing. Tehn.*, 1969, 41: 1059-9.

14

DETONATION WAVES IN GASES

In the case of normal flame propagation, the flame front propagates at relatively low velocities and its rate can be completely determined by the properties of the combustible mixtures. Under certain conditions many explosive gas mixtures propagate flames at speeds of the order of 2000 to 3500 m/s. These flames travel at speeds much faster than the velocity of sound at ordinary pressures and temperatures and are termed detonation waves. The rate of flame propagation can be considered as a physico-chemical constant in two typical cases of flame propagation, viz., normal or slow combustion (deflagration) and detonation. The rate of laminar flame propagation is related to the study of the properties and behaviour of various combustible mixtures, the kinetics of combustion reactions, etc. The theory of detonation waves is related to the study of explosions and explosives, etc. The theory of shocks and detonation waves in gases is mainly based on the work of Chapman[1], Jouguet[2], and Becker[3]. Before discussing detonation waves, we shall briefly review the way in which a shock wave is formed.

14.1 SHOCK WAVE

Consider a long tube closed at the left end by a piston as shown in Fig. 14.1. The steady acceleration of the piston to the right is approximated by a series of instantaneous increases of speed occurring at equal intervals of time t. The piston travels at uniform speed between each pair of impulsive accelerations. Each of these generates a pressure pulse in the gas ahead, which travels with the local speed of sound. But the masses near the piston (such as a) have forward motions greater than those farther from the piston. Moreover, since each pulse must heat the gas adiabatically, the masses nearer the piston have greater sound

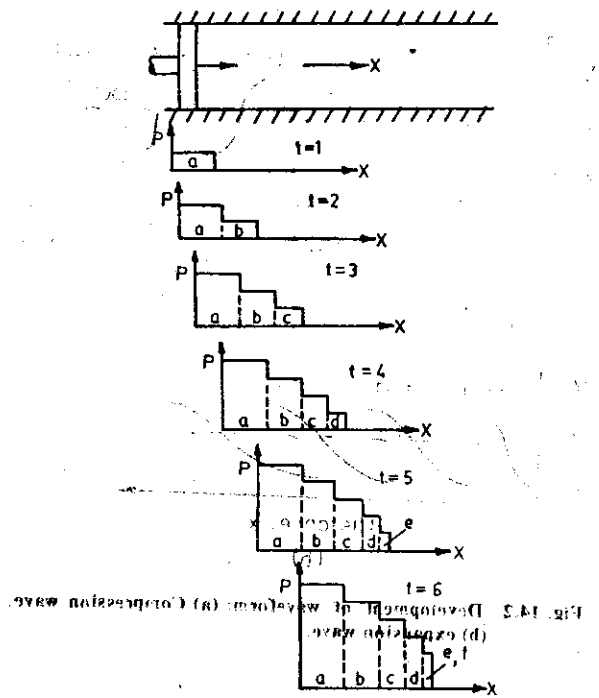

Fig. 14.1 Formation of a shock wave in a tube closed at the left end by a piston.

velocities due to the higher temperatures and pressures. Thus the pressure pulses nearer the piston tend to overtake those farther from it. Consequently, the wave form becomes increasingly steeper until finally the pressure gradient becomes infinite at $t=6$, and a small compression shock is formed which grows in strength as the process continues (Fig. 14.2(a)).

In a similar way it can be shown that if the piston is moved to the left, an expansion wave would be formed at the face of the piston, and the expansion waves become less steep with the passage of time. Thus, we can say that due to the non-linearity of the finite wave motion, compression waves become steeper and finally form a discontinuity, whereas expansion waves spread out and, therefore, are unable to support a discontinuity (Fig. 14.2(b)).

After the piston has accelerated to a constant speed and then has started moving with constant velocity (say W), a column of gas of ever increasing length is formed which gets pushed ahead of the piston at

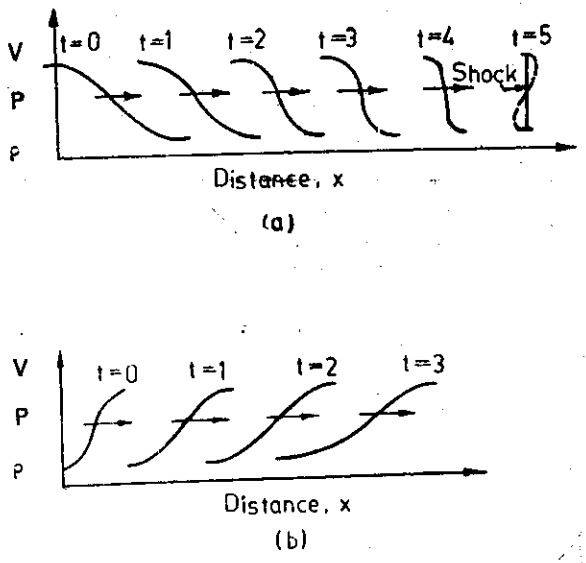

Fig. 14.2 Development of waveform: (a) Compression wave, (b) expansion wave.

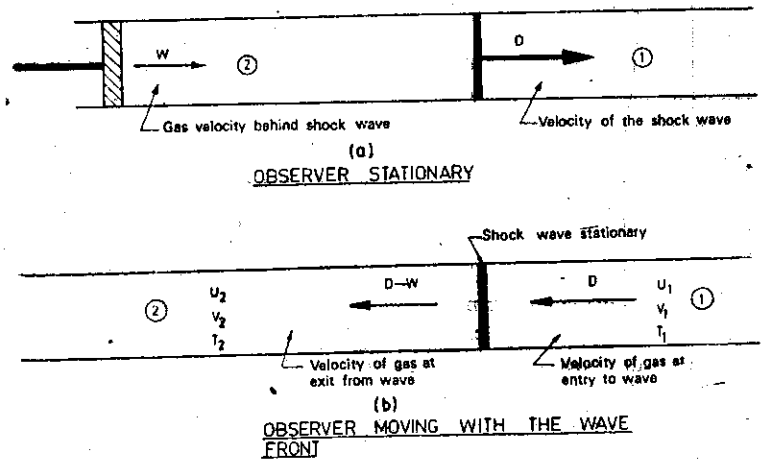

Fig. 14.3 Description of a shock wave.

the same velocity W. The head of this column is a shock wave, travelling at a constant, but greater velocity D than the column of the gas behind it, as shown in Figure 14.3(a). Figure 14.3(b) shows a coordinate system moving with the front. As the shock wave is considered stationary, the application of the mass, momentum, and energy equations for a unit mass of gas passing through a unit area leads to the following expressions.

Conservation of mass: $$\frac{u_1}{v_1} = \frac{u_2}{v_2} \tag{14.1}$$

Conservation of momentum: $$\frac{u_1^2}{v_1} + p_1 = \frac{u_2^2}{v_2} + p_2 \tag{14.2}$$

Conservation of energy: $$E_1 + \frac{u_1^2}{2} + p_1 v_1 = E_2 + \frac{u_2^2}{2} + p_2 v_2 \tag{14.3}$$

where u_1 and u_2 = velocities of gas at entry to and exit from the wave front in planes (1) and (2) respectively

E_1 and E_2 = internal energies of the unit of mass before and after passage through the wave

p_1 and p_2 = pressure of the gas before and after compression

v_1 and v_2 = specific volume of the gas before and after compression.

From Eqs. (14.1) and (14.2),

$$p_2 - p_1 = \frac{u_1^2}{v_1} - \frac{u_2^2}{v_2}$$

$$= \frac{u_1^2}{v_1^2}\left(v_1 - \frac{v_1^2}{u_1^2} \cdot \frac{u_2^2}{v_2}\right)$$

$$= \frac{u_1^2}{v_1^2}(v_1 - v_2)$$

Therefore, $$u_1^2 = \frac{v_1^2 (p_2 - p_1)}{(v_1 - v_2)} \tag{14.4}$$

Similarly, $$u_2^2 = \frac{v_2^2 (p_2 - p_1)}{(v_1 - v_2)} \tag{14.5}$$

Substituting values of u_1^2 and u_2^2 from Eqs. (14.4) and (14.5) into Eq. (14.3), we have

$$E_2 - E_1 = \frac{u_1^2 - u_2^2}{2} + p_1v_1 - p_2v_2$$

$$= \frac{1}{2} \cdot \left(\frac{p_2 - p_1}{v_1 - v_2}\right) \cdot \left(v_1^2 - v_2^2\right) + p_1v_1 - p_2v_2$$

$$= \frac{1}{2}\left[p_2(v_1 - v_2) + p_1 (v_1 - v_2) \right]$$

Therefore, $E_2 - E_1 = \Delta E = \frac{1}{2} (p_1 + p_2) (v_1 - v_2)$ (14.6)

Equation (14.6) is called the Hugoniot equation which describes a curve on a p-v diagram connecting the states which can be achieved by a shock transition. The gas which enters the wave front is compressed according to Eq. (14.6) and not according to the adiabatic equation. In the case of an actual shock wave, the piston is represented by the column of compressed gas moving in the direction of the shock wave.

The velocity of propagation of the shock wave, D into the gas at rest is given by:

$$D = u_1 = v_1 \sqrt{\frac{p_2 - p_1}{v_1 - v_2}} \quad (14.7)$$

and the velocity of the gas behind the wave, W is:

$$W = D - u_2 = u_1 - u_2$$

$$= (v_1 - v_2) \sqrt{\frac{p_2 - p_1}{v_1 - v_2}} \quad (14.8)$$

The velocities D and W are quite often expressed in a dimensionless form by Mach number (M), defined as the ratio of the velocity of the wave (or gas) to the velocity of the sound in that medium.

For a perfect gas, the equation of state determines the pressure and temperature in the wave for any flow velocity W:

$$pv = nRT \quad (14.9)$$

where n = moles per unit mass of the gas

R = molar gas constant.

The energy equation is

$$\Delta E = \bar{C}_v (T_2 - T_1) \quad (14.10)$$

where $\bar{C}_v$ = average specific heat at constant volume,

T_1 and T_2 = the temperatures before and after passage through the wave.

Therefore, we have

$$p_2v_2 - p_1v_1 = R(T_2 - T_1) \quad (14.11)$$

$$\bar{C}_v (T_2 - T_1) = \frac{1}{2} (p_1 + p_2) (v_1 - v_2) \quad (14.12)$$

If $\frac{p_2}{p_1}$ is given, we can find D, W, $\frac{v_1}{v_2}$, T_2, etc., from Eqs. (14.7), (14.8), (14.11) and (14.12) as shown in Table 14.1 calculated by Becker.

TABLE 14.1 Shock Waves in Air for Different Flow Velocities (T_1=273 K)

$\frac{p_2}{p_1}$	$\frac{v_1}{v_2}$	W m/s	D m/s	T_2 (*shock wave* K)	T_2 (*adiabatic compression* K)
2	1.63	175	452	336	330
5	2.84	452	698	482	426
10	3.88	725	978	705	515
50	6.04	1795	2150	2260	794
100	7.06	2590	3020	3860	950
1000	14.3	8560	9210	19100	1710
2000	18.8	12210	12900	29000	2070

The values shown in Table 14.1 can also be found by using the normal shock tables.

For example, if $\frac{p_2}{p_1} = 2$, from normal shock tables

$M_1 = 1.36$

$M_2 = 0.7572$

$\frac{T_2}{T_1} = 1.229$

$\frac{v_1}{v_2} = 1.6202$

Also at $T_1 = 273$ K, velocity of sound, $C = 335$ m/s. Therefore,

$D = M_1C = 1.36 \times 335 = 455$ m/s

$u_2 = 0.7572 \times$ velocity of sound at $T_2 = 0.7572 \times 366 = 280$ m/s

$W = D - u_2 = 455 - 280 = 175$ m/s

$T_2 = 1.229 \times 273 = 336$ K

14.2 DETONATION WAVE

We consider here that a shock wave is travelling in a medium of combustible mixture, and the chemical reaction occurs in the wave front and goes to completion. As in the preceding section, we use (1) and (2) respectively for the planes which lie in the unburned and burned gas. Equations (14.1) to (14.3) for conservation of mass, momentum and energy remain unchanged, and consequently, Eqs. (14.6) to (14.8) also remain unchanged.

For a reactive system in which chemical equilibrium is achieved, the state p_2v_2 must also include the energy liberated by the reaction.

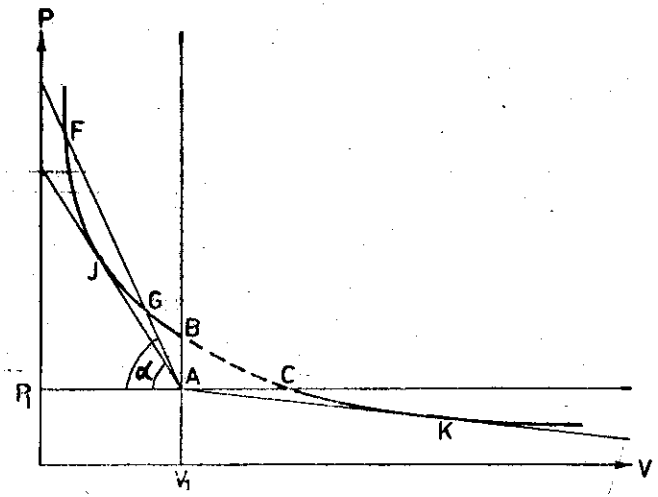

Fig. 14.4 Chapman-Jouguet analysis of combustion waves.

The Hugoniot curve as shown in Fig. 14.4 is displaced to higher values of p and v so that the point A (p_1,v_1) which represents the initial conditions does not lie on the curve. As the energy difference given by the Hugoniot curve represents only the change in the internal energy due to compression, the temperature of the gas in plane (2) has been increased due to the energy release Q in the chemical reaction. We shall, therefore, write the following equation instead of Eq. (14.10).

$$\bar{C}_v(T_2 - T_1) - Q = \frac{1}{2}(p_1 + p_2)(v_1 - v_2) \tag{14.13}$$

where $\bar{C}_v$ is the mean specific heat of burned gas at constant volume between T_1 and T_2.

If n_2 is the number of moles per unit mass of the burned gas

$$p_2v_2 = n_2RT_2 \tag{14.14}$$

Now we have only five equations, viz., (14.6), (14.7), (14.8), (14.13) and (14.14), and six unknowns: p_2, v_2, T_2, D, W, and ΔE. Hence, one additional relation is required. Later we shall consider the way in which the sixth relation is obtained. But first we consider the behaviour of the system on a p-v diagram.

For given values of p_1, v_1, and Q, we can construct a curve to satisfy Eqs. (14.13) and (14.14) as shown in Fig. 14.4 on which lie all pairs of values p_2,v_2. This is known as the Hugoniot curve. The point A (p_1, v_1) which represents the initial condition does not lie on this curve. If $Q=0$, point A will lie on the curve. We can obtain a family of Hugoniot curves or H-curves for a given initial state A and different values of Q.

In order to compute D and W, we should know in what terminal condition p_2,v_2, the gas will change. As stated above, a large number of terminal conditions are possible to satisfy Eq. (14.13). Therefore, no definite value can be assigned for D. However, this is contrary to experimental investigations.

If the gas is burned adiabatically at constant volume ($v_1=v_2$), point B will be obtained corresponding to pressure p_2. Therefore, we have $\bar{C}_v(T_2 - T_1) - Q = 0$ from Eq. (14.13), i.e., $\bar{C}_v(T_2 - T_1) = Q$. Point C corresponds to combustion at constant pressure ($p_1 = p_2$). Therefore, $\bar{C}_v(T_2 - T_1) = Q = p_1(v_1 - v_2)$. In a neutral gas, $Q = 0$ and $n_2=n_1$. Therefore, points B and C would merge with A. If α is the angle between the line FA and the abscissa, the values of D and W corresponding to any pair of values p_2, v_2 are obtained from the following equations:

$$D = v_1\sqrt{\tan\alpha} \tag{14.15}$$

$$W = (v_1 - v_2)\sqrt{\tan\alpha} \tag{14.16}$$

where $\tan\alpha = (p_2 - p_1)/(v_1 - v_2)$.

Thus if a straight line (commonly called the Rayleigh line) joining the two points, A (p_1,v_1) and some other point (p_2,v_2) on the H-curve, representing the initial and final conditions across the shock transition, is drawn, the velocities D and W can be found from the slope:

$$\tan\alpha = \frac{D^2}{v_1^2} = \frac{p_2 - p_1}{v_1 - v_2} \tag{14.17}$$

It can be seen from Fig. 14.4 that $\tan\alpha$ would be negative between points B and C on the H-curve. The value of D in Eq. (14.15) would be imaginary since $\sqrt{\tan\alpha}$ would be imaginary. Therefore, a transition from point A (p_1,v_1) to the region between B and C does not correspond to any actual process.

In the region CK, representing the lower part of the H-curve to the right of (p_1,v_1), $p_2 < p_1$ and $v_2 > v_1$. This corresponds to rarefaction, and $W = (v_1 - v_2)\sqrt{\tan\alpha}$ is negative, i.e., the burned gas no longer moves in the same direction as the wave but in the opposite direction. This part of the curve corresponds to the propagation of an ordinary combustion wave or "deflagration". Using the subscripts u and b for 1 and 2, and replacing D by S_u in Eq. (14.17) we have

$$\frac{S_u^2}{v_u^2}(p_u - p_b) = (v_u - v_b)$$

or

$$p_uS_u^2\left(\frac{p_u}{p_b} - 1\right) = p_u - p_b \tag{14.18}$$

which is the equation for normal flame propagation [see Eqs. (9.24) and (10.33)].

In the region on the H-curve from point B upwards, to the left of

(p_1,v_1), $p_2 > p_1$ and $v_2 < v_1$. This portion of the curve describes the detonation process. The point corresponding to the actual detonation would lie on this part of the curve. Here W is positive, i.e., the burned gas moves in the same direction as the flame front.

We draw a Rayleigh line from (p_1,v_1) which intersects the H-curve at two points such as F and G. This refers to two possible final states except for the tangent to the curve at J and passing through A. The state described by point J is called the *Chapman-Jouguet* (C-J) state. On decreasing the slope tan α from line AGF to tangent AJ, we see:

(i) The lower points of intersection such as G (to the right of J) move to higher pressures and lower specific volumes, and W increases.

(ii) The value of D decreases and attains a minimum value at J.

(iii) The upper points of intersection such as F (to the left of J) move to lower pressures and higher specific volumes, and W decreases.

The question is what point on the curve above B corresponds to actual detonation. Chapman proposed that this is the point of contact J. Let us consider the suggestion in detail. If we draw a reversible adiabatic through J, it can be shown that it touches the H-curve at J, whereas reversible adiabatics through other points on the H-curve intersect the curve. Therefore, the slope of the tangent A-J and that of the adiabatic through J are the same, i.e.,

$$\left(\frac{p_2 - p_1}{v_1 - v_2}\right)_J = -\left(\frac{dp}{dv}\right)_{\text{adia, J}} \tag{14.19}$$

From Eqs. (14.15) and (14.16), we have

$$D = W + v_2\sqrt{\tan\alpha}$$

At point J, therefore,

$$D = W + v_2\sqrt{-\left(\frac{dp}{dv}\right)_{\text{adia}}}$$

or
$$D = W + C \tag{14.20}$$

where C is the velocity of sound in medium 2, i.e., the burned gas. Equation (14.20) shows that the detonation velocity equals the sum of the burned gas velocity and the sound velocity in the burned gas. This is the mathematical statement of the *Chapman-Jouguet* (*C-J*) *hypothesis*. Equation (14.20) enables the prediction of detonation velocity from the thermodynamic properties of the burned gas.

At points above J toward F

$$\left(-\frac{dp}{dv}\right)_{\text{adia}} > \left(\frac{p_2 - p_1}{v_1 - v_2}\right) \tag{14.21}$$

Therefore,

$$D < (W + C) \tag{14.22}$$

At points below J toward G

$$\left(-\frac{dp}{dv}\right)_{\text{adia}} < \left(\frac{p_2 - p_1}{v_1 - v_2}\right) \tag{14.23}$$

Therefore,

$$D > (W + C) \tag{14.24}$$

An explanation of the way in which a detonation wave, corresponding to a state above J, would automatically change to state J or lower, has been given by Jouguet. A rarefaction wave, behind the detonation front, to the left of C-J state, would follow the detonation front with a velocity $(W+C)$, i.e., the sum of the sound velocity, C and the burned gas velocity W. Since at points above J, $(W+C) > D$, the rarefaction wave would overtake the detonation wave, and weaken it or slow it down. Hence, D will decrease so that the terminal state moves towards J. As shown above, since at point J, $(W+C) = D$, the rarefaction wave would not be able to overtake the detonation wave. The following considerations apply for the part of the curve below J as given by Becker. For a given value of $D = v_1\sqrt{\tan\alpha}$ or a given value of tan α, these correspond to two terminal states F and G. It is possible to show that the entropy of the gas at F is always greater than at G. The burned gas at the moment of its formation would tend to attain the state of greatest entropy. The part of the curve to the right of the C-J state would not correspond to an actual process as the gas would prefer point F and not point G. We conclude, therefore, that the detonation wave is mechanically unstable above J and thermodynamically improbable below J. Hence, the detonation wave must travel with a velocity corresponding to point J.

The picture of the detonation wave as presented above is a simplified one, and the argument in support for excluding the part of the curve below J are not considered necessary, if we assume that the chemical reaction does not instantaneously proceed to completion and, therefore, a single H-curve is not sufficient to describe the pressure and density changes in the detonation wave. As the reaction rate is finite, there is a reaction zone of finite thickness with existing temperature and pressure gradients.

A more realistic concept of the detonation wave was independently provided by Zeldovich[4], Neumann[5] and Doring[6]. They suggested that steep temperature and pressure gradients exist at the front of the detonation wave, and the conditions are similar to a shock wave travelling in a neutral gas. The fresh incoming gas is subjected to a sudden rise in pressure and temperature, which initiate the chemical reaction in the gas followed by the energy release behind the shock wave. Hence, different layers of the detonation wave represent a family of Hugoniot curves corresponding to successive fractions, ξ of the completion of chemical reaction as shown in Fig. 14.5. ξ increases from zero in the plane of unreacted gas to $\xi = 1$, in the plane of complete reaction.

As the detonation wave is a steady-state phenomenon, the various

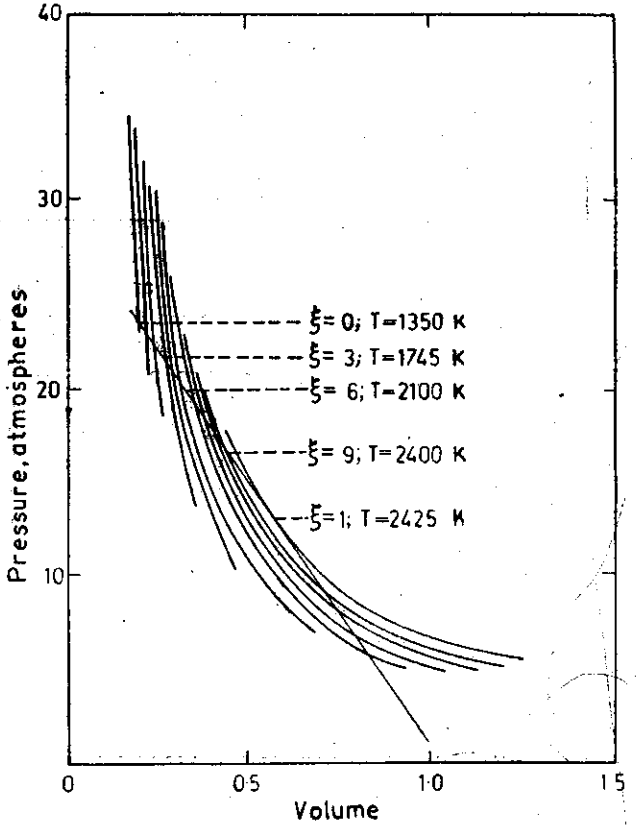

Fig. 14.5 Family of Hugoniot curves corresponding to different extents of reaction (ξ) (for 20% H_2–air).

planes move with the same velocity D. It follows, therefore, that the pressure p and volume v, at any intermediate state, is determined by the intersection of the H-curves with a straight line drawn from the initial state p_1, v_1 at the slope D^2/v_1^2. From Eq. (14.17) we have

$$p_2 = p_1 + \frac{D^2}{v_1^2}(v_1 - v_2)$$

At any of the H-curve, therefore,

$$p = p_1 + \text{const}\,(v_1 - v) \tag{14.25}$$

since $\frac{D}{v_1}$ is a constant. Equation (14.25) represents the straight lines passing through A. If the straight line through A is tangent to the curve $\xi = 1$, it intersects the curves $\xi < 1$ at two points. This shows that there are two alternate paths by which a mass element passing through the

wave from $\xi = 0$ to $\xi = 1$ may satisfy the conservation laws (14.6), (14.13) and (14.17), and also change its pressure and volume without any discontinuity with distance of travel.

Consider that the mass element enters the detonation wave through the upper sequence of (p, v) states from $\xi = 0$ and moves along the upper part of the straight line ending at $\xi = 1$. This sequence starts with a shock front capable of initiating the chemical reaction in the gas and represents the real physical process taking place in the wave. In this process, between planes corresponding to $\xi = 0$ and $\xi = 1$, p decreases, v increases and T also increases. If the mass element enters through the lower sequence of (p, v) states on the curve $\xi = 0$, and moves along the lower part of the straight line ending at the point of tangency at $\xi = 1$, then this sequence starts with the initial point (p_1, v_1) itself where no chemical reaction occurs and is, therefore, impossible. The lower points on the curve, are thus unattainable. The plane corresponding to the point of tangency J is called the Chapman-Jouguet or C-J plane. The reaction zone lies between the shock front and the C-J plane. The pressure decreases in the direction from the unburned to burned gas. Thus, the detonation wave may be visualized as a simple shock transition with a reaction zone of finite width within which the pressure decreases, volume increases, and the temperature rises.

14.3 CALCULATION OF DETONATION VELOCITY

We have considered the following system of equations on the basis of a single Hugoniot curve:

$$D = v_1\sqrt{\frac{p_2 - p_1}{v_1 - v_2}} \tag{14.7}$$

$$W = (v_1 - v_2)\sqrt{\frac{p_2 - p_1}{v_1 - v_2}} \tag{14.8}$$

$$\bar{C}_v(T_2 - T_1) - Q = \frac{1}{2}(p_1 + p_2)(v_1 - v_2) \tag{14.13}$$

$$p_2 v_2 = n_2 R T_2 \tag{14.14}$$

Also at the C-J point

$$\left(\frac{p_2 - p_1}{v_1 - v_2}\right) = -\left(\frac{dp_2}{dv_2}\right)_{\text{adia}} \tag{14.19}$$

For a reversible adiabatic compression process, we have

$$p_2 v_2^{\gamma_2} = \text{const}$$

Therefore, the differential equation is written as

$$\left(-\frac{dp_2}{dv_2}\right)_{\text{adia}} = \frac{\gamma_2 p_2}{v_2} \tag{14.26}$$

Equation (14.19) may now be written as

$$\frac{p_2 - p_1}{v_1 - v_2} = \frac{\gamma_2 p_2}{v_2} \tag{14.27}$$

The above five Eqs. (14.7), (14.8), (14.13), (14.14) and (14.27) enable us to calculate the five unknown quantities D, W, p_2, v_2 and T_2. Equation (14.7) may be re-written in the following form:

$$D^2 = v_1^2 \frac{p_2 - p_1}{v_1 - v_2}$$

or
$$D^2 = v_1^2 \gamma_2 \frac{p_2}{v_2} = \frac{v_1^2 \gamma_2 n_2 R T_2}{v_2^2}$$

or
$$D = \frac{v_1}{v_2}\sqrt{\gamma_2 n_2 R T_2} = \frac{v_1}{v_2}\sqrt{\gamma_2 p_2 v_2} \tag{14.28}$$

Equation (14.13) may be reduced to the following form:

$$\overline{C_v}(T_2 - T_1) - Q = \frac{1}{2}\left(\frac{v_1}{v_2} - 1\right)(p_1 v_1 + p_2 v_2) = \frac{1}{2}\left(\frac{v_1}{v_2} - 1\right)\left(p_1 v_1 \cdot \frac{v_2}{v_2} + p_2 v_2\right)$$

or
$$\overline{C_v}(T_2 - T_1) - Q = \frac{R}{2}\left(\frac{v_1}{v_2} - 1\right)\left(n_2 T_2 + n_1 T_1 \cdot \frac{v_2}{v_1}\right) \tag{14.29}$$

Equation (14.27) may also be re-written in the following form:

$$\frac{p_2 - p_1}{p_2} = \gamma_2 \frac{v_1 - v_2}{v_2}$$

or
$$1 - \frac{n_1 R T_1}{v_1} \cdot \frac{v_2}{n_2 R T_2} = \gamma_2\left(\frac{v_1}{v_2} - 1\right)$$

or
$$1 - \frac{v_2}{v_1} \cdot \frac{n_1 T_1}{n_2 T_2} = \gamma_2\left(\frac{v_1}{v_2}\right) - \gamma_2$$

Multiplying by $\frac{v_1}{v_2}$

$$\frac{v_1}{v_2} - \frac{n_1 T_1}{n_2 T_2} = \gamma_2 \frac{v_1^2}{v_2^2} - \gamma_2 \cdot \frac{v_1}{v_2}$$

or
$$\frac{v_1}{v_2}(1 + \gamma_2) - \gamma_2 \frac{v_1^2}{v_2^2} - \frac{n_1 T_1}{n_2 T_2} = 0$$

or
$$\left(\frac{v_1}{v_2}\right)^2 - \frac{v_1}{v_2}\left(1 + \frac{1}{\gamma_2}\right) + \frac{n_1 T_1}{\gamma_2 n_2 T_2} = 0 \tag{14.30}$$

Also Eq. (14.14) may be written as

$$\frac{p_2}{p_1} = \frac{v_1}{v_2} \cdot \frac{n_2 T_2}{n_1 T_1} \tag{14.31}$$

Equations (14.28), (14.29) and (14.30) enable us to find v_2, T_2 and D. Equations (14.8) and (14.31) can then be used to calculate p_2 and W.

It can be seen from Eq. (14.28) that the detonation velocity equals v_1/v_2 times the velocity of sound in the burned gas.

The procedure for calculating the four unknown quantities p_2, v_2, T_2, and D is as follows: The known quantities are p_1, v_1, T_1, n_1, and Q. The values of $\overline{C_v}$ and γ_2 can be calculated from the tables of thermodynamic properties. If dissociation is considered, then n_2 is different from n_1. The four unknown quantities can be determined by solving Eqs. (14.28) to (14.31) by trial and error. Assume a suitable value of T_2 and calculate the value of γ_2 at this temperature. Now substitute the values of n_1, n_2, T_1, T_2, and γ_2 in Eq. (14.30) to calculate v_1/v_2. The value of v_1/v_2 so calculated is substituted in Eq. (14.29) to determine an improved value of T_2. These trials are made till the values of v_1/v_2 and T_2 satisfy Eqs. (14.29) and (14.30). Equations (14.7) and (14.31) are then used to calculate p_2 and D. The value of the fifth unknown quantity W can be found from Eq. (14.8). The procedure becomes much more complicated if the equilibrium dissociation effects are taken into consideration. However, the results may not be affected significantly.

Lewis and Friauf[7] applied the Chapman-Jouguet theory of detonation for hydrogen-oxygen mixtures with additions of different gases and the following dissociation equilibria were considered:

$$H_2O \rightleftharpoons H_2 + \tfrac{1}{2}O_2$$

$$H_2O \rightleftharpoons \tfrac{1}{2}H_2 + OH$$

$$H_2 \rightleftharpoons 2\,H$$

The results are shown in Table 14.2.

TABLE 14.2 Comparison of Calculated and Experimental Detonation Velocities

Explosive mixture	Initial pressure, p_1 atm	Initial temperature, T_1 K	Detonation velocity, D m/s		Concentrations of burned gas, %	
			Calculated	Experimental	H_2O	H
$(2H_2 + O_2)$	18.05	333	2800	2819	25.8	6.9
$(2H_2 + O_2) + O_2$	11.4	289	2302	2314	28.5	1.8
$(2H_2 + O_2) + H_2$	11.4	289	2970	2925	13.5	0.2
$(2H_2 + O_2) + 5\,O_2$	14.13	2620	1732	1700	6.3	6.07
$(2H_2 + O_2) + 1\,N_2$	17.37	3367	2478	2407	14.7	3.3
$(2H_2 + O_2) + 3\,N_2$	15.63	3003	2029	2055	15.5	0.9
$(2H_2 + O_2) + 5\,N_2$	14.39	2685	1850	1822	15.9	0.2
$(2H_2 + O_2) + 2\,H_2$	17.28	3314	3354	3273	5.9	6.5
$(2H_2 + O_2) + 4\,H_2$	16.07	2976	3627	3527	1.2	3.0
$(2H_2 + O_2) + 6\,H_2$	14.18	2650	3749	3532	0.3	1.1

Analogous to the limits of inflammability for normal combustion waves, there exist limits of detonability for detonable mixtures. Experimental work has provided information on the limits of detonability. A number of such limits have been collected in Table 14.3[8]. In principle, detonation waves should be obtained for all combustible mixtures, but limits are imposed from chemical kinetic considerations.

TABLE 14.3 Limits of Detonability

Mixture	*Lower limit (% fuel)*	*Upper limit (% fuel)*
H_2–O_2	15	90
H_2–Air	18.3	59
CO–O_2, moist	38	90
CO–O_2, well dried	...	83
(CO+H_2)–O_2	17.2	91
(CO+H_2)–Air	19	59
NH_3–O_2	25.4	75
C_3H_8–O_2	3.2	37
i-C_4H_{10}–O_2	2.8	31
C_2H_2–O_2	3.5	92
C_2H_2–Air	4.2	50
$C_4H_{10}O$(ether)–O_2	2.6	>40
$C_4H_{10}O$–Air	2.8	4.5

For any mixture below the upper limit, the steady-state theory predicts a certain value of the detonation velocity. For example, a mixture of 5% H_2 in air, which is well below the limit of inflammability, gives a detonation velocity of 900 m/s.[9]

14.4 INITIATION OF DETONATION

Detonation waves are initiated in combustible mixtures in two ways: either by a local heat source or by a shock wave. They do not occur instantaneously. If initiation is by a shock wave, ignition takes place at some distance from the shock front, and a detonation front forms immediately which overtakes the shock front ahead. If initiation is by a local heat source, a laminar steady-state flame front develops and transition to detonation occurs at the end of a predetonation run of the flame. During the run, the combustible mixture in the tube is set in motion and turbulence develops due to friction at the wall. Turbulence leads to greater flame surface thereby causing more rapid reaction. The burning velocity increases as the unburned gas ahead of the flame is preheated and precompressed by the compression waves, generated by the mass acceleration in the combustion wave. The compression and heating of the unburned gas leads to self-ignition of the mixture and a detonation wave is formed.

Example 14.1

A steady-state explosion wave is travelling in a hydrocarbon-air mixture for which the constant pressure heat of reaction is 416 kcal/kg of mixture. The combustible mixture is initially at rest and at a temperature of 16°C and pressure of 1 atm. Assume that the friction is negligible and the properties of both the unburned and burned gas are equivalent to air in respect of specific heat and molecular weight. Determine the following: (*a*) The steady-state detonation velocity and the velocity of the burned gas and (*b*) the pressure and temperature of the burned gas.

Solution:

The two values of M_1 which correspond to the maximum flame front speed for slow combustion and the minimum for detonation are found from the following equation (which can be derived by means of equations of gas dynamics as applied to a reactive detonation wave propagating in a medium of combustible mixture):

$$\left(\frac{\Delta H}{C_p T_1}\right)_{M_2=1} = \frac{(1-M_1^2)^2}{2(\gamma+1)M_1^2}$$

The given data are: $\Delta H = 416$ kcal/kg

$$C_p = 0.24 \text{ kcal/kg °C}$$
$$T_1 = 273+16 = 289 \text{ K}$$
$$\gamma = 1.4$$

Substitution of the known values in the above equation yields:

$$\frac{416}{0.24\times 289} = \frac{(1-M_1^2)^2}{2(2.4)M_1^2}$$

Solving the equation gives

$$M_1 = 5.54 \text{ or } 0.18$$

The steady-state velocity (minimum) for detonation is given by

D = 5.54 × velocity of sound in unburned gas, C_1

$$C_1 = \sqrt{\gamma g_c R T_1} = \sqrt{1.4\times 9.81\times 29.27\times T_1}$$
$$= 20.05\sqrt{T_1}$$
$$= 20.05\sqrt{289}$$
$$= 340.85 \text{ m/s}$$

Therefore, $D = 5.54\times 340.85$

$$= 1888.31 \text{ m/s}$$
$$\simeq 1888 \text{ m/s}$$

We know at the C-J point

$D = W +$ velocity of sound in burned gas, C_2

$C_2 = \sqrt{\gamma g_c R T_2}$

To find the pressure and temperature of the burned gas, we use the Rayleigh Line tables:

At $M_1 = 5.54$, $\frac{T_1}{T^*} = 0.09346$; $\frac{P_1}{P^*} = 0.05587$

Therefore, $T^* = T_2 = \frac{289}{0.09346} = 3100$ K

$P^* = P_2 = \frac{1}{0.05587} = 17.9$ atm

Substituting the values in the expression for C_2, we have

$$C_2 = \sqrt{1.4 \times 9.81 \times 29.27 \times T_2}$$
$$= 20.05\sqrt{T_2}$$
$$= 20.05\sqrt{3100}$$
$$= 1116.32 \text{ m/s}$$
$$\simeq 1116 \text{ m/s}$$

Therefore, the velocity of burned gas, W is given by

$$W = D - C_2$$
$$= 1888 - 1116$$
$$= 772 \text{ m/s}$$

Mach number of burned gas is

$$M_2 = \frac{\text{velocity of the burned gas, } W}{\text{velocity of sound in burned gas, } C_2}$$
$$= \frac{772}{1116}$$
$$= 0.692$$

If the stagnation pressure and stagnation temperature of the burned gas (viz. P_{O_2}, T_{O_2}) are required, we use isentropic tables and values of P_2/P_{O_2} and T_2/T_{O_2} corresponding to $M_2 = 0.692$ can be obtained by interpolation. The temperature behind the shock wave travelling at the velocity of the detonation wave can be determined by the use of normal shock tables corresponding to $M_1 = 5.54$.

REFERENCES

1. D.L. Chapman, *Phil. Mag.*, 1899, 5:47, 90.
2. E. Jouguet, *J. Mathematiqué*, 1905, p. 347; 1906, p. 6.
3. R. Becker, *Z. Physik* 1922, 8: 321; *Z. Elecktrochem.*, 1936, 42: 457.
4. Ya. B. Zeldovich, *J. Exptl. Theoret. Phys.*, U.S.S.R., 1940, 10: 542.
5. J. Von. Neumann, *O.S.R.D. Rept.*, 1942, p. 549, Ballistic Research Lab. File No. X-122.
6. W. Doring, *Ann. Physik*, 1943, 43:421.
7. B. Lewis and J.B. Trianp, *J. Ann. Chem. Soc.*, 1930, 52: 3905.
8. B. Levis and G. Von Elbe, *Combustion, Flames and Explosion of Gases*, Academic Press, New York, 1961, p. 535.
9. R. Wendlandt, *Z. Physik. Chem.*, 1924, 110: 637; 1925, 116: 227.

15

IGNITION

The influences of chemical and physical factors set limits of ignition or flame propagation in fuel-air mixtures. An inflammable mixture is one which is capable of propagating a flame away from, and in the absence of, a source of ignition. That is to say, an inflammable mixture will continue to propagate a flame even after the ignition source such as a spark is removed or turned off, but a non-inflammable mixture will not.

The rate of a chemical reaction strongly depends upon the initial temperature of the combustible mixture. If the temperature of the mixture is raised slowly, it is observed that up to a certain temperature, the reaction is not noticeable, but at a critical temperature, the mixture will suddenly explode. The sudden explosion is because as the temperature of the mixture is raised, the rate of heat release is increased. If the rate of heat generation is less than the rate of heat dissipation, the chemical reaction proceeds under almost isothermal conditions, the rate being determined by the initial temperature of the mixture. However, with the increasing initial temperature, a stage may come when the rate of heat release will exceed the rate of heat dissipation. At such a stage, the mixture will start self-heating. The heating in turn will further increase the reaction rate. The cumulative effect of heating and increase in reaction rate will lead to explosion. The lowest temperature at which the heat lost from the mixture overbalanced by the heat generated by the chemical reaction is referred to as the "ignition temperature". Similarly, if the mixture is kept at a sufficiently high temperature and its pressure is raised gradually, a condition is reached when sudden explosion, i.e., ignition may occur.

A combustible mixture can be ignited in two different manners. In the first method, the whole of the mixture may be heated slowly so that its temperature is raised. In this case, at a particular temperature, the whole of the mixture will spontaneously ignite, consuming all the reactants. This process is called self-ignition. In the second method,

a small portion of the combustible mixture can be heated to a high temperature by an external heat source. In this case, the mixture near the heat source will ignite and the heat released by this burning will force the surrounding mixture to burn. Thus, a flame will start propagating from the ignition source with a determined spatial velocity of propagation. The external source of heat may be an outside flame, an incandescent body, or an electric spark, etc. This method of ignition is called "forced-ignition". Although the characteristics of the two methods are different, the foundation of the two methods of ignition is the same, i.e., heat liberation and its dissipation.

15.1 THE PROCESS OF SELF-IGNITION

N.N. Semenov[1] first proposed the thermal theory of ignition. In a combustible mixture, reacting in a vessel, the rate of a chemical reaction will depend upon the concentration of the reactants and their temperature. Because of heat generation during the reaction, the rate of reaction will differ at different locations in the vessel. Near the walls due to the heat loss, the rate of reaction and the temperature of mixture will be appreciably less than at a location far off from the wall where the concentration of the reactants will be rapidly reduced because of the higher reaction rate. Due to this non-uniformity of the reaction rate at various points, there will be transfer of mass and heat in the vessel. In general, one will have to solve two differential equations, the equation of thermal conduction and the equation of diffusion. Even in the simplest case for the reaction in an immobile medium the equations take the following form:

$$-\frac{\partial C}{\partial \tau} = \operatorname{div}\left(\frac{D}{T}\operatorname{grad} CT\right) - k_0 C^{\nu} e^{-E/RT} \tag{15.1}$$

and

$$\rho C_p \frac{\partial T}{\partial \tau} = \operatorname{div}(k \operatorname{grad} T) + Q k_0 C^{\nu} e^{-E/RT} \tag{15.2}$$

or

$$\frac{dc}{d\tau} = \frac{d}{dx}\left\{\frac{D}{T}\frac{d(CT)}{dx}\right\} - k_0 C^{\nu} e^{-E/RT} \tag{15.1}$$

and

$$\frac{dT}{d\tau} = \frac{1}{\rho C_p}\frac{d}{dx}\left(\frac{k\,dT}{dx}\right) - \frac{Q}{\rho C_p} k_0 C^{\nu} e^{-E/RT} \tag{15.2}$$

where D is the diffusion coefficient and k is the coefficient of thermal conductivity. The solution of the above non-linear system of equations is quite difficult. To simplify the analysis either the process is considered to be in steady-state or it is assumed that within the vessel there is no transfer of mass or heat, thus assuming the reaction to be taking place uniformly in the vessel.

Consider that a volume V of the gas is enclosed in a constant volume chamber, the walls of the chamber being maintained at constant tem-

perature T_0. Also assume that during the reaction the temperature of the mixture is T and is kept uniform throughout the entire volume. The temperature difference between the gas and walls is confined to a very narrow boundary near the wall, there being no mass transfer. Therefore, we may write the equations for heat generation and heat loss for the system as given below.

The rate of heat generation will be given by:

$$q_1 = QWV \text{ cal/s} \tag{15.3}$$

where Q is the heat of reaction in cal/mol

W is the reaction rate given by equation

$$W = k_0 C^\nu e^{-E/RT} \tag{15.4}$$

Therefore $$q_1 = Qk_0 C^\nu V e^{-E/RT} \tag{15.5}$$

A part of the heat generated will be lost to the surroundings and the rest will raise the temperature of the gas.

The heat lost will be given by

$$q_2 = \alpha S(T - T_0) \tag{15.6}$$

where α is the coefficient of heat transfer from the gas to the walls and S is the surface area of the vessel.

Now, to understand Semenov's method, consider Fig. 15.1 where the temperature is indicated along the x-axis and the ordinate represents the rate of heat generation or the rate of heat loss. The exponential curve q_1 represents the rate of heat generation with respect to temperature and straight lines (1), (2) and (3) represent the rate of heat loss. With an increase in the initial wall temperature, the straight line, giving the heat transfer rate, will shift to the right. The intersection of lines (1), (2) and (3) with the x-axis gives the initial temperature of the vessel walls, i.e. T_0. If we consider the initial temperature of the vessel walls to be T_0', from T_0' to T_1, the heat generated is higher than the heat lost, and the mixture gets heated. But after temperature T_1 is attained, the rate of heat loss will increase as compared to the rate of heat generation. Thus, the temperature of the mixture will be brought back to temperature T_1 and a steady-state of the reaction will be maintained, it being assumed that the concentration of the reactants remains constant. Otherwise, in actual practice, the rate of reaction will start reducing, because of the decreasing concentration of the reactant with time.

Now, if the temperature of the reaction vessel is raised to T_0, the curve (2) of heat loss will shift to its right and will remain parallel to curve (1), provided the value of α remains constant. In this case, up to temperature T_0 the mixture will be heated and an equilibrium will be attained at temperature T_b. A slight increase in the initial temperature T_0 to T_0'' will shift the curve of heat loss further to the right. Thus, the heat loss will always be less than the heat generation. Therefore, the self-heating of the mixture will lead to increasing reaction rate, and ultimately to explosion. It is necessary for a steady-state reaction that the curves of heat generation and heat loss must intersect each other. The point of turnover from steady reaction to that of explosion is given by curve (2) of heat loss, i.e., one corresponding to the wall temperature T_0' where the mixture will be in equilibrium at the temperature T_b and a slight change of temperature will lead to explosion. At this point, the rate of heat generation q_1 will be equal to the rate of heat loss q_2, and their rate of change with temperature will also be equal, i.e.,

$$dq_1/dT = dq_2/dT$$

These two conditions determine in a definite manner, the temperature T_b which specifies the boundary conditions for the ignition of the system with a given mixture and given vessel. This particular temperature is called the "ignition temperature" or the "self-ignition temperature"

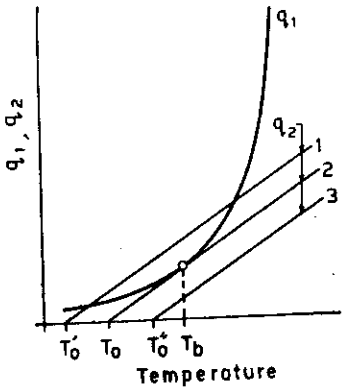

Fig. 15.1 Self-ignition temperature of a gaseous mixture.

of the gaseous mixture. From Fig. 15.1 it is clear that for a particular mixture and vessel, once the temperature of the vessel is T_0, the temperature T_b is automatically attained. Thus, the temperature which separates the steady reaction state to the explosion state is T_0. As the measurement of T_b is difficult because of the rapidly changing mixture temperature, the ignition temperature is usually defined as the lowest temperature of the vessel walls at which the explosion occurs, i.e., T_0 is the ignition temperature. It is clear that T_b will be always greater than T_0. Practically the difference between T_b and T_0 is small. Figure 15.1 corresponds to the condition of ignition at constant pressure, but varying temperature of the combustion vessel, and, consequently, that of the gas mixture.

We may also consider the condition for the change in the initial pressure of the mixture at constant initial temperature. Figure 15.2 shows one straight line q_2, i.e., the heat loss corresponding to initial temperature T_0 and three heat generation curves corresponding to three different pressures. With an increase in pressure, the mass of the mixture at constant volume of the vessel will increase, and hence the heat generation rate will also increase. Thus the heat generation curve will shift up in Fig. 15.2. At low pressure P_1, the mixture will attain

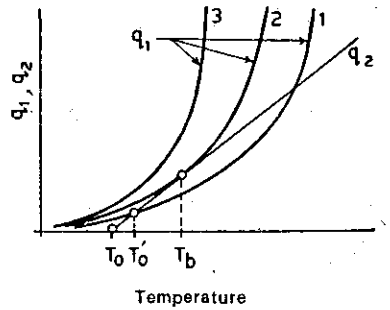

Fig. 15.2 Rate of heat generation and heat loss as a function of mixture temperature within a vessel.

a steady-state position at temperature T_0'. With increasing pressure a position will reach when T_b will attain equilibrium such that $q_1 = q_2$ and $dq_1/dT = dq_2/dT$. The ignition point is now reached at a higher pressure corresponding to P_2 and the explosion will take place immediately.

As already explained, T_0 is usually taken as the ignition temperature. The two temperatures T_0 and T_b may be related mathematically by using the condition at the critical point, i.e.,

$$q_1 = q_2 \quad \text{and} \quad \frac{dq_1}{dT} = \frac{dq_2}{dT}$$

Substituting the values of q_1 and q_2 from Eqs. (15.5) and (15.6)

$$Qk_0C^v V e^{-E/RT} = \alpha S(T_b - T_0) \tag{15.7}$$

and

$$Qk_0C^vV \frac{e^{-E/RT}}{RT_0^2/E} = \alpha S \tag{15.8}$$

Dividing Eqs. (15.7) and (15.8) we get

$$\frac{RT_b^2}{E} = T_b - T_0 \tag{15.9}$$

or

$$T_b^2 + \frac{E}{R} T_b + \frac{E}{R} T_0 = 0$$

By taking the square root, we get

$$T_b = \frac{E}{2R} \pm \sqrt{\left(\frac{E}{2R}\right)^2 - \frac{E}{R} T_0}$$

By neglecting the positive sign, which corresponds to a very high temperature and expanding the equation we get

$$T_b = \frac{E}{2R} - \frac{E}{2R}\sqrt{1 - \frac{4RT_0}{E}}$$

Taking the first three terms of the expansion and neglecting the higher terms, we have

$$T_b \simeq \frac{E}{2R} - \frac{E}{2R}\left[1 - \frac{2RT_0}{E} - \frac{2R^2T_0^2}{E^2} + \ldots\right]$$

or

$$T_b \simeq T_0 + \frac{T_0^2 R}{E}$$

or

$$T_b - T_0 = \frac{RT_0^2}{E} \tag{15.10}$$

It can be shown that the difference between T_b and T_0 is very small, i.e., for $T_0 = 600°C$ and $E = 40{,}000$ cal/mol we get $T_b - T_0 \simeq 18°C$. It is clear that if the gas temperature is increased by a very small percentage, the mixture will change from an almost no reaction state to that of the explosion state. As the ignition temperature thus defined depends upon the apparatus and the surrounding conditions, it cannot, therefore, be called a physico-chemical constant.

15.2 THE INDUCTION PERIOD OR DELAY OF IGNITION

As mentioned above, the temperature T_0 is taken as the ignition temperature while the explosion takes place at temperature T_b. It is, therefore, obvious that some time is needed before the mixture temperature becomes T_b after the vessel wall attains temperature T_0. This time will depend upon the rate of heat generation, the rate of heat loss, and upon the thermal capacity of the system. Now, the heat gained by the mixture per unit time will be the difference between the heat generated and heat lost and will be given as

$$q_1 - q_2 = Qk_0\, C^v V e^{-E/RT} - \alpha S(T - T_0) \text{ cal/s} \tag{15.11}$$

If the heat capacity of the system is $C_v V$, then the rate of temperature rise will be given as

$$\frac{dT}{d\tau} = \frac{q_1 - q_2}{C_v V} = \frac{Q}{C_v} k_0 C^v e^{-E/RT} - \frac{\alpha S}{C_v V}(T - T_0) \tag{15.12}$$

The increase in temperature of mixture with respect to time can be plotted with the help of either Fig. 15.1 or 15.2 by measuring the difference in q_1 and q_2 at different points, and identifying it with the rate of temperature rise. The curve shown in Fig. 15.3 will be obtained. The lowest curve corresponds to curve (3) of Fig. 15.1 where q_2 is always greater than q_1 and the explosion is not possible. The middle curve corresponds to the boundary condition, i.e., curve (2) of Fig. 15.1

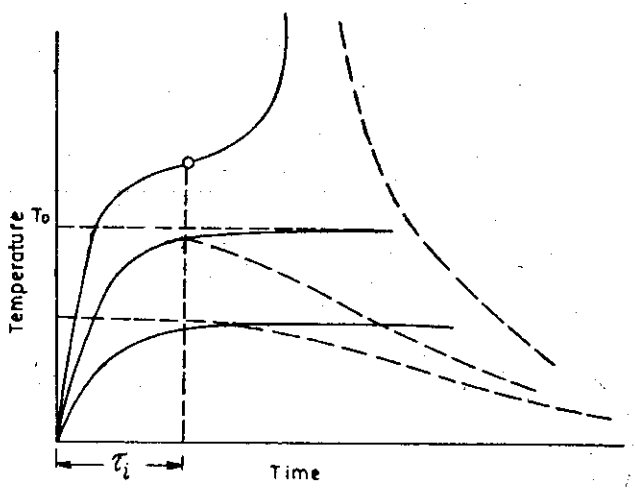

Fig. 15.3 Delay period and ignition temperature of a gaseous mixture.

when the mixture temperature approaches temperature T_0. The top curve is for the condition when $q_2 < q_1$ and when explosion takes place. In this curve, the inflexion occurs at time τ_i. This time period, when the rate of reaction starts increasing rapidly, is called the "induction period" or the "delay period".

However, this delay period is also related to the temperature of the vessel, with increasing temperature of the vessel the delay period decreases. Therefore, the value of T_0 is taken to be that temperature when the delay period is infinite, i.e., the minimum temperature of the vessel wall which will cause the explosion irrespective of the time it will take. However, for practical purposes, the value of T_0 is chosen such that the actual explosion occurs after a certain delay. It, therefore, becomes necessary to mention the delay period along with the ignition temperature T_0. The dotted curve in Fig. 15.3 corresponds to the actual condition where the rate of reaction decreases because of the reducing concentration of reactants while the solid line represents the condition for the constant concentration of reactants.

15.3 THE LIMITS OF SELF-IGNITION

It may be observed in Figs. 15.1 and 15.2 that for a particular mixture there exists a fixed value of T_b or T_0. If the concentration of fuel in the mixture or the pressure is changed, the rate of heat generation and hence the ignition temperature T_0 will change. This means that there exists a whole system of limiting conditions which determine the zones where

the explosion sets in. The limits of such zones are called explosion boundaries, explosion limits, or limits of self-ignition.

Semenov gave a mathematical treatment of the condition given in Fig. 15.2. If curve q_1 corresponds to the mixture at a certain pressure, the condition of explosion, $q_1 = q_2$ and $\frac{dq_1}{dT} = \frac{dq_2}{dT}$ leads to the relation given by Eq. (15.10), i.e.,

$$T_b = \frac{RT_0^2}{E} + T_0$$

Substitution of this value of T_b in Eq. (15.7) yields,

$$Qk_0C^vV \exp\left\{-\left[\frac{E}{RT_0\left(1+\frac{RT_0}{E}\right)}\right]\right\} = \alpha S\frac{RT_0^2}{E}$$

and since $\frac{RT_0}{E} \ll 1$, we may write

$$Qk_0C^vVe^{-E/RT_0} = \frac{\alpha SRT_0^2}{E} \tag{15.13}$$

or taking the logarithm, we get

$$\ln\frac{C^v}{T_0^2} = \frac{E}{R}\cdot\frac{1}{T_0} - \ln\frac{QVk_0E}{\alpha SR} \tag{15.14}$$

As for a bimolecular reaction $C^v \approx P^2$

Therefore,
$$\ln\frac{P_{ig}}{T_0} = \frac{E}{2RT_0} + \text{const} \tag{15.15}$$

where P_{ig} is the pressure corresponding to the critical condition of ignition. This relationship is called the Semenov equation. The equation is represented in Fig. 15.4 which shows the explosion and no-explosion zones. The same equation will give a straight line if we choose the coordinates as

$$\ln\frac{P_{ig}}{T_0} \quad \text{and} \quad \frac{1}{T_0}$$

Figure 15.4 is obtained for a fixed composition of the mixture. Similarly, we can obtain the curves giving the relationship between T_b and the composition of mixture for a constant pressure, or P_{ig} vs. composition for a fixed value of the ignition temperature T_b or T_0. Figures 15.5 and 15.6 give the nature of such curves showing the limits of ignition.

It was found that the experimental results corroborated the theoretical results in a limited number of cases. This is because in most of the cases, apart from the thermal explosion, branching chain reactions are also responsible for the change in the reaction rate. The assumption of uniform temperature distribution in the vessel by Semenov is the major

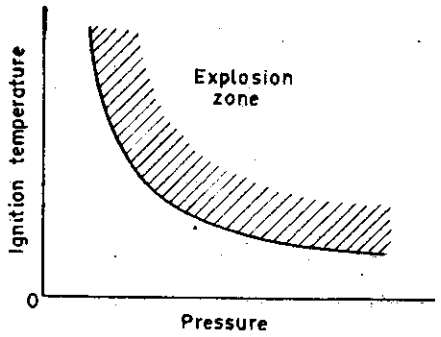

Fig. 15.4 Relation between ignition temperature and pressure of a gaseous mixture

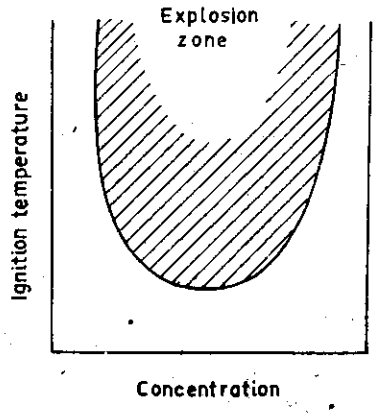

Fig. 15.5 Ignition temperature as a function of mixture concentration at constant pressure.

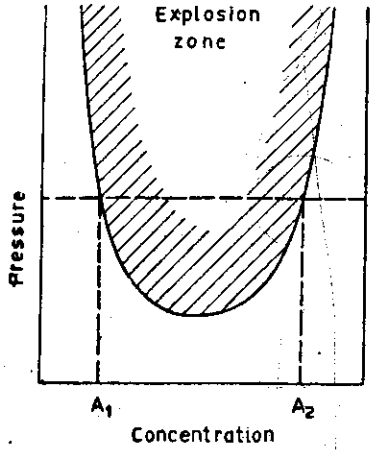

Fig. 15.6 Pressure at ignition boundary as a function of mixture concentration.

drawback of his theory. Frank-Kamenetsky[2] used the conduction Eq. (15.2), neglecting the diffusion effect for steady state:

$$\nabla^2 T + \frac{Q}{k} k_0 C^\nu e^{-E/RT} = 0 \qquad (15.16)$$

where ∇^2 is the Laplacian operator $\left(\frac{\partial}{\partial x^2}+\frac{\partial}{\partial y^2}+\frac{\partial}{\partial z^2}\right)$. The solution of the equation for various vessel geometries gives the following relation for the pre-explosion heating:

$$T_b - T_0 = 1.2 \frac{RT_0^2}{E} \text{ for plane parallel vessel}$$

$$= 1.37 \frac{RT_0^2}{E} \text{ for cylindrical vessel} \qquad (15.17)$$

$$= 1.66 \frac{RT_0^2}{E} \text{ for spherical vessel}$$

The above relations are similar to Semenov's results, only they are multiplied by some numerical constants. Frank-Kamenetsky[2] also assumed that heat is transferred only by conduction and he also neglected the effect of reducing concentration of reactants.

15.4 FORCED IGNITION

In forced ignition, a small portion of the combustible mixture is heated by an external source of heat, the heat liberated during the combustion of that small mass results in further propagation of a flame, thus burning the entire volume. The external source of heat can be any one of following: an incandescent body, a pilot flame, a shock wave, an inductive or capacitance spark, etc. Though the source of heat can vary, the ignition and propagation is because of a single factor, i.e., the heat factor. Here we shall first consider the general theory of forced ignition, and then the ignition by various sources of heat and the effect of various variables.

If we consider that a combustible mixture is brought in contact with an incandescent body or a very hot wall, the temperature of the mixture in the immediate vicinity will rise, dropping gradually away from the wall. The mixture near the wall will react and the heat liberated due to combustion will be transferred to the mixture next to the reacting zone. If the heat liberated is not sufficient, the temperature of the mixture will be reduced with increasing distance. However, if the temperature of the incandescent body or the hot wall is raised so that the mixture near it reacts to liberate sufficient quantity of heat, capable of igniting the layer adjoining it, the reaction wave may propagate in the entire mixture. The minimum temperature of the body which is able to produce a self-supporting combustion wave is called the ignition temperature. This ignition temperature is analogous in meaning to the one defined for self-ignition.

According to Zeldovich, the limiting critical ignition condition should be written in the form $\left(\frac{dT}{dn}\right)_{st} = 0$, where n is the normal to the

surface and st indicates that the gradient refers to the surface of the incandescent body. This condition also indicates that from the moment where $T = T_b$, the source no longer participates in the process, the condition in the gaseous layer, in contact with the highly heated body, becomes the determining factor. The equation governing ignition is the same as Eqs. (15.1) and (15.2), i.e., for thermal conduction and diffusion. For simplification, we can assume the process to be in steady state, i.e., if T and C are independent of time τ, the two equations can be combined into one giving a relation between T and C. For a one-dimensional problem we can write Eqs. (15.1) and (15.2) as

$$\frac{d}{dx}\left\{\frac{D}{T}\frac{d(CT)}{dx}\right\} - k_0 C^\nu e^{-E/RT} = 0 \tag{15.18}$$

and

$$\frac{d}{dx}\left(k\frac{dT}{dx}\right) + Qk_0 C^\nu e^{-E/RT} = 0 \tag{15.19}$$

since $N = \frac{\mu}{\rho} C$, where N is the relative concentration, ρ is the density of the mixture, and μ is its molecular weight.

Equation (15.18) may be written as:

$$\frac{d}{dx}\left(\frac{D}{\mu}\rho\frac{dN}{dx}\right) - k_0 C^\nu e^{-E/RT} = 0$$

Combining this with Eq. (15.19),

$$Qk_0 C^\nu e^{-E/RT} = -\frac{d}{dx}\left(k\frac{dT}{dx}\right) = Q\frac{d}{dx}\left(\frac{D\rho}{\mu}\cdot\frac{dN}{dx}\right) \tag{15.20}$$

By integrating the above equation, we have

$$k\frac{dT}{dx} = -Q\frac{D\rho}{\mu}\frac{dN}{dx} + A'$$

or

$$\frac{dT}{dx} = -\frac{Q}{k}\frac{D\rho}{\mu}\frac{dN}{dx} + A \tag{15.21}$$

Now as

$$D \approx \alpha \approx \frac{k}{C_p\rho}$$

Therefore,

$$\frac{QD\rho}{k\mu} \approx \frac{Q}{C_p\mu} \tag{15.22}$$

and this quantity can be considered constant. Thus the second integration gives

$$T = -\frac{Q}{C_p\mu} + Ax + B \tag{15.23}$$

Constants A and B can be calculated by the boundary conditions. As T must always be finite, therefore, $A = 0$ and

$$T = -\frac{Q}{C_p\mu}N + B$$

At $T = T_0$; $N = N_0$

$$\therefore \quad T - T_0 = \frac{Q}{\mu C_p}(N_0 - N) \tag{15.24}$$

If the mixture is stoichiometric and complete combustion takes place, then $T = T_b$ and $N = 0$ for the adiabatic process.

$$\frac{Q}{\mu C_p}N_0 = T_b - T_0$$

From Eq. (15.24)

$$\frac{N}{N_0} = \frac{T_b - T}{T_b - T_0} \tag{15.25}$$

Equation (15.25) gives the relation between the relative concentration of the combustible and temperature of the mixture at any point, provided there is no heat loss from the system. The concentration and temperature profiles near a hot surface are shown in Fig. 15.7. It is not necessary

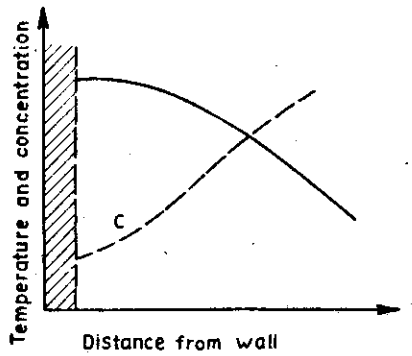

Fig. 15.7 Temperature and concentration of combustible near a heated surface.

that a flame will propagate throughout the mixture if the temperature of the incandescent body is equal to the self ignition temperature. On the contrary, in most cases, the mixure will not ignite until the body temperature is much higher than the self-ignition temperature. This is because near the solid wall the concentration of the reactant will be reduced because of the reaction, thus the mixture near the surface will react, but the flame will not propagate. The difference between the self-ignition temperature and the ignition temperature of the hot surface is much more if the hot surface is one of the catalysts. At first sight this may seem unrealistic, but because of absorption, the concentration near the surface is further reduced, thus requiring

a higher temperature of the surface for the flame to form and propagate. It is also observed that the dimensions of the incandescent bodies also play a part. A body with a larger surface area and mass will ignite the mixture at a slightly lower temperature than a smaller body. In most cases the ignition temperature is reduced linearly at a higher concentration of the fuel, though for some catalyst surfaces and some fuels, this rule does not hold true. Some fuels can give two ignition temperatures. The first one corresponds to the branching chain reactions called the low temperature of ignition. This temperature is found to be independent of the concentration of fuel. The second ignition temperature, which is much higher, corresponds to the thermal ignition. Similar to the ignition delay in the case of self-ignition, an ignition lag is observed in forced ignition. This lag is the time interval between the introduction of the hot body to the actual appearance of the flame. The higher the temperature of the incandescent body, the lower will be the ignition lag. Figure 15.8 shows the effect of ignition temperature on the ignition lag. The

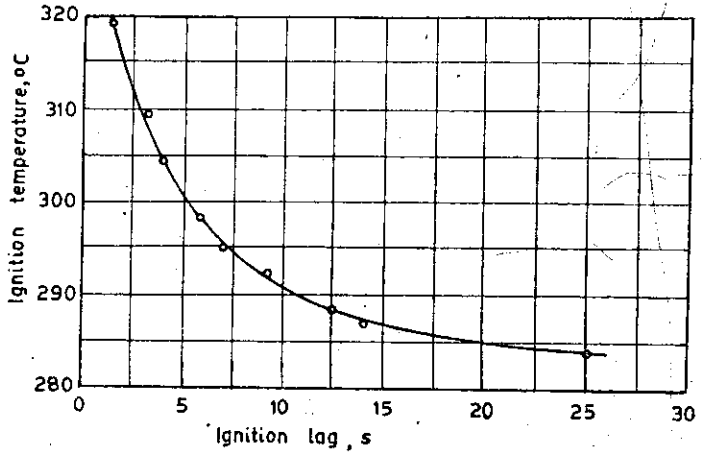

Fig. 15.8 Effect of ignition temperature on ignition lag for gasoline-oxygen mixture.

shape of the curve is hyperbolic, i.e., with lower ignition temperature the ignition lag is appreciably increased. The minimum ignition temperature can be taken as the temperature with infinite lag. But for practical purposes, it is observed that the minimum ignition temperature can be taken with a lag of few seconds and a slight change in lag will not change the ignition temperature.

It is observed that the ignition temperature is continuously reduced with increasing pressure. This is true for almost all fuels. The effect of an inert admixture is to increase the ignition temperature because of the reduced supply of oxygen to the layers near the hot surface.

Ignition by Pilot Flames

A reacting mixture can be very easily ignited with the help of a pilot flame immersed in the mixture, or brought in contact for a very short time with the help of a shutter. The ignition of mixture will depend upon the time of exposure of the flame, size of the flame, flame temperature, mixture composition, turbulence level, etc. Because of high temperature of the flames, the time required for ignition is quite low. For a slightly rich mixture of methane in air, the time taken by a 1.5 cm long flame was found to be about 0.003 to 0.004 s. By reducing the flame height from 1.5 to 1 cm, the time increased to 0.007 s. Similarly, it was observed that if the flame temperature is reduced from 1770° to 1520°C, the time required for ignition increased to nearly six-fold.[3]

Ignition by Hot Gases

This process of ignition by hot gases is one of practical importance, especially when the fuel is in the form of a fine liquid spray. If a gaseous or liquid spray is injected in a hot stationary or moving air, the fuel may ignite. The ignition will depend on many factors, namely, the temperature of hot air, air-fuel ratio just before the flame appears, rate of mixing, type of apparatus, chemical and physical state of fuel, etc. The ignition of propane by hot air was studied by Jackson *et al.*[4] Propane and air were very rapidly mixed in a chamber to avoid thermal cracking of propane before ignition. The mixture flowed through a tube where the ignition was observed with the help of a pressure pulse and photo cell and the ignition lag was measured. Figure 15.9 shows the effect of concentration of propane by volume and the temperature of hot gases on ignition lag. The graph is drawn on a log scale. The ignition lag varies from 0.3 s to as long as 8 s. It is seen that with the increasing concentration of propane, the ignition lag is reduced, and the effect of temperature is also quite predominant. The flow rate of mixture through the tube was also observed to have an appreciable effect, as with the increasing flow rate, the rate of heat transfer increased. However, the change in the diameter of tube was found to have no effect on the ignition lag. A decrease in pressure caused an increase in lag.

Ignition by Shock Waves

Not much work has been done on this aspect. However, this process of ignition has two advantages: (i) the combustion of mixture is much faster because the shock wave travels with the speed of sound, instead of the deflagration flame velocity which is much lower, and (ii) no flame holder is needed and the length of the combustion chamber is also reduced because of faster burning of the mixture.

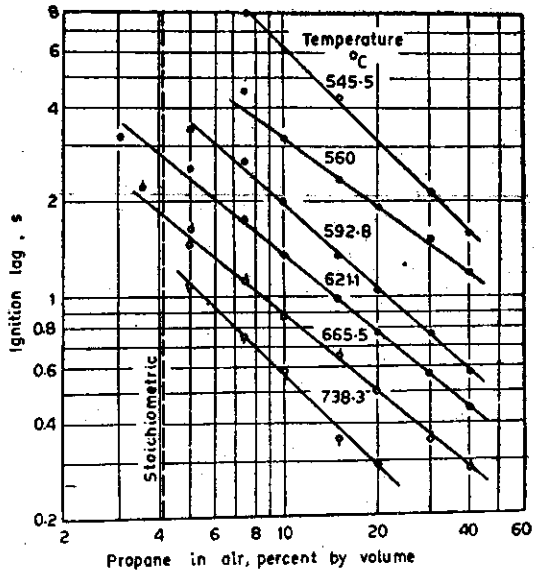

Fig. 15.9 Effect of concentration and temperature on ignition lag of propane-air mixture.

If a shock wave is travelling through a reacting mixture, the heat produced due to the compression of the mixture is sufficient to ignite the mixture. From the hydrodynamic equation it can be calculated that if the ratio of pressure behind the shock wave to the initial pressure is 50, the temperature behind the wave will be 2100°C, as compared to the temperature of 520°C obtained by the adiabatic compression by the same pressure ratio. With increasing pressure ratio, the difference in temperature by two processes also increases. At a pressure ratio of 100, the temperature by shock is about 3590°C, while by adiabatic compression it is 676°C only. In addition, the shock wave contains free atoms and radicals that can promote rapid chemical reaction. It has been observed that the mixture can be ignited by a very weak shock, provided the mixture ratio is within the limits of detonability.

Ignition by Spark

Ignition by means of electric spark is the most widely used mode of ignition. The spark may be an inductive spark or capacitance spark. Both the modes of spark ignition can produce a very high temperature in a small zone and can be treated as a small incandescent gaseous body. The main difference between inductive and capacitance sparks is that in the inductive spark the duration of the spark is long and the current

is low. The spectrum of the spark corresponds to the vapour of the metal electrode. It is produced by opening an inductive circuit of high impedance. The capacitance spark is produced by the discharge of charged condensers into the gas. The duration of the spark is extremely short (0.01 to 100 μs) depending upon the amount of energy released. The current of the capacitance spark is high because of the low impedance of the circuit, and its spectrum corresponds to the spectrum of gas. The duration of the spark may be increased by adding a resistance in the circuit. The energy released by the capacitance spark may be written as

$$E_c = \tfrac{1}{2} C \left(V_2^2 - V_1^2 \right) \tag{15.26}$$

where E_c = energy obtained from the capacitance, J
C = capacitance of the condenser, F
V_2 = voltage on the condenser just before the spark occurs, V
V_1 = voltage remaining on the condenser at the instant spark ceases, V

The above equation does not consider the losses in the circuit. Thus the actual energy released across the spark gap will be slightly less. Unless the system used is of very low voltage, V_1 can be neglected as it is usually quite low as compared to V_2. The energy stored in an inductance is given as

$$E_L = \tfrac{1}{2} L i^2 \tag{15.27}$$

where E_L = energy, J
L = Inductance, H
i = current in the circuit at the instant of sparking, A

Most workers have used the measurement of energy in the primary circuit as a measure of the energy released. This does not give the actual energy released across the gap.

Two theories were proposed for the mechanism of spark ignition: the ionic theory by V. Thornton, and the thermal theory by Taylor, Jones and Morgan. The ionic theory supported the experimental observation that the ignition ability of the spark is proportional to the intensity of current, instead of the square of the current if the ignition is assumed to take place because of heat release. It was observed by Thornton and also by Finch that the reaction at the discharge was directly proportional to the number of ions reaching the cathode in a given time. However, Holm has shown that Finch's results do not contradict the thermal theory if it is considered that during discharge the potential does not change. Many other observations, e.g., the effect of spark gap

and diameter of spark points, etc., also corroborate the thermal nature of spark ignition as predicted by the thermal theory of an incandescent body.

If a spark is passed through a gap in a reacting mixture, a small volume of the mixture will burn, but it is not necessary that the flame will propagate throughout the entire mixture. The ignition of the mixture will depend upon the properties of the mixture, that of spark electrodes and upon the strength or intensity of the spark. It is quite possible to pass a weak spark through a combustible mixture without igniting it.

Lewis and Von Elbe applied the flame stretch concept to give the minimum volume or diameter of the spherical volume that should be burned by the spark so that the whole mixture will ignite. When a spark is passed, a small volume of the mixture is heated to a very high temperature. Immediately, after the spark ceases, the temperature of this volume starts decreasing due to heat dissipation to the adjoining layers of the gas. This heat raises the temperature of the surrounding layers, where the mixture reacts because of high temperature to release further heat. The propagation of this combustion wave very rapidly assumes a spherical shape. Whether the wave propagates to the entire volume of the mixture or not, depends upon the size of this spherical volume at the time when the temperature at the origin has decreased to the order of the flame temperature. If the diameter of this volume is sufficiently large so as to give a temperature gradient between the burned gas in the core to the unburned gas, less than or equal to the gradient in a steady-state wave, the flame will propagate further. If by this time the volume is quite less or the gradient is steep, then the amount of heat dissipation to the outer layer will be much more than the heat generated due to the combustion of the spherical layer resulting in the quenching of the combustion wave. Thus a minimum amount of energy must be released during the spark so that the heat liberated must be sufficient to produce a steady combustion wave.

If we consider a sphere of burned gas which has a diameter d surrounded by a shell of unburned gas of thickness η_0 as shown in Fig. 15.10(a) we can calculate the effect of the flame stretch. Figure 15.10(b) represents the size of a spherical shell after the flame has passed over the thickness η_0. The width of the shell can now be approximately represented as $\eta_0 (\rho_u/\rho_b)$ where ρ_u and ρ_b respectively represent the unburned and burned gas densities. Taking η_0 to be small as compared to d, the ratio of the spherical surface before and after burning will be

$$1+4\,(\eta_0/d)\,(\rho_u/\rho_b)$$

so that the stretch factor K becomes

$$K = 4\frac{\eta_0}{d}\,\frac{\rho_u}{\rho_b} \tag{15.28}$$

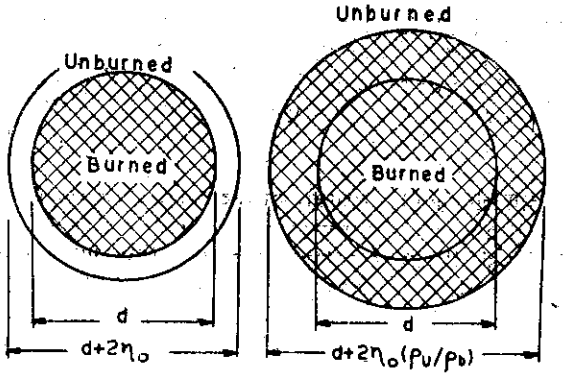

Fig. 15.10 Increase of flame diameter over distance η_0 in the urburned gas (with permission of Academic Press, from B. Lewis and G. Von Elbe: *Combustion, Flames and Explosions of Gases*, 1961, p. 336.)

For minimum ignition energy, d will give the critical minimum diameter. In the above expression, d is identified with the experimental quenching distance that has been determined by separating the spark electrodes to the point of lowest value of the minimum ignition energy. η_0 is calculated from the following expression

$$\eta_0 = \frac{K}{C_p \rho_u S_u} \tag{15.29}$$

ρ_u, C_p, S_u, etc. can be obtained from literature, and the value of K can be calculated.

Lewis and Von Elbe calculated the value of K for various mixtures of fuel-air and fuel-oxygen and found it to mostly vary between 0.5 and 0.1. They also compared the values of experimentally determined ignition energy H with the theoretical amount of excess energy in the small volume given by two different methods, one given by the volume integral of the total heat represented by, say H', such that

$$H' = \frac{\pi}{6}\, d^3 C_p \rho_b\, (T_b - T_u) \tag{15.30}$$

and the second by the volume integral of the calculated heat, say H'' given as

$$H'' = \pi\, d^2 \frac{K}{S_u}\, (T_b - T_u) \tag{15.31}$$

They compared the values of H/H', H/H'' and H''/H', though it should be expected that H' should always be greater than H'', but it was found that for lean mixtures of hydrogen and methane and rich mixtures of propane, H'' was greater than H'. They explained that as hydrogen and methane have higher diffusivity than oxygen, and oxygen has higher diffusivity than propane, therefore, H'' increases more gradually than H', as the more rapidly diffusing mixture component is

made stoichiometrically increasingly deficient. The reason they assigned is that the value of S_u used in the expression is found for a plane wave whereas in the above case the surface is curved. The strongly curved minimal flames are richer in the deficient component than in a plane combustion wave, and the burning velocities used for computing H'' are too low resulting in high values of H'' and η_0. If the effect of the preferential diffusion and curvature of the flame is considered, then it is expected to give a consistent value of H''/H', and this may be used as an approximate similarity constant for correlating minimal flame diameters in the same way as the stretch factor K can be related to the ratio H''/H' by Eqs. (15.28), (15.29), (15.30) and (15.31) which give

$$\frac{H''}{H'} = \frac{6\,k}{dC_p\rho_u S_u} = (6\eta_0/4)\ (\rho_u/\rho_0) = 1.5\ K \qquad (15.32)$$

The experimental value of H is always much lower than H' and H'', because the small volume of the gas receives heat from the chemical reaction and the ignition source.

Apart from the heat conducted to the unburned gas, the mixture in the small volume is cooled because of the heat conducted to the electrodes. Watson has shown that for a large capacitance spark in argon, a fair amount of energy is lost in the form of a shock wave produced at the spark gap. This energy loss can be reduced for a long duration capacitance spark by adding a resistance in the circuit.

Similarly the experimental values of the minimum ignition energy can be reduced by changing the shape and material of the electrode.

Now we shall consider the effects of various variables on ignition energy.

15.5 FACTORS AFFECTING IGNITION ENERGY

Effect of Mixture Composition

It has already been mentioned that a combustible mixture may or may not ignite by passing a spark. Thus, for every combustible mixture there is a fixed value of ignition energy below which the flame will not propagate. If we consider the mixture of a particular fuel with air or oxygen and plot the minimum ignition energy for various compositions, a plot as shown in Fig. 15.11 will be obtained. For a particular value of the ignition current there will be two values of limiting mixture compositions. Above and below these values the mixture will not ignite. It can be observed from the figure that with increasing value of ignition energy these limits do not vary much. Thus a very high value of energy will not be able to ignite a very lean or rich mixture. Such limits of concentration, as already defined, are known as the limits of flammability or the limits of forced ignition.

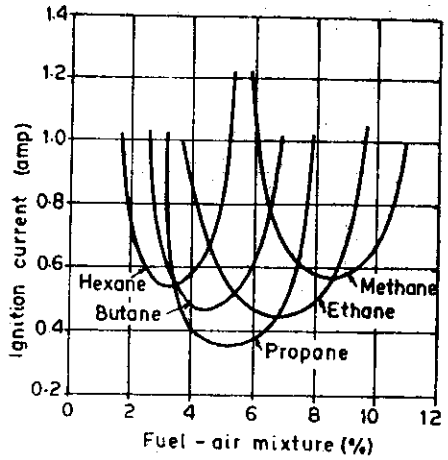

Fig. 15.11 Minimum spark intensity for ignition as a function of mixture composition.

Now as the value of ignition energy rises asymptotically, it can be said that there exists a value of the spark energy above which the limit of ignition does not change. This spark is usually known as the saturation spark. It should be further noted that a minimum spark energy is needed to ignite a fuel-oxidant mixture which has a composition slightly richer than the stoichiometric composition.

Effect of Electrode Type

Electrode size, spacing, and materials affect the amount of minimum ignition energy, because the quenching effect of the solid surface of the electrode reduces the reaction rate near the solid surface. It has been observed that the minimum ignition energy is reduced by increasing the gap between the two electrodes. Figure 15.12 shows the effect of electrode spacing on the minimum ignition energy. Two different types of electrodes were used, one of 0.159 cm (1/16") stainless steel wire and the second flanged by two glass discs of 2.54 cm diameter at the tips.

For the flanged electrodes it was observed that below a particular distance there was a sudden rise in ignition energy, indicating that below this distance ignition by flanged electrodes is impossible. This is because of the quenching effect of the flanges. This minimum distance is known as the quenching distance. It was further observed that the material of the flanges has no effect on this minimum distance, the flange may be of any metal or insulating material.

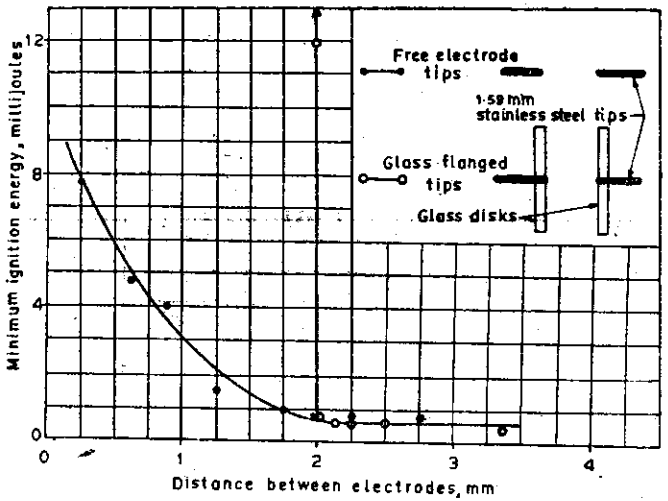

Fig. 15.12 **Minimum ignition energies for free and flanged electrode tips as function of electrode distance (with permission of the American Institution of Physics from *Journal of Chemical and Physics*, Nov. 1947, 15:(11).**

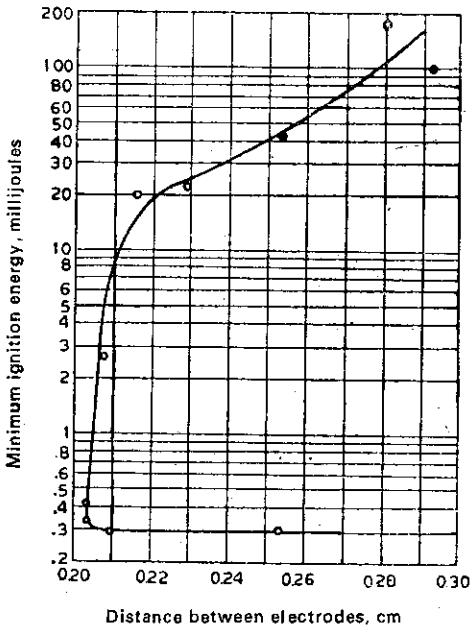

Fig. 15.13 **Increase of quenching distance at large spark energies of plate electrodes, 8.5% methane in methane-air mixture (with permission from *J. Chem. Phys.*, op. cit., 11).**

In contrast to the sudden rise of ignition energy given by the flanged electrodes, the rise in ignition energy was found to be gradual when the gap of the unflanged electrodes was reduced. This showed that the quenching effect of the small tip surface can be compensated by the increased supply of energy. At a distance more than the quenching distance, the two electrodes behave in similar fashion. Another interesting result of electrode spacing versus ignition energy is shown in Fig. 15.13. It is seen that if the energy supplied is very high, the quenching distance increases instead of decreasing in the case of flanged electrodes. This effect is explained as follows: due to the very high ignition energy, turbulence is generated between the electrode gas which increases the heat transfer, thereby requiring more energy. In general, for a short duration capacitance discharge, electrode materials are found

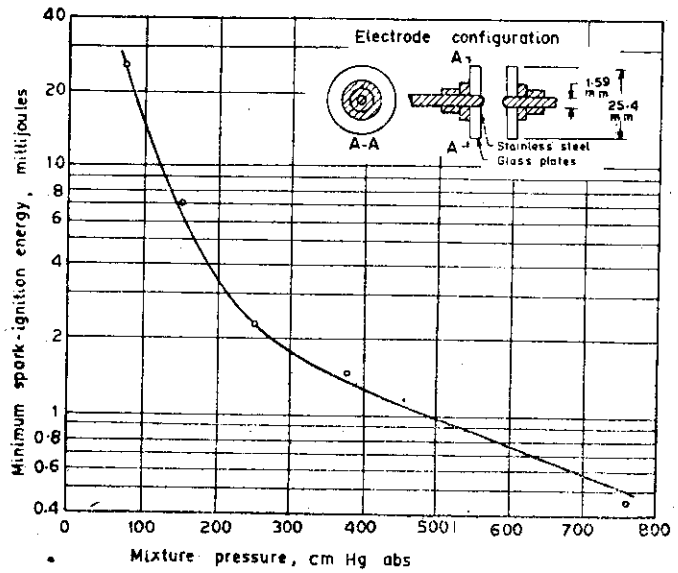

Fig. 15.14 **Effect of pressure on minimum ignition energy for flanged electrodes (with permission from *J. Chem. Phys*, op. cit., 11).**

to have no significant effect on the minimum ignition energy. However, C.C. Swett found that for a long duration capacitance discharge, stainless steel electrodes, which produces a glow discharge, had ignition energies 50% higher than cadmium electrodes, which produce a discharge starting as an arc discharge and changing to glow discharge. The electrode materials were found to have no effect for glow discharge

Effect of Pressure

Pressure has been found to have a pronounced effect on the ignition energy. In general, the minimum ignition energy increases with decreasing pressure. For most fuels the energy approximately varies as the second power of pressure. Below a certain pressure called the "minimum

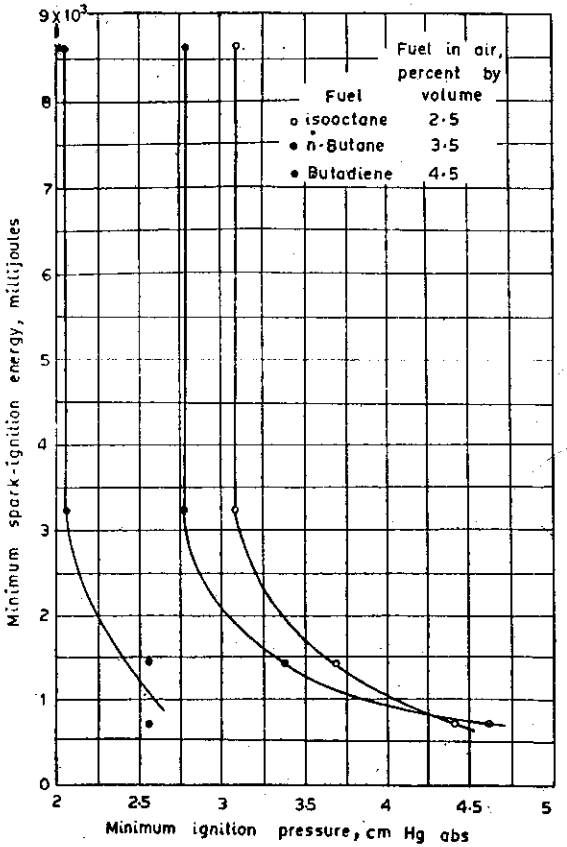

Fig. 15.15 Effect of pressure on minimum ignition energy for various fuel-air mixtures with constant electrode spacing.

ignition pressure" the ignition is limited by some factors of the apparatus, e.g., electrode spacing, size of ignition chamber, etc. This pressure, of course, changes with a change in apparatus. As the change in pressure has a marked effect on the quenching distance, the effect of pressure on the minimum ignition energy with respect to the maximum pressure is shown in Fig. 15.14. Figure 15.15 shows the effect of

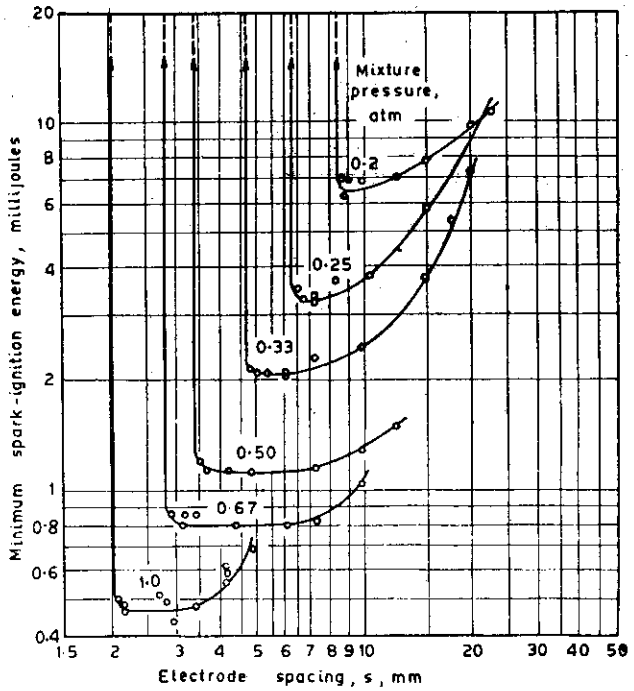

Fig. 15.16 Effect of electrode spacing and pressure on minimum spark ignition energy for methane-air mixture glass flanged electrodes (with permission from *J. Chem. Phys.*, op. cit., 11).

mixture pressure on ignition energy with fixed electrode distance. A complete relation between the mixture pressure, electrode spacing, and minimum ignition energy is given in Fig. 15.16.

Effect of Temperature

It is obvious that with increasing temperature of the mixture, lesser ignition energy will be needed. J.B. Fenn measured the effect of temperature on ignition energy and proposed a relation of the form

$$E_{ig} = Ce^{KT} \tag{15.33}$$

where C and K are constants which have different values for different mixtures.

Effect of Diluents

When a mixture is diluted by any inert gas, the minimum ignition energy required is changed. This change depends upon the absorptive and

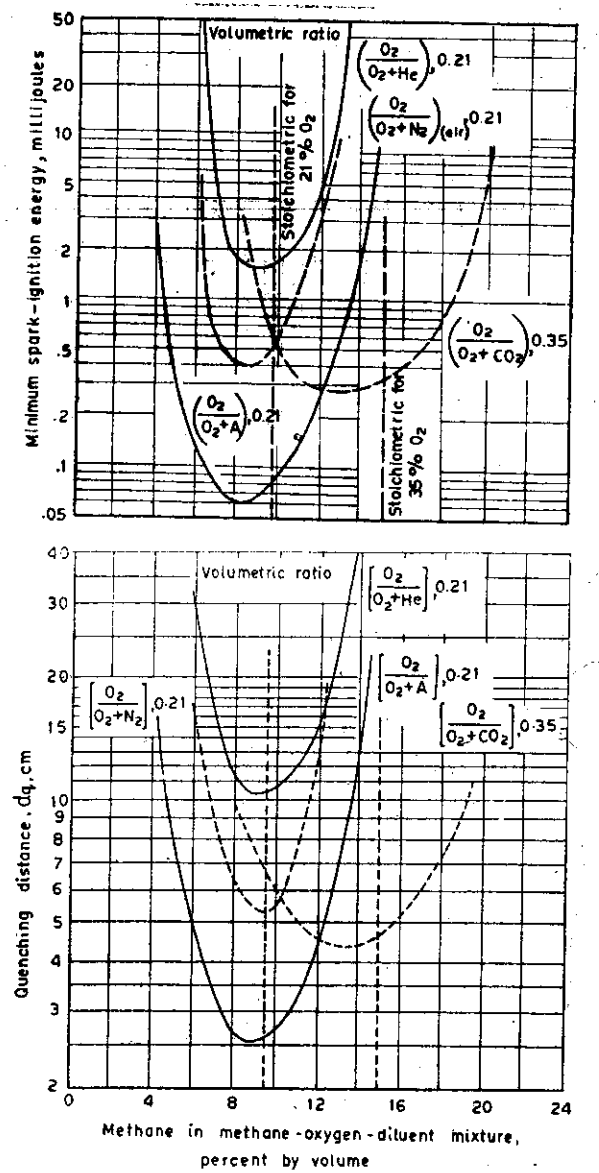

Fig. 15.17 Effect of diluents on minimum spark ignition energy and quenching distance (with permission from *J. Chem. Phys.*, op. cit., 11).

conductive qualities of the diluents. The effect of diluent also increases with increasing concentration. For most cases, the minimum ignition

energy is increased by the addition of the diluent. One exception is the methane-oxygen-argon mixture. The effect of diluents on minimum ignition energies for n-butane-oxygen mixtures with diluents such as argon, nitrogen, carbondioxide, and helium is shown in Fig. 15.17.

Effect of Mixture Velocity and Turbulence

If the combustible mixture is moving with respect to the electrode, the heat transfer from the ignition zone will increase with the increasing velocity of flow. Thus, the amount of energy required will also increase. It has been found that the energy required for ignition increases almost linearly in a velocity range of 2 to 16 m/s, but increases more rapidly at higher velocities. Figure 15.18 shows the effect of flow velocity on the minimum ignition energy. It has been found that with increasing flow, the arc across the spark gap is stretched and blown downwards. This

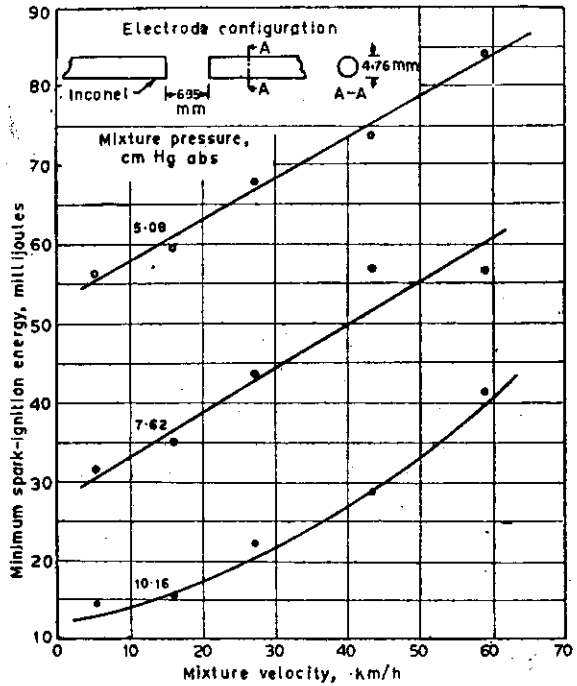

Fig. 15.18 Effect of mixture velocity and pressure on minimum spark ignition energy.

assumes a U-shape, causing the energy to be distributed over a large volume.

The effect of turbulence is somewhat similar. If, in a moving mixture, turbulence is generated by placing a wire screen, the ignition energy has been found to increase with an increasing diameter of screen wires and with a decreasing distance between the screen and electrode. Figure 15.19 shows the effect of turbulence promoter on the ignition energy for various promoter diameters and distanoes.

Spark Duration

It has been found that if the spark duration is high more amount of energy will be needed. The effect is shown in Fig. 15.20 for a time range

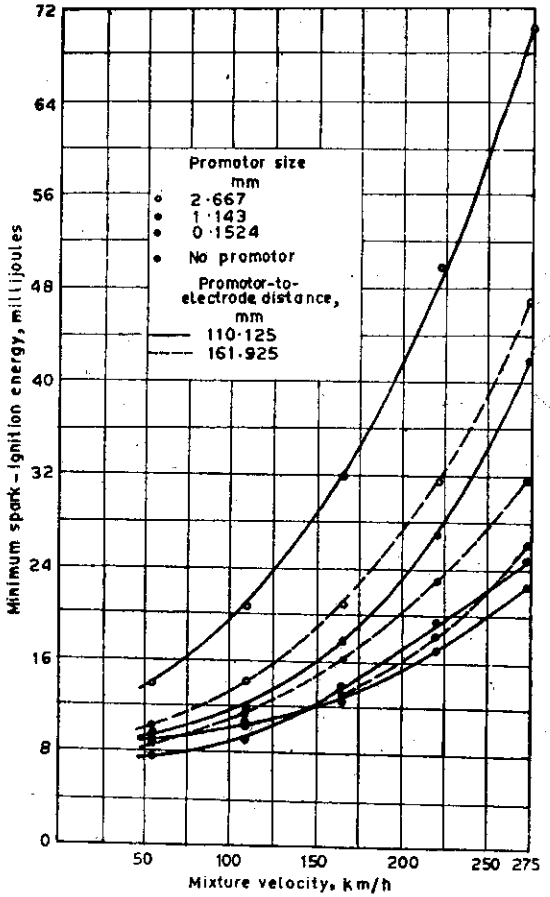

Fig. 15.19 Effect of mixture velocity, promoter size and distance from promoter to spark electrode on minimum spark ignition energy.

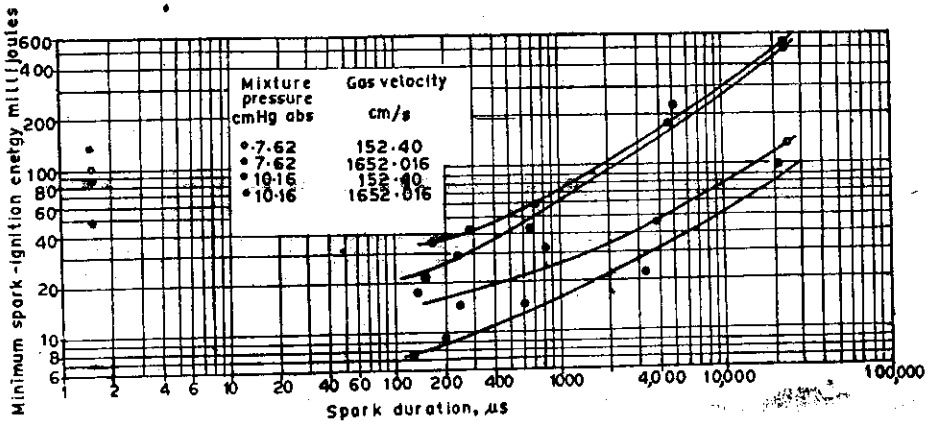

Fig. 15.20 Effect of spark duration on minimum spark ignition energy.

of 125 to 25,000 μs. However, it has been found that for a very short duration spark (2 μs), the amount of energy needed is much more.

REFERENCES

1. N.N. Semenov, *Progr. Phys. Sci.*, U.S.S.R., 1940, 24 (English Trans. in NACA Tech. Mem. 1026, 1942).
2. D.A. Frank-Kamenetsky, *Diffuziye i teploperedacha V khimicheskoi kinetike* (*Diffusion and Heat Transfer in Chemical Kinetics*), p. 255, Izdatel'stvo Akademii Nauk, SSSR.
3. J.D. Morgan, *Principles of Ignition*, Isaac Pitman and Sons, London, 1942.
4. J.L. Jackson and R.S. Brokaw, NACA *RME* 54 B19, 1954.

16

COMBUSTION OF LIQUID AND SOLID FUELS

Fuels in liquid and solid forms may be considered from the same point of view as the more conventional gaseous fuels. Some of the combustion characteristics of liquid and solid fuels are similar to those of gaseous diffusion flames, but there are sufficient differences which necessitate a separate discussion here. The burning of liquid and solid fuels may be called heterogeneous combustion as the fuels are mostly in the liquid or solid form, while the oxygen is supplied in the gaseous form. The first step is to bring the fuel and air in contact so that reaction can take place. For dispersible fuels, this process involves atomization and mixing. In the case of volatile fuels, evaporation may occur so that a part of the mixing process involves fuel vapour and air.

The surface area of the liquid and solid fuels exposed to the air or oxygen is usually very small, as the densities of liquids and solids are much higher than those of the gases. The surface area per unit mass can be increased manifold by reducing the size of liquid drops or the size of particles of a solid fuel. It is interesting to observe that a single cube of 1 cm side (volume 1 cm^3) has a surface area of 6 cm^2, while the same cube, if crushed to a powder form with cubical particles each of 0.01 mm side, will give a surface area of 6000 cm^2. The amount of the fuel to be evaporated, therefore, depends upon its surface area.

The liquid fuel can be evaporated and mixed with the air before combustion by breaking the liquid into small particles and providing sufficient space for these processes to take place. It is important to keep the volume of the combustion chamber to a minimum, e.g., in gas turbines and jet engines. But sufficient volume is generally not available so that the complete evaporation of the fuel can take place and the liquid fuel enters the flame zone in the form of droplets. The combustion of a liquid fuel consists of the following processes: the mixing of the spray with air, its evaporation, and the combustion of the mixture. For the practical design of combustors, these processes must be fully understood. However, no suitable information is yet available in literature. But for simple systems such as fuel jets or single droplets of fuel, combustion characteristics have been successfully predicted from the mixing rates which are determined by heat and mass-transport processes. Chemical reaction rates are not considered.

In the case of a solid fuel, the atomization step can be eliminated if it is injected inside the combustion chamber as a dust, e.g., coal. Also, the processes of atomization and mixing are eliminated if a solid fuel bed is used. The combustion of a solid fuel also includes the evaporation process, which is negligible in most cases. However, the early stages of the reaction which lead to ignition, will depend on the mechanism and the rate of the surface reactions. These reactions will increase the surface temperature leading to the evaporation and/or the combustion of the solid fuel. This is the major difference between solid and liquid fuels: the combustion of all hydrocarbon fuels occurs in the vapour phase. But solids such as naphthalene may be considered to evaporate according to the equations established for liquid fuels.

16.1 COMBUSTION OF LIQUID FUELS

A liquid fuel can be burned in the form of vapour, small drops, or in a pool. If the size of the drop is extremely small, say less than 100μ in diameter, the liquid will vaporize in the pre-heat zone and the combustion phenomenon will resemble the process of combustion in a premixed gaseous mixture, e.g., in spark ignition (SI) engines, gasoline burns in the vapour form. If the liquid droplet exceeds the critical size, but is smaller than, say about 1 mm, the combustion takes place in the form of spherical diffusion flame around the droplet. This form of combustion resembles the burning of a candle of a paraffin lamp, and the process is much slower than the first one. If the liquid dimension is greater than 1 cm, the fuel no longer behaves as a drop but as a pool. Where the liquid is confined in a pan and the surface burns, it is called "pan-fire", e.g., the fire on a petrol tank in an open atmosphere. In large pools, the rising column of hot gases restrict the air from reaching the fuel. Due to the limited amount of oxidant reaching the fuel, a rich flame is produced, generally accompanied by soot. The heat for evaporation is supplied by radiation.

16.2 COMBUSTION OF A FUEL DROPLET

The study of the combustion of a single fuel droplet is of practical importance as the combustion behaviour of a fuel in the combustion chambers of I.C. engines, gas turbines, liquid propellant rocket engines, and industrial burners cannot be understood unless the burning mechanism of individual droplets is known.

Droplet-combustion can be divided into two types: (i) bipropellant combustion, and (ii) monopropellant combustion.

In bipropellant combustion fuel vapour and oxidant diffuse from opposite directions and a flame is formed at the contact surface at some distance from the drop. Monopropellant droplets, e.g., hydrozine, ethylenitrate, etc., evaporate and decompose exothermally. Here we shall confine our discussion only to bipropellant combustion.

Three different types of experimental techniques have been developed to study the combusion of fuel droplets. In the first type, the fuel is supplied through a porous sphere at a steady rate and a liquid film is maintained at the sphere surface. In the second type, fuel droplets are suspended in air on a silica or quartz fibre, held either horizontally or vertically. The rate of decrease in the diameter of the fuel drop is recorded after ignition. In the third type, usually applied to very small droplets, a freely falling droplet is ignited and the rate of decrease in the diameter observed. Each technique has its own advantages and disadvantages.

In the first method, it is easy to obtain the steady state and a relation of the following form may be written.

$$\dot{m} = K' r_1 \tag{16.1}$$

where $\dot{m}$ = mass of fuel burned per s

r_1 = radius of sphere

K' = constant, independent of r_1

It has been found by experiments on the second and third type, that after the initial unsteady state, the square of the droplet diameter decreases linearly with time, viz.

$$d_{1,0}^2 - d_1^2 = K(t - t_0) \tag{16.2}$$

when $d_{1,0}$ is the initial diameter of the liquid droplet at time t_0, and d_1 is the diameter of the droplet at time t; K is called the evaporation constant, and is independent of time t in the absence of combustion.

Equation (16.2) also expresses the relationship between the droplet diameter and the time for vaporization of the droplet in the absence of combustion.

The general method for predicting the mass burning rate and the structure of the flame of a burning droplet involves the use of the general conservation equations. However, because of the complex boundary conditions and the exponential form of the Arrhenius expression for the chemical reaction rate, the analytical solution of such equations is not possible. Therefore, a number of theories based on a simplified physical model have been proposed. Most of the theories deal only with the combustion of a droplet in stagnant surroundings and in the absence of convection.

In the generally accepted steady-state theory, an ideal model consisting of a single spherical burning droplet is considered, surrounded by a spherical symmetrical flame front. In addition to the spherical symmetry, the following assumptions are usually made:

1. The droplet surface and the flame form concentric spheres.
2. At an infinite distance from the drop lies a boundary at which the gas composition is that of the ambient gas.
3. The fuel vapour diffuses from the drop surface to the flame front, and the oxygen from the boundary in the ambient gas to the flame surface. The resulting combustion products diffuse from the flame to the surroundings.
4. The exothermic chemical reaction between the fuel vapour and the oxidant takes place at the surface in stoichiometric proportion.
5. Combustion occurs under isobaric quasi steady state conditions.
6. The chemical reaction occurs instantaneously and hence the reaction zone is infinitely thin.
7. The chemical reaction goes to completion and requires no activation energy.
8. A part of the heat of combustion is transmitted by conduction to the droplet to effect vaporization, while the rest enters the ambient gas beyond the stagnant film.
9. The droplet temperature is uniform and equal to the boiling point of the liquid.
10. Radiation and thermal diffusion effects are negligible.

A general physical picture of the way in which a fuel droplet burns based on the above assumption is given in Fig. 16.1. The fuel evaporates from the drop surface and diffuses through region A, while the oxygen diffuses through region B. The fuel and oxygen react to form the product at a radius r_c where the fuel and oxidant are in stoichiometric ratio.

Figure 16.2 shows the temperature profile as a function of the radial distance from the centre of the drop for a benzene droplet, 0.01 cm in diameter, burning in air at atmospheric pressure. Figure 16.3 shows the profiles of mass fractions of fuel Y_F, Oxygen Y_O and inert gas Y_I as a function of the radial distance from the centre of the drop. $Y_{O,0}$ and

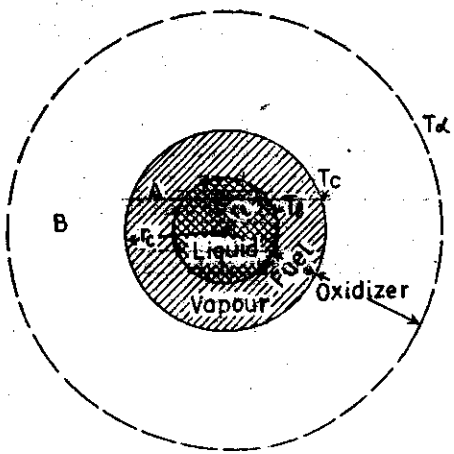

Fig. 16.1 Model of the burning of a fuel droplet.

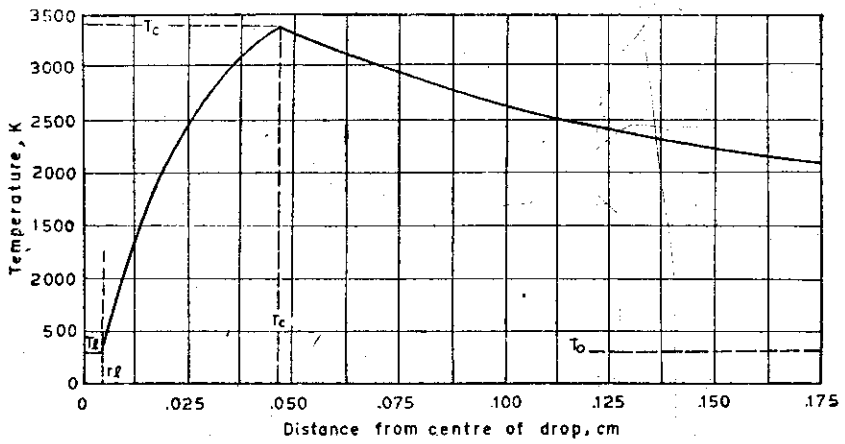

Fig. 16.2 Temperature profile for a burning fuel droplet as a function of distance from centre of drop.
r_c Radial distance of the combustion surface from the centre of the liquid drop
r_1 Radius of liquid drop
T_1 Temperature of the droplet
T_0 Temperature of the oxygen inert gas mixture at a large distance from the combustion surface.

$Y_{I,0}$ represent the mass fractions of oxygen and inert gas in ambiant air.

The conservation of mass and energy is considered for the above simplified model. The equations of Wise *et al.*[1] are presented here.

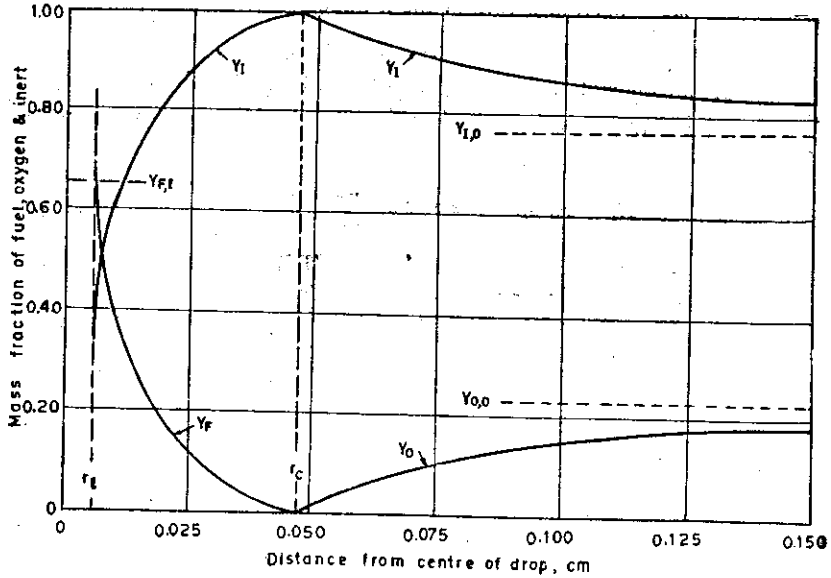

Fig. 16.3 Mass fraction profiles of fuel, oxygen, and inert as a function of distance from centre of drop (benzene droplet diameter 0.01 cm).

Equation for Conservation of Mass and Energy

The mass rate of fuel m_F leaving the liquid surface in region A (between r_1 and r_c) may be written as:

$$\dot{m}_F = 4\pi r^2 \rho \left(Y_F v - D_A \frac{dY_F}{dr} \right) \tag{16.3}$$

where $\dot{m}_F$ = mass flow rate of fuel, gm/s

ρ = liquid density, gm/cc

Y_F = mole fraction of liquid reactant

v = velocity with which fuel vapours are convected out, $\left(\frac{dr}{dt}\right)$, cm/s

D_A = Diffusion coefficient in region A, cm²/s

The products of combustion also diffuse to the region A, but there cannot be a continuous flow of the products towards the centre. Therefore,

$$\dot{m}_P = 0 = 4\pi r^2 \rho \left(Y_P v - D_A \frac{dY_P}{dr} \right) \tag{16.4}$$

where $\dot{m}_P$ = mass flow rate of the products

Y_P = mole fraction of the products.

Under steady state condition, the total enthalpy flux H_F at any point within this region must be equal to the total enthalpy flux at the liquid surface $H_{F,l}$ or

$$H_F = \dot{m}_F h_F - 4\pi r^2 k_A \frac{dT}{dr}$$

$$H_{F,l} = \dot{m}_F h_{F,l} - \left[4\pi r^2 k_A \frac{dT}{dr} \right]_l$$

where k_A is the thermal conductivity (cal/cm s K) in region A

h is the enthalpy per unit mass of the gaseous component (cal/g)

Subscript l refers to the liquid surface

F refers to the fuel

Therefore,

$$\dot{m}_F(h_F - h_{F,l}) = \left[4\pi r^2 k_A \frac{dT}{dr} \right]_l - \dot{m}_F L \tag{16.5}$$

where

$$\left[4\pi r^2 k_A \frac{dT}{dr} \right]_l = \dot{m}_F L = \dot{m}_F \left[L^* + C_l (T_l - T^*) \right] \tag{16.6}$$

where L^* = heat of vaporization (cal/g)

T^* = arbitrary reference temperature

In the absence of a source or sink of heat within the liquid droplet, the total rate of heat transfer at the spherical surface r_l must be equal to the rate of vaporization of the liquid fuel.

Considering the oxidizer flow rate in region B (between r_c and ∞), the mass flow rate of the oxidizer is given by

$$\dot{m}_0 = 4\pi r^2 \rho \left((Y_0 v)_0 - D_B \frac{dY_0}{dr} \right) \tag{16.7}$$

since at $r = r_c$, the fuel and oxygen meet in stoichiometric ratio i, therefore,

$$\dot{m}_0 = -i \dot{m}_F \tag{16.8}$$

Similarly, in region B, the mass flow rate of the products will be given by the difference in the mass flow rate of the fuel and the oxidizer, therefore,

$$\dot{m}_P = \dot{m}_F - \dot{m}_0 = 4\pi r^2 \left(Y_P v - D_B \frac{dY_P}{dr} \right) \tag{16.9}$$

Considering the conservation of energy, the following equation is obtained.

$$\dot{m}_0 h_0 + \dot{m}_P h_P - \dot{m}_F h_{F,l} = 4\pi r^2 k_B \frac{dT}{dr} - \dot{m}_F L \tag{16.10}$$

Thermodynamic Relationships

$$h_F + i h_0 = q + (1 + i) h_P$$

$$h_P = C_P (T - T^*)$$

$$h_0 = C_0 (T - T^*) + q/i$$

$$h_F = C_F (T - T_l) + L$$

where q = heat of reaction (cal/g)

c_p = specific heat at constant pressure (cal/g K)

It is assumed that $C_P = C_F = C_0 = C$.

Boundary conditons are:

At $r = r_l$, $T = T_l$

$r = r_c$, $T = T_c$, $Y_0 = 0 = Y_F$

$r = \infty$, $T = T_\infty$, $Y_0 = Y_{0,\infty}$

Integration of Differential Equations

Based upon the above relationships, the following differential equations are obtained for the condition $T^* = T_l$.

In region A:

$$\frac{dY_F}{dr} = \frac{\dot{m}_F (Y_F - 1)}{4\pi \rho D_A r^2} \tag{16.11}$$

$$\frac{d(T - T_l)}{dr} = \dot{m}_F [C(T - T_l) + L] / 4\pi k_A r^2 \tag{16.12}$$

and in region B:

$$\frac{dY_0}{dr} = \frac{\dot{m}_F (Y_0 + i)}{4\pi \rho D_B r^2} \tag{16.13}$$

$$\frac{d(T - T_l)}{dr} = \frac{\dot{m}_F [C(T - T_l) + (L - q)]}{4\pi K_B r^2} \tag{16.14}$$

These equations may be integrated in the closed form, if the assumption is made that c/k and ρD are constant and independent of Y and T. The results of integration yield the following explicit solutions for the mass and flow rate of fuel $\dot{m}_F$, temperature T_s at the reaction surface and at a radius r_c:

$$\dot{m}_F = \frac{4\pi k_B r_1}{C_B} \ln \left[\frac{q}{L} \left(1 + \frac{Y_{0,\infty}}{i} \right)^{\alpha k_B/k_A} - \frac{C_B}{L} \left(\frac{q-L}{C_B} + T_1 - T_\infty \right) \left(1 + \frac{Y_{0,\infty}}{i} \right)_\alpha^{[(k_B/k_B)-1]} \right] \tag{16.15}$$

$$T_C - T_i = \frac{q-L}{C_B} - \left(\frac{q-L}{C_B} + T_1 - T_\infty \right) \left(1 + \frac{Y_{0,\infty}}{i} \right)^{-\infty} \tag{16.16}$$

$$\frac{Y_0}{r_1} =$$

$$\frac{\ln \left[\frac{q}{L} \left(1 + \frac{Y_{0,\infty}}{i} \right)^{\alpha k_B/k_A} - \frac{C}{L} \left(\frac{q-L}{C} - T_1 - T_\infty \right) \left(1 + \frac{Y_{0,\infty}}{i} \right)_\alpha^{[(k_B/k_A)-1]} \right]}{\alpha \frac{k_B}{k_A} \ln \left(1 + \frac{Y_{0,\infty}}{i} \right)} \tag{16.17}$$

where $\alpha = C_P D_B / k_B$.

This ratio of Prandtl to Schmidt number is nearly unity for most gases with a specific heat ratio between 1.3 and 1.4.

These equations can be further simplified by assuming the same values of transport parameters in the two regions, A and B. Thus the simplified equation can be written as:

$$\dot{m} \simeq \frac{4\pi k r_b}{C} \ln \left(\frac{q}{L} \frac{Y_{0,\infty}}{i} \right) \tag{16.18}$$

$$T_C - T_L = \frac{q-L}{C} - \frac{\left(\frac{q-L}{C} T_1 - T_\infty \right)}{\left(1 + \frac{Y_{0,\infty}}{i} \right)} \tag{16.19}$$

$$\frac{r_c}{r_1} \simeq \frac{\ln \left(\frac{q}{L} \frac{Y_{0,\infty}}{i} \right)}{\ln \left(1 + \frac{Y_{0,\infty}}{i} \right)} \tag{16.20}$$

The Evaporation Constant K

The mass of the droplet is $\frac{1}{6} \pi \rho_1 D_1^3$, therefore, the mass burning rate is given by:

$$\dot{m}_F = -\frac{1}{2} \pi \rho_1 D_1^2 \frac{dD_1}{dt} \tag{16.21}$$

From the empirical Eq. (16.2),

$$D_1^2 = D_{1,0}^2 - K(t - t_0)$$

Differentiating this, we get

$$-2D_1 \frac{dD_1}{dt} = K \tag{16.22}$$

From Eqs. (16.21) and (16.22)

$$K = \frac{4\dot{m}_F}{\pi \rho_1 D_1} = \frac{2\dot{m}_F}{\pi r_1 \rho_L} \tag{16.23}$$

K is a convenient parameter for characterizing the burning rate of a single droplet.

Comparison between Observed and Calculated Results

Experimental studies relating to the effect that the square of the droplet diameter decreases linearly with time have been conducted by Godsave[2] and many other workers and are in accord with the theoretical model. Similarly, it has also been verified that the burning rate is directly proportional to the droplet radius. The experimental values of K have been found to be in good agreement with the theoretical predictions. The effect of the concentration of oxygen on the mass burning rate of a fuel droplet in natural convection has also been investigated and it is found to be in a good agreement with the calculated trend. The discrepancy between the theoretical and experimental values may be due to the uncertain values of the coefficients, and to the incorrect prediction of the flame temperature, without taking dissociation into consideration. It is also suggested that the discrepancy may be due to the convection currents during the burning of a droplet, but the later investigations by Kumagai *et al.*[3] in a freely falling chamber, where the convection currents were absent, have shown that the experimental values with convection are in better agreement with the theory than those obtained in the absence of convection.

Effect of Pressure and Flame Radius on Burning Rate

The present simplified theoretical model of the droplet burning suggests that the burning rate is independent of the pressure except that there is a slight change in the values of the boiling point and the latent heat of vapourization of the liquid fuel with pressure. However, the experimental results of Hall and Diederichsen[4] for burning with natural convection have shown that the burning rate is roughly proportional to one-fourth of the power of the pressure. According to the theory, the burning rate increases with pressure as the latent heat of evaporation decreases with the increase in the boiling temperatures associated with increased pressure.

It does not seem likely that the effect of pressure on the burning rate can be quantitatively accounted for without a further extension of the present theory.

The experimental data also suggest that the ratio of the flame radius to the droplet radius increases during combustion, and this ratio is greater for the smaller initial diameter. However, the quasi-steady-state theories suggest this ratio to be independent of both the time and the drop

size. The most likely explanation of these differences is given by Kolake and Okazaki[5]. They have shown that the combustion of a droplet is a non-steady process. The numerical calculations on the basis of their model show that the values of $d(d^2)/dt$ attain constant values, equal to those of the quasi-steady-state model after the initial period, and that the values of $d(d^2)/dt$ increases with time. These predictions are in line with the observed phenomenon.

16.3 SHAPE OF FLAME SURFACE DURING BURNING OF A DROPLET WITH NATURAL CONVECTION

Although the simplified spherical model may be assumed to be valid for extremely small droplets, there is no correlation between the actual flame shapes and the spherical flame surface. It is of interest to briefly describe the observations of Kumagai and Kimura[6] who showed the way in which a more realistic qualitative description for a single fuel droplet burning with natural convection could be obtained.

Natural convection currents are produced as a result of droplet burning. Let the velocity of such currents be U at some distance upstream from the undisturbed initial flame front. The model acts as a source in a uniform flow field. Under steady conditions of burning, a flow pattern as shown in Fig. 16.4 is established. The stream surface through the lower stagnation point, may be thought of as dividing initially the streamlines originating from the source (fuel droplet) and

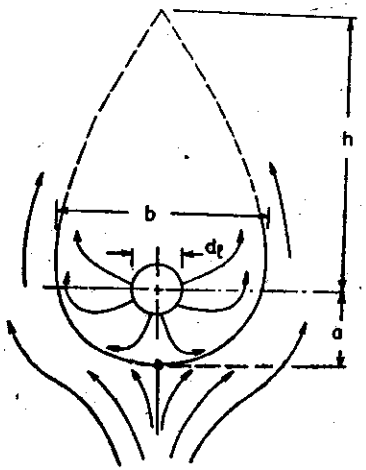

Fig. 16.4 Shape of flame surface surrounding a single fuel droplet during burning with natural convection.

the streamlines established by convective flow. This situation, however, is unstable, and the diffusive transport of the oxidizer and fuel across the stream surface must be established. The tangential flow velocities at the stream surface of the fuel vapour and air are initially equal. Presumably, the concentration and temperature gradients are established during steady burning in such a way that the diffusive transport of the fuel and oxygen brings a stoichiometric mixture roughly to the stream surface, thereby making the lower stream surface a flame surface.

Figure 16.4 also shows the shape of the flame boundary. Most of the fuel vapour is deflected around the stream surface and ultimately moves vertically upwards through a cylinder of diameter b. On the upper half, a flame shape as of one over-ventilated diffusion flame is formed. The height of the flame h can be calculated by the procedure of Burke and Schumann[7], described in Chapter 13.

It may be again stated here, that the effect of free convection is, in the first approximation, a distortion of the spherical flame front to a flame surface whose lower boundary is the stream surface which corresponds to a source of strength $\dot{m}_F/\rho_F$ ($\dot{m}_F$ = mass rate of burning of fuel droplet and ρ_F = density of fuel vapour) in a uniform flow of velocity U; the upper flame surface can be described as the flame front for a cylindrical diffusion flame with the inside cylinder of diameter l and flow velocities of fuel and air equal to U.

The observations of Kumagai and Kimura are in accord with the results obtained by the above model. Thus,

$$b = \sqrt{\frac{2\dot{m}_F}{\rho_F \pi U}} \tag{16.24}$$

and

$$\frac{b}{a} = 2\sqrt{2} \tag{16.25}$$

Furthermore, since $U \sin\theta$ (i.e., the tangential flow velocity of air stream surface) must be equal to the tangential flow velocity of the fuel vapour, one would expect that U and $\dot{m}_F$ are proportional to each other. Thus,

$$U \simeq d_1 \tag{16.26}$$

where d_1 is the diameter of the spherical droplet.

16.4 DROPLET INTERFERENCE DURING BURNING

Experimental studies have been carried out on the burning of fuel droplets, in close proximity to other burning drops. A configuration of two drops, five drops (four on corners and one at the centre) and nine drops (eight on cubical corners and one at the centre) was used. It has been found that the value of the evaporation constant does not change unless

the drops are so close that their combustion zone interfere with one another. If the combustion zones of two drops are merged, then the value of K is reduced by about 40%. This is because of the less penetration of the air or oxidant upto the surface of the droplets. Contrary to expectation, the value of K has been found to increase slightly if another droplet is burning close by. This may be because of the decrease in heat transfer from the flame surface of the droplet to the ambient atmosphere.

16.5 DIFFUSION FLAMES IN SPRAY COMBUSTION

The mode of combustion of fuel droplets in sprays can be considered as:

(i) If the drops are extremely small and their concentration is large, they may evaporate and mix by diffusion with the air in the preheat zone of an established flame front.

(ii) If the drops and the distance between the individual spheres are large, they may burn as diffusion flames in the local atmosphere surrounding them.

A theoretical study of the evaporation or burning of liquid fuel droplets in sprays has been carried out by Probert[8]. He assumed that the fuel spray drop size distribution follows the Rosin-Rammler relation

$$\psi = \exp\left[-\left(\frac{d_{l,0}}{\bar{d}_{l,0}}\right)^n\right] \tag{16.27}$$

where ψ is the volume or weight fraction of the spray composed of drops greater in diameter than $d_{l,0}$, $\bar{d}_{l,0}$ is called the size constant, and n is referred to as the distribution constant. If the size of the drops is more uniform, n will assume a higher value. If all the drops were of equal size, n would be infinite. However, it has been found that the atomizing nozzles give a spray which have values of n between two and four.

Probert defines a mean diameter d_m in such a way that a single droplet per unit volume of diameter d_m burns at the same rate as the liquid in a unit volume of the spray. For steady burning the approximate relation is

$$d_m = \frac{\bar{d}_{l,0}}{\sqrt{2}} \tag{16.28}$$

The fraction of the spray unevaporated for limited evaporative time t_r was also considered. The fraction of the spray unevaporated is plotted against $K t_r/\bar{d}^2_{l,0}$. For sprays in which the distribution constant n is 2, 3, or 4 is shown in Fig. 16.5. The dashed line shows the behaviour

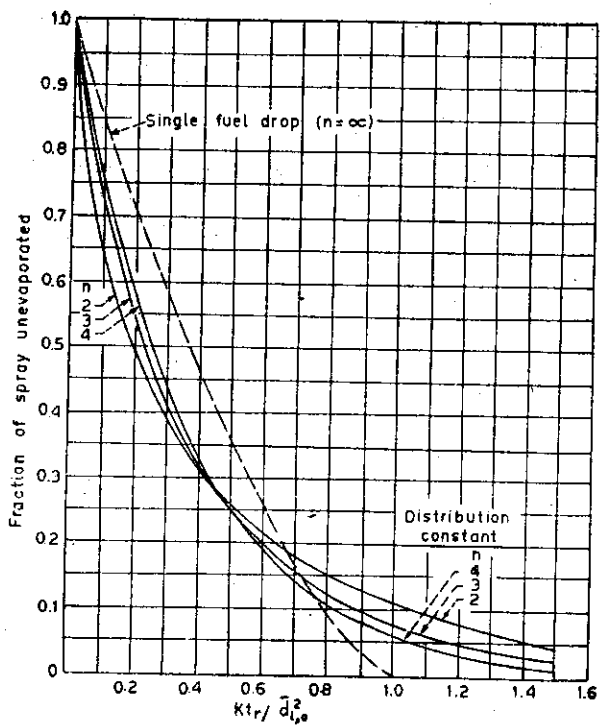

Fig. 16.5 Evaporation of fuel spray (with permission of Taylor and Francis, from *The Philosophical Magazine* XXXVII: 265).

of a single droplet, or a spray in which all drops are of the same size ($n=\infty$). It is observed that for sprays of low distribution constant n, the evaporation is most rapid in the early stages as more number of small droplets are present. However, in the later stages, sprays of uniform size distribution (large n), evaporate faster. It is, therefore, concluded that the size constant n is the most important factor for the evaporation or combustion of fuel sprays. Although the distribution constant is important, it has a much smaller effect on the evaporation rate. For a large value of the distribution constant, the evaporation is more complete, although the initial evaporation rate of the injected spray will be lower.

Droplet distribution laws other than the Rosin-Rammler distribution law, have also been applied, but the experimental data suggest that the values of K for a single droplet cannot predict the behaviour of spray combustion.

Wolfhard *et al.*[9] have also studied the burning of kerosene spray in still air. They have found that kerosene drops of size up to 10 μ evaporate if the preheat zone thickness is 2.5 mm or more, but the larger drops can pass through the combustion zone without being fully evaporated. In the case of fine sprays, a bunsen flame, similar to that for a premixed gaseous mixture, can be obtained. The burning velocity and the flammability limits for fine sprays closely correspond to those for vaporized fuel air mixtures. The larger size drops burn when surrounded by diffusion flames.

16.6 COMBUSTION OF SOLID FUELS

Solid fuels may be coal, wood, metals, or other chemical compounds. However, almost all of the energy used comes from coal. Other solid fuels are mostly of an academic nature, except when they used in solid fuel rockets. Apart from coal, few metals have the requisite properties of a fuel, i e., they release large amounts of energy while oxidizing. But because of their limited supply and slight difficulty in ignition, the oxidation of metals will not be dealt with in this chapter. Another disadvantage of metallic fuels is that they absorb a large amount of energy for melting and vapourizing before they are consumed. In the solid state, the slow oxidation process does not yield an appreciable amount of energy. As a fuel, the slow oxidation of metals can be neglected. We consider here the combustion of coal or coke only, because of its importance as a fuel.

16.7 COMBUSTION OF COAL

The coal samples from different mines vary considerably in respect of their properties and composition. One factor which is common to all the types of coal is that they contain a fixed amount of carbon and volatile matter, although their composition may vary. We consider here the combustion of coal in general and the description can be applied to various types of coal available.

Let us examine what happens to a piece of coal which is gradually heated in a furnace in the presence of air. Firstly the water vapour from the coal is released as its temperature is raised. This process gets over at about 100°C. Next, the decomposition of its unstable compounds starts. This coal now starts emitting volatile matter. If the furnace temperature is sufficient to ignite the volatile gases, they will burn like the liquid fuel droplets which continuously supply the vapours as the drops are consumed; the rate controlling factor being the diffusion mechanism. The coal piece remains dark during these processes.

Because of the burning of the volatile matter around the coal piece, its temperature is raised but normally does not exceed 600 to 700°C. The flame gradually shortens and is extinguished when all the gases get consumed. The piece which now remains is coke. If the rate of heating is very fast and the size of the coal is very small, the coal particles may be ignited before the volatile matter is completely burned. In this case, the coal will become red-hot and the combustion of volatile matter and coke may take place simultaneously.

The period when the coal gets dried and its volatile matter burned, is called the "preparation period" of coal or the first stage of burning. During the second stage, or the stage when the coke gets roasted, the solid carbon burns and most of the energy is liberated during this period. The coke temperature increases to about 1100°C and remains almost constant until the end of burning. The burning is for all practical purposes, flameless.

As stated earlier, the burning in the first stage is similar to the burning of liquid fuel drops. Also, very little heat is released. Therefore, we consider here the combustion of coke or the burning of coal during the second stage.

Oxidation Mechanism of Carbon

The rate of the oxidation of carbon in coal depends upon the reaction rate between carbon and oxygen and upon the rate of the supply of oxygen to the coal surface. These factors further depend upon the size and shape of the coal particles, velocity of the air supply, temperature of the coal surface and surroundings, diffusion coefficient of oxygen and the products, etc. The first part in the burning process is the diffusion of oxygen to the surface. This is a physical process. The second part of the process is the reaction of oxygen with solid carbon. This is a chemical process and the reaction is called the primary reaction. Rhead and Wheeler[10] assumed that the reaction of carbon with oxygen, resulting in the formation of carbon monoxide and carbon dioxide, are via an intermediary physicochemical complex of the form C_xO_y, which afterwards splits into CO and CO_2 in a ratio depending on the burning conditions.

Since it is not possible to observe any compound such as C_xO_y, the reaction is supposed to produce either carbon monoxide or carbon dioxide according to one of the following mechanisms:

(i) Formation of both CO and CO_2 in a surface reaction between C and O_2.

(ii) Formation of CO_2 from C and O_2 at the surface, with some CO_2 later reduced to CO.

(iii) Formation of CO at the surface from C and O_2 or C and CO_2, the CO being oxidized to CO_2 later in a gas phase reaction.

Initially, a two-zone theory of the burning of carbon was proposed, which assumed that the main product of the primary reaction of oxygen with carbon was CO_2 and not CO. In the second stage, this CO_2 was reduced to CO in the gas phase reaction with O_2.

However, Arthur, Bangham and Bowring, Mertens and Hellinckx, and Mertens[11] have definitely shown that the third mechanism, the reaction of carbon to primarily form carbon monoxide, prevails. Strickland–Constable[12] studies also support the third mechanism. It has not been confirmed whether the oxygen reaches the surface as oxygen or carbon dioxide, although both may reach the surface to form carbon monoxide. The three-zone theory is now almost accepted. According to this theory, the combustion of carbon takes place in three stages.

In the first stage, the oxygen from the air diffuses to the solid carbon surface and reacts as

$$2C + O_2 \rightarrow 2CO \tag{16.29}$$

In the second stage, the carbon monoxide diffuses from the surface to react in a homogeneous manner with oxygen as

$$2CO + O_2 \rightarrow 2CO_2 \tag{16.30}$$

In the third stage, the product CO_2 also diffuses to the surface where it reacts with carbon heterogeneously as

$$CO_2 + C \rightarrow 2CO \tag{16.31}$$

In the above three reactions, the second reaction takes place rapidly as compared to the first and third reactions. The rapid gas phase reaction of carbon monoxide with oxygen gave false results regarding the production of CO or CO_2. Arthur[13], using $POCl_3$ as a gas phase reaction inhibitor, showed that the ratio CO/CO_2 obeys the temperature dependent equation:

$$\frac{CO}{CO_2} = Fe^{-E/RT} \tag{16.32}$$

where F is the frequency constant and E the activation energy of value 12.4 kcal/mol. The calculations indicate that at temperatures above 1000°C, the proportion of CO_2 is negligible. Meyer[14] reported his observations on carbon filaments burning in the range of 730 to 1230°C. According to him, at a low pressure (below 0.1 mm), the CO/CO_2 ratio is one, and is independent of the temperature and pressure changes over the specified range. In the range 1530 to 2230°C, CO/CO_2 ratio is two, and it is again found to be independent of temperature and pressure. Strickland–Constable reported that in a range of 900 to 2000°C, only carbon monoxide is the primary product of the surface reaction. It may be concluded from this that only CO is formed at the higher temperatures.

Jones and Townend[15] investigated the oxidation of carbonaceous materials at temperatures below 350°C. Gulbrasen and Andrew[16] have studied the oxidation of graphite in the range of 425 to 575°C and have found that the rate constant has an exponential temperature dependence:

$$k = Ze^{-E/RT} \tag{16.33}$$

Different values of activation energies are reported for various temperature ranges by many workers.

16.8 KINETICS OF HETEROGENEOUS REACTION

The heterogeneous combustion of carbon is principally a chemisorption/desorption process. The oxygen molecules are first chemically bounded with certain atoms at the surface and then desorbed along with bonded carbon atoms. This leaves a bare carbon surface for further adsorption. The chemisorbed layer is believed to be only one molecule thick. The reaction can be represented as

$$F + S \underset{k_3}{\overset{k_1}{\rightleftharpoons}} (F.S)_{ads} \underset{k_4}{\overset{k_2}{\rightleftharpoons}} S + P \tag{16.34}$$

where F and S represent the fluid and solid molecules respectively. $(F.S)_{ads}$ is the adsorbed molecule and P is the product, k_1, k_2, k_3 and k_4 are the velocity constants of various steps. The specific reaction rate is given by the Langmuir[17] adsorption isotherm:

$$K = \frac{k_1 k_2 p_f}{k_1 p_f + k_3} \tag{16.35}$$

where p_f is the partial pressure of the reacting fluid immediately adjacent to the solid surface. It has been found both theoretically and experimentally that the reaction rate constant k_3 is negligible, but k_4 is not small. When the partial pressure of the products p_p is appreciable, then the equation becomes

$$K = \frac{k_1 k_2 p_f}{k_1 p_f + k_2 + k_4 p_p} \tag{16.36}$$

This equation has been experimentally tested for the CO_2 reduction reaction. The reaction rate is also temperature dependent as given by Eq. (16.33). The activation energy and the heat of adsorption are the two important quantities which control the reaction rate. The residence or reaction time (τ) that an adsorbed molecule will spend on the solid surface is controlled by the heat of adsorption. It is given by De Boer as:

$$\tau = \tau_0 e^{Q/RT} \tag{16.37}$$

Where τ_0 is the frequency factor. For carbon, it has a value of about 5×10^{-14}. Q is the heat of adsorption. In Eqs. (16.35) and (16.36), the value of p_f is the partial pressure of the fluid immediately adjacent to the solid surface. Usually, because of the diffusing product gases, it is quite different and difficult to measure and so it is calculated theoreti-

cally. If k_0 is the velocity constant for diffusional transport, then the reaction rate which must be proportional to the net number of gas molecules migrating from the mainstream to the solid surface through the stagnant film is given by

$$K = Ck_0 (p_0 - p_f) \tag{16.38}$$

where C is a conversion factor to keep the unit consistent and p_o is the partial pressure of the gas in the mainstream away from the solid surface. k_o can be experimentally measured or can be calculated theoretically. By integrating Ficks' equation for diffusional transport without convection, k_o is given by:

$$k_0 = \frac{D}{L} \tag{16.39}$$

where D is the diffusion coefficient, L is the film thickness. This film thickness decreases with increasing gas velocity.

After diffusing through the stagnant gas film, the oxidant has to reach the solid surface. If the solid reacting surface is perfectly smooth, then it will be immediately adjacent to the stagnant gas film. But usually the reacting surface is inside the solid. The oxidant has to diffuse through the pores of the porous solid surface, either of ash or the solid coal itself. Wheeler,[18] considering a uniform number of pores in the solid surface through which the oxidant gas has to diffuse, predicted the rate equations. These equations are quite complex, but under the limiting conditions they show that the reaction rate is proportional to the square root of the true velocity constant. This means that the values of the activation energy determined experimentally under the conditions of pores diffusion were half the true values for the surface reaction on the wall of the pores. These predictions were subsequently confirmed by Wicke[19] and Blyholder *et al*[20]. Thus Eqs. (16.35) and (16.36) can be used, assuming the reaction at the smooth surface provided the modified values of k and E are used.

By combining Eqs. (16.35) and (16.38), the unknown pressure p_f can be eliminated to give a complex quadratic in K involving p_0, k_1, k_2, and k_0. The overall reaction rate is controlled by three processes, viz., diffusion, chemisorption, and desorption. Normally at different temperature and pressure ranges, one or the other process dominates the other two. In that particular range, only one reaction rate controls the overall reaction rate, while the other two rates can be neglected. However, in the transition region, any two or all the three processes may have equal control. Three different temperature ranges have been identified as

1. The low temperature region where T is less than T_L, i.e., the lower critical temperature. For oxidation reactions, T_L is about 800°C.
2. The intermediate temperature region: $T_L < T < T_H$ where T_H is the higher critical temperature. For the oxidation reactions, T_H is about 1200°C.

3. The high temperature region: $T > T_H$.

In the low temperature region Tu *et al*.[21] found that $k_2 \ll k_1 p_f$. Therefore, Eq. (16.35) reduces to:

$$k = k_2 = K_2 e^{-E_2/RT} \tag{16.40}$$

The value of E_2 is between 20 to 40 kcal and K_2 lies in the range of 10^4 to 10^7. The reaction is found to be of zero order. This means that the solid surface is fully saturated with oxygen molecules, and only the desorption process controls the reaction rate.

In the intermediate temperature region Semechkova and Frank-Kamenetsky[22] reported the reaction to be of fractional order with respect to oxygen concentration. This region is a transition region and as such the full quadratic equation should be used. But as an approximation the Freundlich isotherm

$$K + k_0 p_0^n \tag{16.41}$$

is applicable, though k_o and n must be obtained empirically.

At high temperature regions Tu *et al*.[23] and others reported the reaction to be of first order. In this region, $k_2 \gg k_1 p_f$. So, combining the result with Eq. (16.38) gives

$$\frac{1}{K} = \frac{1}{Ck_0 p_0} + \frac{1}{k_1 p_0} = S_0 + S_1 \tag{16.42}$$

where S_0 and S_1 are known as diffusional and chemical resistances respectively. Equation (16.42) shows that K is directly proportional to p_0, irrespective of the ratio S_0/S_1. Ratio S_0/S_1 is a function of the aerodynamic conditions. If S_1 is small

$$K = \frac{1}{S_0} = \left(\frac{Cp_0 D_0}{L}\right)\left(\frac{T}{T_0}\right)^m \tag{16.43}$$

where D_0 is the diffusion coefficient at a standard temperature T_0 and L is the film thickness. If S_0 is small

$$K = \frac{1}{S_1} = K_1 p_0 e^{-E_1/RT} \tag{16.44}$$

for the oxidation reaction. Essenhigh[24] and Hadman *et al*.[25] reported the value of E to be about 4 kcal.

If at the solid surface, carbon dioxide penetrates, it reacts to form carbon monoxide. The rate equations and mechanism is similar to the one described for the oxidation reaction, only the values of activation energies and critical temperatures are different. For the heterogeneous reduction of carbon dioxide T_L seems to lie between 1000 and 1200°C. The value of T_H is not well defined. The experimental value of E_2, i.e., the activation energy of desorption in the low temperature region is

reported to lie between 40 to 80 kcal. At 1200°C, Walker *et al.*[26] and Nichols and Thring[27] reported that it drops to between 25 and 30 kcal. Nichols and Thring observed that at 1540°C, the activation energy jumped from 25 to 50 kcal. However, the exact cause for this is not known. They have explained this by stating that either the pores in the solid surface become large so that the effect of pore diffusion is removed, thus, automatically doubling the activation energy, or it may be due to some spurious effect of the experimental conditions.

The overall burning rate of coal also depends upon the particle size, because it changes the surface to mass ratio of the coal. Small coal particles give large surface area. This principle is used in the development of pulverised coal burners, where a moving coal dust cloud is burned in a hot combustion chamber. The flame produced has something in common with both solid and the liquid fuel combustion.

16.9 THE TRANSFER NUMBER IN HETEROGENEOUS COMBUSTION

Many practical combustion systems involve heterogeneous combustion where a liquid or solid fuel burns in an oxidizing gaseous atmosphere. In general, a gas stream containing oxygen flows past a fuel body and the chemical reaction occurs at, or in the immediate neighbourhood of the fuel surface, and the fuel is transferred in some form or other into the gas stream. The rate of mass transfer from the unit area of fuel surface is of considerable interest in heterogeneous combustion which finds application in spray and droplet combustion, metal combustion, hybrid rockets, etc. Most commonly, the chemical aspects of the problem do not need any attention, as the rate controlling processes involve heat and mass transfer. The mass transfer rates, which here mean the combustion or vaporization rates, can be described in terms of a driving force, commonly referred to as the transfer number denoted by the letter B. Spalding[28] did pioneering work in this field and was one of the first to describe the mass transfer rates in terms of the driving forces, expressed in a dimensionless form. Although present in the expression for B, such characteristics of the system of chemical reaction as the composition of gas streams, the carbon-hydrogen ratio of the fuel, its enthalpy of combustion, or the gas temperature are not present in the solution.

Spalding[29] defined the transfer number B, in analogy with ohm's law for the flow of electricity, as

$$B = \dot{m}''/g \tag{16.45}$$

where g is the conductance, and B, which can be calculated from thermodynamic considerations, is thought of as a driving force for mass transfer. B has also been referred to as the "Spalding transfer number" or "phase-change number" in literature. B can have either positive or

negative values. If B is positive, mass transfer is outwards from the interface; if B is negative, mass transfer is into the interface. The maximum and minimum possible values of B are ∞ and -1 respectively. $B=-1$ implies that a pure fluid is wholly absorbed.

Transfer Number of Liquid Fuels

Spalding has presented a method of deriving the transfer number of a liquid fuel from the fundamental balance equations.[30] A less formal method presented by him, giving the same result, is given below.

The differential equation

$$q''' + \frac{H}{r}\,\dot{m}'''_{O_2} = 0 \tag{16.46}$$

implies that heat release occurs within the gas where oxygen disappears, and the amount equals the full heat of combustion of the fuel H. In Eq. (16.46), q''' is the heat produced in unit volume and time $\dot{m}_{O_2}'''$ is the mass flow of oxygen into unit volume; r is the weight of oxygen that combines with unit weight of the fuel.

We assume that the molecular diffusion coefficient of oxygen D_{O_2} equals to the terminal diffusivity $\alpha = \frac{k}{c\rho}$.

This is very nearly true. A new variable b may be introduced as follows:

$$b \equiv \frac{Hm_{O_2}/r + cT}{Q} \tag{16.47}$$

where Q is the amount of heat reaching the fuel surface from gas per unit weight of the fuel vaporized, m_{O_2} is the mass concentration of oxygen, c is the specific heat at constant pressure, and T is the temperature. The variable b satisfies the boundary condition

$$v_s = \alpha \left(\frac{\partial b}{\partial y}\right)_s \tag{16.48}$$

where y and v are the direction and velocity respectively at right angles to the surface.

Equation (16.48) states that the heat absorbed in vaporizing is equal to the heat conducted to the surface. Thus

$$\alpha \left(\frac{\partial b}{\partial y}\right)_s = \frac{K}{Q} \cdot \left(\frac{\partial T}{\partial y}\right)_s \tag{16.49}$$

Also $m_{O_2,s}$ and $(\partial m_{O_2}/\partial y)_s$ are both zero for the thermodynamic equilibrium and no reaction at the surface.

We know that in heat transfer, the rate depends on the temperature difference between the fluid stream and the solid surface. Likewise, in mass transfer, the rate depends on the difference in the values of the variable b in the gas stream and at the surface. The difference $B \equiv (b_g - b_s)$ occurs very frequently in mass transfer and is termed as the transfer number. As stated earlier, the transfer number is the driving force for mass transfer expressed in a dimensionless form.

The transfer number thus becomes

$$B = \frac{H}{Q} \quad \frac{m_{O_{2,g}}}{r} + c\frac{(T_g - T_s)}{Q} \tag{16.50}$$

Usually all the quantities occurring on the right hand side of Eq. (16.50) are given in the problem for calculating the value of the transfer number. The value of T_s, the temperature at the fuel surface, although not known precisely, is nearly equal to the boiling temperature of the fuel. T_g is the temperature in the gas stream.

There are different forms of the transfer numbers for a given problem. As there can be only one value of the mass transfer rate, each of the many forms of the transfer number for a given system must have the same numerical value. The transfer numbers can be defined in terms of the temperatures (or enthalpies) or concentrations.

From Eq. (16.50) it can be seen that if a liquid fuel is burned in pure oxygen ($m_{O_2} = 1$) instead of air ($m_{O_2} = 0.232$), the value of transfer number is increased. If $T_g = T_s$, then

$$\frac{B_{O_2}}{B_{air}} = 4.31 \tag{16.51}$$

Transfer Number of Solid Fuels

For solid fuels, the temperature at the fuel surface T_s can never exceed the temperature of the reaction zone. As T_s increases, the value of the transfer number B decreases and approaches a lower limit appropriate to a solid fuel. The concentration of both oxygen and fuel is zero at the reaction zone where the temperature T_r can be determined from the enthalpy balance for the process such that the fuel is just sufficient to consume all the oxygen. Thus we have

$$c(T_r - T_s) = \frac{\frac{m_{O_{2,g}}}{r}(H - Q) + c(T_g - T_s)}{1 + \frac{m_{O_2}}{r}} \tag{16.52}$$

If the reaction zone and fuel surface have the same temperature, i.e., $T_r = T_s$, it can be seen from Eq. (16.52):

$$c(T_s - T_g) = \frac{m_{O_{2,g}}}{r}(H - Q) \tag{16.53}$$

Substituting the above value of $c(T_s - T_g)$ in Eq. (16.50), we get

$$B = \frac{m_{O_{2,g}}}{r} \tag{16.54}$$

Equation (16.54) gives the transfer number of a solid fuel.

Liquid and Solid Fuels as One Family

It can be seen from Table 16.1[30] that for less volatile liquid fuels with high boiling points and large latent heats, the value of transfer numbers is generally smaller. We may, therefore, consider a continuous series of fuels of increasing boiling points (T_s) with constant values of other properties, thereby giving lower transfer numbers. As shown in Eq. (16.53), when

$$(T_s - T_g) = \frac{m_{O_{2,g}}}{r}\left(\frac{H - Q}{c}\right)$$

the transfer number becomes simply $m_{O_{2,g}}/r$, all the heat terms having disappeared.

TABLE 16.1 Transfer Numbers of Liquid and Solid Fuels

Fuel formula	*Condition*	B	*Condition*	B
n-Pentane (C_5H_{12})		8.23		7.78
n-Hexane (C_6H_{14})	Combustion	9.00	As before,	6.39
n-Heptane (C_7H_{16})	in atmospheric air	9.15	except	5.45
n-Octane (C_8H_8)	$T_g - T_s = 0$,	9.70	Q = latent	5.02
n-Decane ($C_{10}H_{22}$)	Q = latent	10.02	heat and sensible	4.11
Benzene (C_6H_6)	heat of fuel	7.74	heat to raise	6.09
Toluene ($CH_3C_6H_5$)	CO formation	8.35	liquid from	5.85
Cyclohexane ($CH_2)_6$	neglected	8.25	15°C to	6.22
Methyl alcohol (CH_3OH)	$m_{O_{2,g}} = 0.232$	2.67	B.P.	2.37
Ethyl alcohol (C_2H_5OH)	$m_{CO_{2,g}} = 0$	3.50	$m_{O_{2,g}} = 0.232$	2.95
Solid carbon (C)		0.174	$m_{CO_2} = 0$	0.087
Water (H_2O)	Vaporizing into gas stream at 2000°C	0.77		—
n-Decane ($C_{10}H_{22}$)	Vaporizing into gas stream at 2000°C	2.98		—

It can be seen from Eq. (16.54) that solid fuels belong to the same family as liquid fuels, with the extreme condition that the boiling temperature of the solid fuels is equal to or above the reaction temperature. Therefore, we may say that the heavier fuels burn less rapidly than those of the low molecular weight. The transfer number steadily decreases as the average boiling point (which is closer to T_s) increases.

Combustion of Carbon

If we consider that the carbon is completely oxidized to CO and any CO_2 reaching the surface is instantly consumed, then CO is the sole carrier of carbon.

Therefore, $$B = \frac{12}{16} m_{O_2,g} \tag{16.55}$$

If it is considered that no CO is formed at all, then CO_2 is the sole carrier of carbon.

Therefore, $$B = \frac{12}{32} m_{O_2,g} \tag{16.56}$$

i.e., the value of B from Eq. (16.56) is just one-half of the value of B from Eq. (16.55).

Combustion of Metals

The combustion of metals finds application in many important processes, e.g., in oxygen cutting where the metal is burned away as an alternative to machining and in the steel industry where the oxidation of the molten metal has to be avoided. Metals are different from other solid fuels, as the oxides of the metals do not generally vapourize at the temperatures attained by the metal surface. The transfer number of metals is negative due to the mass transfer being predominantly inwards to the surface. In the case of very pure oxygen and iron, Spalding[80] showed that the transfer number tends to be equal to -1, corresponding to an infinite inward transfer rate.

16.10 BURNING TIME OF FUEL PARTICLES

We consider that the mass transfer occurs through a stagnant film of thickness δ, and the concentrations of the diffusing substance are $m_{j,s}$ at the phase boundary and $m_{j,g}$ at the opposite face of the gas film. Let y be the direction normal to the film. The transfer of component j is in two ways, by convection and by diffusion as given by the two terms on the right side of the following equation:

$$\rho v_s = \rho m_{j,s} v_s - D\rho \left[\frac{dm_j}{dy}\right]_s \tag{16.57}$$

where the left side of the equation ρv_s represents the mass transfer rate at the surface. Equation (16.57) may be rewritten as follows:

$$v_s = \frac{D\left(\frac{dm_j}{dy}\right)_s}{m_{j,s} - 1} \tag{16.58}$$

Introducing the variable $b = \frac{m_j}{m_{j,s} - 1}$, Eq. (16.58) reduces to:

$$v_s = D\left(\frac{db}{dy}\right)_s \tag{16.59}$$

The differential equation for mass transfer can be written as

$$D\left(\frac{d^2 m_j}{dy^2}\right) - v\frac{dm_j}{dy} = 0 \tag{16.60}$$

Dividing Eq. (16.60) by $(m_{j,s} - 1)$ and rearranging the terms, we have

$$D\frac{d^2 b}{dy^2} - v\frac{db}{dy} = 0 \tag{16.61}$$

If density is assumed to be a constant, then from the continuity equation, v — constant. We integrate Eq. (16.61) keeping v = constant, from 0 to y

$$D\frac{db}{dy} - v(1 + b - b_s) = 0 \tag{16.62}$$

The further integration of Eq. (16.62) from 0 to δ (the stagnant film thickness) gives

$$D \log_e (1 + b - b_s) = v\delta \tag{16.63}$$

As $\dot{m}'' = \rho v$, we get

$$\frac{\dot{m}''\,\delta}{D\rho} \log_e (1 + B) \tag{16.64}$$

It may be mentioned here that as the mass transfer rate increases, the flow causes the increasing curvature in the b profile. However, for low values of mass transfer rate, Eq. (16.64) reduces to

$$\frac{\dot{m}''\,\delta}{D\rho} \approx B \tag{16.65}$$

This means that at low values of B, the mass transfer rate is directly proportional to B, and the curvature of the b profile is negligible.

The rate of mass transfer from a sphere in a stagnant infinite atmosphere may also be derived in a similar way. The resulting equation would be given by

$$\frac{\dot{m}''\,d}{D\rho} = 2 \log_e (1 + B) \tag{16.66}$$

where d is the sphere diameter.

Equation (16.66) may be used to calculate the burning time t_b of a fuel particle (vaporizing droplet or other spherical droplet). The relationship between the mass transfer rate and the rate of the change of radius r is given by

$$\dot{m}'' = -\rho_f \left(\frac{dr}{dt}\right) \tag{16.67}$$

where ρ_f is the fuel density (or the density of the sphere).

The burning time is given by

$$\frac{t_b D \rho_g}{d_0^2 \rho_f} = \frac{1}{8 \log_e (1 + B)} \tag{16.68}$$

where d_0 is the initial diameter. ρ_g is the gas density (assumed constant). This equation can be used to calculate the burning time of liquid and solid fuel particles.

Example 16.1

Determine the transfer number of a liquid hydrocarbon $(CH_2)_n$ fuel droplet burning in an atmoshere of air. The latent heat of vaporization of the hydrocarbon fuel is 83.5 cal/g and the specific heat of gases at constant pressure may be taken as 0.3 cal/g°C. Assume the value of the heat of combustion of fuel (H) as 10,550 cal/g. Take $T_g - T_s = 565$°C.

Solution

The transfer number derived from heat balance is written as

$$B = \frac{\frac{H.m_{O_2,g}}{r} + C(T_g - T_s)}{Q}$$

The stoichiometric ratio r, i.e., the mass of oxygen required to burn a unit mass of fuel is calculated by writing the chemical equation

$$C_nH_{2n} + \frac{3n}{2}(O_2 + 3.76\ N_2) \rightarrow n\ CO_2 + n\ H_2O + \frac{3n}{2}(3.76)\ N_2$$

Therefore $$r = \frac{48n}{14n} = 3.43$$

Other data are: $m_{O_2,g} = 0.232$

$C = 0.3$ cal/g°C

$T_g - T_s = 565$°C

$Q = 83.5$ cal/g

$H = 10{,}550$ cal/g

Substitution of the above values in the expression for transfer number yields

$$B = \frac{\frac{10{,}550 \times 0.232}{3.43} + 0.3 \times 565}{83.5}$$

$$= 10.57$$

Example 16.2

What is the time of disappearance in seconds of a liquid droplet of a $(CH_2)_n$ hydrocarbon fuel burning in still air when the following data in addition to those given in Example 16.1 apply:

Density of droplet $(\rho_f) = 0.8$ g/cm³

Initial radius of droplet $(r_0) = 2 \times 10^{-3}$ cm

Exchange coefficient $(\gamma = D\rho_g) = 0.413 \times 10^{-3}$ g/cms.

Solution

The burning time of a fuel droplet is given by:

$$\frac{t_b D \rho_g}{(d_0)^2 \rho_f} = \frac{1}{8 \log_e (1 + B)}$$

or $$t_b = \frac{r_0^2}{2} \cdot \frac{\rho_f}{\gamma} \cdot \log_e (1 + B)$$

The value of the transfer number calculated in Example 16.1 is:

$$B = 10.57$$

Substituting the values of known data in the above expression we have

$$t_b = \frac{(2 \times 10^{-3})^2 \times 0.8}{2 \times 0.413 \times 10^{-3} \times 2.449}$$

$$= 1.58 \times 10^{-3}\ s$$

Example 16.3

Estimate the life-time of an ethyl alcohol fuel droplet burning in stagnant air. The initial droplet diameter is 20×10^{-3} cm. The following data may be used:

Heat of combustion of fuel $(H) = 6{,}700$ cal/g

Latent heat of vaporization of fuel $(L) = 238$ cal/g.

Specific gravity of ethyl alcohol $= 0.8$

Exchange coefficient $(\gamma = D\rho_g) = 0.413 \times 10^{-3}$ gm/cm. s

The temperature of the droplet (T_s) may be assumed to be equal to the atmospheric temperature (T_g).

Solution

The expression for transfer is:

$$B = \frac{\frac{H.m_{O_2,g}}{r} + C(T_g - T_s)}{Q}$$

For ethyl alcohol (C_2H_5OH), the stoichiometric ratio, r may be calculated from the following chemical equation:

$$C_2H_5OH + 3O_2 \rightarrow 2\ CO_2 + 3\ H_2O$$

$$r = \frac{3\ (32)}{46} = 2.087$$

Other data are: $H = 6{,}700$ cal/g

$$m_{O_{2,g}} = 0.232$$

$$T_g - T_s = 0.0$$

$$Q = L = 238 \text{ cal/g}$$

Substitution of the above data yields

$$B = \frac{6700 \times 0.232}{2.087 \times 238}$$

$$= 3.13$$

The burning time of a fuel droplet is given by

$$t_b = \frac{\rho_f d_0^2}{8 D \rho_g \log_e (1 + B)}$$

$$= \frac{0.8\ (20 \times 10^{-3})^2}{8 \times 0.413 \times 10^{-3} \times \log_e 4.13}$$

$$= 0.0684 \text{ s}$$

REFERENCES

1. H. Wise, J. Lorell, and B.J. Wood, *Fifth Symposium (International) on Combustion*, (Reinhold. New York), 1955, 132-141.
2. G.A.E. Godsave, *National Gas Turbine Establishment (England)*, Report Nos. R 86 1950, R 87 1951, and R 88 1952.
3. S. Kumagai, T. Sakai, and S. Okajima, *Thirteenth Symposium (International) on Cumbustion*, (The Combustion Institute, Pennsylvania, 1971, 779.
4. A.R. Hall, and J. Diederichsen, *Fourth Symposium (International) on Combustion*, (Williams and Wilkins, Baltimore), 1953, 837.
5. S. Kolake, and Okazaki, *Int. J. of Heat and Mass Transfer*.
6. S. Kumagai, and A. Kimura, *Science of Machine* 1951, 3: 431.
7. S.P. Burke, and T.E.W. Schumann, *Ind. and Eng. Chem.*, Oct. 1928, 20(10): 98-1004.
8. R.P. Probert, *Phil. Mag*, Ser. 7, XXXVIII (265): 94-105, 1946.
9. H.G. Wolfhard, and W.G. Parker, *Jour. Inst. Petroleum*, 1949, 35 (302): 112-125.
10. R.F.E. Rhead and R.V. Wheeler, *Trans. Chem. Soc.*, 1912, 10: 846.
11. J.R. Arthur, D.H. Bangham and J.R. Bowring, *Third Symposium on Combustion, Flame and Explosion Phenomena*, Williams and Wilkins, 1949, 466-474.
    E. Mertens, and Hellinckx, *Third Symposium on Combustion, Flame and Explosion Phenomena*, Williams and Wilkins, 1949, 474-475.
    E. Mertens, *International Symposium on Combustion of Carbon, J. Chem. Phys.*, 1950, 47: 313-378, 523-585.
12. R S Strickland-Constable, *Chemistry and Industry*, 1948,771-774.

13. J.R. Arthur, *Trans. Farad. Soc.*, 1951, 47 (Part 2):164,
14. L. Meyer, *International Symposium on Combustion of Carbon, J. Chim. Phys.* 1950, 47: 313-378, 523-585.
15. Jones, and Townend, *Third Symposium on Combustion, Flame, and Explosion phenomena*, Williams and Wilkins, 1949.
16. Gulbrasen, and Andrew, *Symposium on Theoretical Aspects of Combustion and Gasification, Ind. Eng. Chem.* 44: 1952, 1028-1082, 1547-1575.
17. I. Langmuir, *J.A.C.S.*, 1916, 38: 2221.
18. A. Wheeler. *Advances in Catalysts*, III, Academic Press, 1951, N.Y., 250.
19. E. Wicke, *Fifth Symposium (International) on Combustion*, Reinhold, Paper 17, 1955, 245.
20. G.D. Blyholder, and H. Eyring, *U.S. Air Force Office of Scientific Research Report*, Technical Note O.A., XX, 1956.
21. C.M. Tu, H. Davis, and H.C. Hottel, *Ind. Eng. Chem.* 1934, 26: 749.
22. A.D. Semechkova, and D.A. Frank-Kamentskii, *Zhur Fi Chim.* 1940, 14: 231.
23. C.M. Tu, and H.C. Hottel, *Ind. Eng. Chem.*, 1934, 26: 749.
24. R.H. Essenhigh, J. Sheff. *Univ. Fuel Soc.*, 1955, 6: 15.
25. T. Hadman and C.N. Hinshelwood, *Proc. Roy. Soc.*
26. P.L. Walker, R.J. Forlsti and C.C. Wright, *Ind. Eng. Chem.* 1953, 45: 1703.
27. L.F. Nichols and M.W. Thring, "Physical Processes in a Bed of Fuel", *J. Inst. Fuel*, 1940.
28. D.B. Spalding, "The Combustion of Liquid Fuels", *Ph D Thesis*, Mech. Engg. Dept., Cambridge University, 1951.
29. ———, *Convective Mass Transfer*, McGraw-Hill, New York, 1963.
30. ———, "The Combustion of Liquid Fuels", *Fourth Symposium (International) on Combustion*, Williams and Wilkins, Baltimore, 1953, 847.